Towards Quantifying Groundwater Resources of the Paloluoma Buried Bedrock Valley in Western Finland Using Groundwater Modelling

by

Ameerah Binte Rashid

A thesis

presented to the University of Waterloo

in fulfilment of the

thesis requirement of the degree of

Master of Science

in

Earth Sciences

Waterloo, Ontario, Canada, 2022

Author's Declaration

This thesis consists of material all of which I authored or co-authored: see Statement of Contributions included in the thesis. This is a true copy of the thesis, including any required final revisions, as accepted by my examiners. I understand that my thesis may be made electronically available to the public.

Statement of Contributions

This research project was designed by Martin Ross, René Lefebvre, Niko Putkinen, and myself.

I am the sole author of Chapter 1.

Chapter 2 is intended for publication with co-authors Martin Ross, René Lefebvre, and Niko Putkinen. The geological model surfaces from chapter 2 were received from the Geological Survey of Finland.

Chapter 3 is also intended for publication with the same co-authors from chapter 2 as well as Jean-Marc Ballard who guided the construction of the numerical model. Application and analysis of the numerical model were performed by me.

I am the sole author of Chapter 4.

Abstract

Groundwater provides about 60 percent of drinking water in Finland. In western Finland, drinking water for the town of Kurikka (pop. ~21 700) comes from glaciofluvial aquifers confined underneath thick glaciomarine aquitards along structurally-controlled bedrock valleys. One such valley is called the Paloluoma Buried Bedrock Valley (BBV) – an area that experiences a subarctic climate with no dry season and cool summers. The nearby town of Vaasa (pop. ~70 000) currently uses river water, which is more prone to near-surface sources of contamination than groundwater. As such, Vaasa intends to get its water supply from the same aquifer as Kurikka, especially because the aquifer of interest is seemingly highly productive. With increased interest and demand, it is important to understand key hydrogeological characteristics of the Paloluoma BBV aquifer system, its flow dynamics, and response to pumping in order to assess its sustainable exploitation rate. Such an assessment of the groundwater system has yet to be completed for this region. Hence, research on key hydrogeological characteristics and behaviour of the groundwater system is necessary to determine sustainable usage and develop plans to better protect and manage this groundwater resource.

An understanding of groundwater systems is commonly developed by coupling a conceptual model with a flow model. The conceptual hydrogeological model of the Paloluoma BBV aquifer system was developed using methods such as water balances and pumping test analyses, which estimate hydraulic parameters such as groundwater recharge and hydraulic conductivity, respectively. The conceptual model also includes the 3D subsurface hydrostratigraphic structure consisting of a series of aquifers and aquitards for a total of 14 sedimentary hydrostratigraphic units (HSU) and bedrock. Important hydrogeological characteristics based on the conceptual model include the lack of groundwater interaction between surface water bodies and subsurface units, the delineation of spatial recharge on the basis of surficial geology where good recharge zones are found along raised Holocene beach ridges and topographic highs, indication of aquifer behaviour as confined and leaky, and local flow pathways indicating interaction between shallow and deep aquifers. The conceptual model is the foundation and framework of the groundwater flow model as it is an amalgamation of key processes and parameters of the Paloluoma BBV groundwater system.

From the conceptual model, parameters are applied to the flow model, which is constructed using a finite element numerical model grid and set up as a fully saturated and confined aquifer system. The calibrated model parameters include a recharge rate of 50 mm/a, hydraulic conductivity of aquifers ranging within 10^{-4} ms^{-1} to 10^{-3} ms^{-1}, hydraulic conductivity of aquitards at a magnitude of 10^{-7} ms^{-1},

hydraulic conductivity of bedrock gradually decreasing with depth from 10^{-7} ms^{-1} to 10^{-10} ms^{-1}, and bedrock hydraulic conductivity anisotropy (K_h/K_v) of 1000. The flow model is critical to obtain quantitative understanding of the Paloluoma BBV hydrogeological system. To this end, four simulation goals/scenarios were addressed: (1) produce steady-state stabilized conditions, (2) verify the model with field pumping observations, (3) understand where water is coming from and going to, and (4) explore what could be the future maximum sustainable pumping rate of the existing production wells. These scenarios are studied and quantified using rate budgets at specific boundaries of interest. The change and comparison between scenarios at each boundary provided insight into how key areas of the model react to varying pumping rates. Key characteristics derived from the flow model include flow pathways and source areas during groundwater extraction. Specifically, it was found that the pumping well at the center of the study area is likely receiving water from overlying aquifers or underlying bedrock. In contrast, the water extracted from the pumping well at the downgradient south end of the study area is mainly sourced from captured discharge that would have otherwise flowed out of the system in the absence of pumping.

While under the maximum pumping scenario (5500 m^3d^{-1}), water is drawn from outside the watershed and outflow out of the watershed is reduced, there is no lack of groundwater as even during pumping, flowing artesian conditions in monitoring wells remain present (for the purpose of this thesis, when artesian wells are specified, it is meant as flowing artesian wells). Nonetheless, groundwater production in the valley impacts the adjacent watershed, which must be considered when designing pumping plans.

Using conventional flow modelling processes from conceptual model development to numerical modelling, the Paloluoma BBV is characterized and its groundwater resource is successfully quantified. The flow model is a critical tool for the town of Kurikka to aid in making informed decisions surrounding their freshwater resource and further the advancements of their freshwater program.

Acknowledgments

I would like to express my sincere gratitude to my supervisors Dr. Martin Ross (UWaterloo) and Dr. René Lefebvre (INRS) for their dedicated support and guidance every step of the way. Their insights have taught me invaluable lessons that have made this experience incredibly worthwhile.

I also extend my thanks to my committee members Dr. David Rudolf and Dr. Andrea Brookfield for providing critical feedback at the most pivoting of times.

This research would not have been possible without the support and collaboration of the Geological Survey of Finland (GTK), the Water Services Public Company of Kurikka, Finland (Kurikan Vesihuolto Oy), and the Water Services Public Utilities of Vaasa, Finland (Vaasan Vesi). I thank them for entrusting me with this research for their municipal development. I was also fortunate to receive the Farvolden Scholarship (UWaterloo) which helped provide more academic opportunities and research exposure.

I also give great thanks to Niko Putkinen (GTK) for his expertise and enthusiasm throughout the entire thesis period. Through his hospitality, I had the honour to experience Finnish culture and learn more about the country. I also give many thanks to Elina Lindsberg for her help with finding and translating Finnish data. Kiitos!

Additionally, from INRS, I would like to extend my thanks to Melanie Raynauld, Maxime Claprood, and Erwan Gloaguen for having shared their problem-solving ideas. I would especially like to thank Jean-Marc Ballard for his guidance from the very beginning stages of modelling and for being an all-around incredible mentor.

From the University of Waterloo, I thank everyone in the Quaternary research group; Bob, Caroline, Jessey, Rebecca, Robin, Thomas, Tyler, Wenyao, and especially Grant. Also, many thanks to all my peers and good friends for making my time at UWaterloo as amazing as it was, especially Simon, Jaki, and Tong.

Lastly, I would like to thank my family for their unbelievable support not only throughout my entire academic career but with every endeavour I pursue. For always encouraging me to follow my interests and passions and for never missing an opportunity to celebrate together.

Table of Contents

List of Figures

List of Tables

Chapter 1

Introduction

Groundwater systems of regions that were covered by the Laurentide ice sheet in North America and the Fennoscandian ice sheet in Scandinavia (Dyke, 2009; Stroeven et al., 2016) are unique to most other regions of the World as relatively cold and humid climates allow for high rates of groundwater recharge through glacial deposits (Barthel et al., 2021; Person et al., 2007). However, fractured rock and glaciofluvial aquifers in some of these regions are confined underneath thick glaciolacustrine and glaciomarine aquitards along Quaternary buried valleys forming pressurized hydrogeological systems that have intricate connectivity to surface systems (Beaudry et al., 2018; Cloutier et al., 2006; Ross et al., 2005). These areas are also populated with many municipalities relying on groundwater for their water supply. This is the case for large areas of southwestern Finland (Katko, 2016), where semi-confined and confined hydrogeological systems are prominent and are increasingly used to supply water to municipalities and towns.

Groundwater is a critical resource for the Finnish population as 60% of drinking water usage is sourced from granular aquifers (Katko, 2016; Kløve et al., 2017). While these granular aquifers contain high permeability materials, high exploitation rates could still lead to unsustainable exploitation of aquifer systems relative to their recharge rates. Consequences of unsustainable exploitation include, but are not limited to, lowering of the water table, land subsidence, deterioration of groundwater quality, and changes in the local ecosystem (Gleeson et al., 2011; Savard et al., 2013; M Sophocleous, 2000). As such, it is important to determine sustainable rates of extraction. In order to determine safe groundwater extraction rates, a good understanding of the aquifer system is required. This understanding begins with the conceptualization of the study area that will model the subsurface architecture and assess key hydraulic parameters. Alongside conceptual model building, key processes such as recharge mechanisms and flow dynamics may begin to be investigated.

Under the basis and conditions of the conceptual model, a numerical flow model must be developed. The numerical flow model is used to quantify freshwater resources and help construct management plans (Anderson & Woessner, 1992). Failures of numerical models to represent aquifer systems are often related to poor conceptual models (Kresic & Mikszewski, 2013). A flow model is especially useful for understanding complex systems such as the previously mentioned glaciofluvial aquifers with intricate connectivity between surface water and groundwater systems. The flow model can further explore flow dynamics under natural conditions and pumping conditions. Moreover, using

the flow model, varying pumping conditions can be simulated in order to explore the aquifer's response to varying stress levels (Anderson & Woessner, 1992; Rushton, 2003). This will be especially helpful when determining safe extraction rates for the aquifer system. In many regions, especially those less populated, an exhaustive assessment of groundwater resulting from the product of a conceptual model and flow model, has yet to be completed. As such, further investigation of the groundwater system in these regions will lead to an improved understanding of key processes that are necessary to support sustainable groundwater usage.

One such region requiring an improved understanding of its aquifer system is the Paloluoma Buried Bedrock Valley (BBV) in western Finland (Fig. 1.1). The Paloluoma BBV has historically sustained its water levels with artesian conditions, suggesting a prospective future in terms of its groundwater supply potential. On that account, groundwater usage is proposed to increase in order to supply water to other nearby municipalities. Specifically, the city of Vaasa, which currently supply their drinking water from rivers. Surface water bodies like rivers are more susceptible to contamination and changes to climate compared to groundwater.

With the aquifer system proposed to undergo more pumping and its current limited understanding, sustainable groundwater extraction rates cannot be confidently estimated. Therefore, to improve understanding of the Paloluoma BBV, a conceptual model and a groundwater flow model are required. This research is a first attempt at developing these models for this region of western Finland. This study presents a multidisciplinary approach to acquire a better understanding of the aquifer system. From the hydrostratigraphic framework, characterization of hydrogeological properties, to quantification of groundwater availability, this study acquires and integrates all data and interpretations to form an applicable model for decision-making purposes surrounding the usage of groundwater of the Paloluoma BBV. Developing such an understanding of the Paloluoma BBV aquifer system will constitute a crucial first step towards meeting heavier demands of its freshwater resource in a sustainable manner and will greatly contribute to the region's groundwater management plans.

Figure 1.1: Paloluoma study area located in West Finland near the Town of Kurikka.

1.1 Background Information

Buried valleys in glacial landscapes can have complex origins related to tectonics, pre-glacial fluvial processes, as well as glacial erosion during the Quaternary (Cummings et al., 2006). Glacially carved out valleys are filled with unconsolidated sediments composed of sand and gravel, resulting in highly productive aquifers (Van Der Kamp & Maathuis, 2012). Often, such an aquifer area transitions upward into an aquitard related to lacustrine and/or marine depositional environments, which are in turn discontinuously overlain by minor perched aquifers made of deposits of postglacial origin (e.g., fluvial, eolian, organics). The aquitard units of low permeability till deposits form a complicated internal structure to the sediment assemblage. Detailed characterization of buried valley aquifers is essential to ensure consistent representation and useful quantitative analysis of the groundwater flow system.

Buried valleys can be modelled to represent three-dimensional subsurface structures and the lithological stratigraphy and sedimentology of valley fill units (Hickin et al., 2008; Ross et al., 2005; Sandersen & Jørgensen, 2003; Stumpf & Ismail, 2013). These geological models can then be used to provide important insights into the spatial distribution and hydraulic connectivity of aquifer and aquitard units within aquifer systems (e.g., Ross et al., 2005). Accordingly, a geological model of the geometry of the aquifer and aquitard units provide key insights into the hydrostratigraphic architecture, which is the basic framework for developing a sound hydrogeologic conceptual model.

Based on the geological model, the hydrogeological model is obtained by assigning hydraulic parameters such as hydraulic conductivity and recharge. There are multiple methods cited in the literature to determine these hydraulic properties such as analysing hydrofacies and pumping tests for hydraulic conductivity (Van Der Kamp, 2001; Wen et al., 2010; Zhu et al., 2016); and analysing hydrometeorological data and surficial geology for recharge and recharge distribution, respectively (Rivard et al., 2014; Scanlon et al., 2002).

Another important component of developing an understanding of the hydrogeological system of buried valleys is to investigate the effect of pumping in different aquifers within the valley. Multiple methods to assess groundwater withdrawal with pumping have been developed and include; volume-based methods using hydraulic head changes, remote sensing, groundwater flow models, and water balance methods using hydrological models (Bierkens & Wada, 2019). Groundwater flow models (simulated groundwater levels and head declines multiplied by the respective storage coefficient and drainable porosity) coupled with hydrological models (withdrawal rates subtracted from recharge rates) are also used to assess sustainable pumping rates and manage flow systems (De Graaf et al., 2014).

Another important strategy is the use of geochemical data to understand flow dynamics within the system. The most relevant radioactive isotopes in the hydrological cycle, tritium and ^{14}C, are commonly used to support conceptual hydrogeological models and to form the basis for numerical simulations (Beaudry et al., 2018; Blackport et al., 2014; Janos et al., 2018; Kazemi et al., 2006; Mook, 2006; Rey et al., 2018). The relative ages and evolution of a series of water samples provide important constraints to groundwater flow patterns and the degree to which certain aquifers in a buried valley are connected to the regional system.

The uncertainty that remains surrounding groundwater flow models is heightened in semi-confined to confined systems. For confined systems, replenishment is slower due to infiltration and recharge processes being more complex than for unconfined systems. Complexity for confined aquifer recharge arises due to the fact that they are fed by interconnected unconfined aquifer areas that are heterogeneously distributed over the region (Rey et al., 2018). These confined aquifers are prevalent in previously glaciated areas, especially along the former southern margins of Pleistocene ice sheets which were inundated by glacial lakes and short-lived inland seas, whose fine-grained sediments covered previously deposited glaciofluvial sediments from the melting of the ice sheets. Confined aquifers are becoming increasingly exploited for the purpose of water supply as they generally offer more protection from near-surface sources of contamination than surface water and unconfined aquifers (Bajc et al., 2011).

1.2 Scope and Objectives

The main goal of this study is to improve the overall understanding of the groundwater flow system of the Paloluoma BBV, which currently supplies water to the Town of Kurikka. Presently, only the topmost aquifer of the buried valley is exploited. However, the deepest aquifer will also be exploited in order to expand the distribution of the valley's freshwater resource to other nearby municipalities, like Vaasa (Fig. 1.1). More specifically, the particular objectives of this study are to:

1. Assess recharge to the granular aquifers within the valley;
2. Develop a conceptual hydrogeological model of the Paloluoma BBV;
3. Build a steady-state numerical groundwater flow model of the study area;
4. Analyse groundwater flow dynamics under different pumping scenarios.

The first two sub-objectives are essential steps prior to developing a numerical groundwater flow model. The recharge estimates and conceptual model are critical to establish the boundary

conditions of the flow model. The groundwater flow model will in turn allow for an understanding of the system dynamics and its response to various pumping scenarios.

Understanding groundwater recharge mechanisms and aquifer connectivity are especially important when considering sustainable exploitation of the aquifer system as pumping should only draw on the renewable groundwater of the aquifer system, rather than the stored capital. Provided that the objectives are met, the municipality of Kurikka will have the tools to sustainably manage their freshwater resources.

1.3 Methods Overview

1.3.1 Assess recharge to the granular aquifers within the valley

Recharge assessment is problematic because it cannot be directly measured, hence, it must be quantified using indirect methods (Healy and Cook, 2002; Wen et al., 2010). It is difficult to estimate groundwater recharge reliably using any one single method due to uncertainties and limitations of each method (Scanlon et al., 2002). Therefore, often recharge is estimated using multiple methods to cross-check the results and constrain the values obtained (Rivard et al., 2014). For example, a water budget method may be implemented using available hydrometeorological data and soil information. Hydrometeorological data such as, but not limited to, evapotranspiration, temperature, and precipitation is publicly made available online by the Finnish Meteorological Institute. In order to provide additional support for the results from the water balance method, a groundwater flux analysis is performed as a secondary method to estimate recharge.

To analyse recharge in more detail, surficial maps are enhanced for delineating recharge zones using sediment texture information, as areas of coarse gravel may identify preferential areas of recharge into the groundwater system. In contrast, surface areas that are overlain with thick clay deposits may represent poor recharge areas that are more suited for runoff or areas of potentially high evaporation rates.

1.3.2 Develop a conceptual hydrogeological model of the Paloluoma valley

Development of a hydrogeological conceptual model can be initiated with information from pumping data, borehole data, geophysical data, and lithological information from a three-dimensional geological model, which is provided by the Geological Survey of Finland (GTK).

1.3.2.1 Primary data

Subsurface geology interpreted from borehole data is used to build a 3D geological map using Groundhog (britishgeologicalsurvey.github.io), which is a widely used software by the British Geological Survey (BGS) and GTK. One of the greatest challenges that is associated with determining groundwater flow is the construction of an accurate 3D geological model. This is especially challenging when encountered with Quaternary deposits due to the highly variable geology. Ensuring that the interpreted geology accounts for, if present, discontinuity in units and variable thicknesses, are key responsibilities of the model.

1.3.2.2 Use and Modification of Primary Data

The hydrogeological model building process is divided into two major steps. The first step is outlining the conceptual physical structure. This includes classifying the geological units into aquifers and aquitards. Layers of the model must be relevant in the context of the hydrogeological cycle. For example, consecutive sandy units are combined to represent an aquifer for the hydrogeological model. With hydraulic context given to the geological units, the stratigraphy is simplified and results in the hydrostratigraphy of the valley. Simplification is important as it is impossible to reconstruct reality.

The second step is to outline the conceptual processes which include identifying aquifer properties such as hydraulic head from monitoring wells, transmissivity and storage from pumping tests, and other hydraulic properties from well hydrographs. Numerous techniques have been employed for investigating aquifer hydraulic properties. A traditional method of estimating aquifer hydraulic parameters is the slug test (useful for unconfined low permeability aquifers; Campbell et al.,1990) and pumping test method (useful for confined aquifers).

Pumping tests will be especially important to identify hydraulic limits, which may be present in the laterally restricted aquifer system within the buried valley. Groundwater response rate to pumping will indicate storage of the aquifer and the size of the capture zone (Meyer et al., 2014; Pétré et al., 2019). The transmissivity and storage coefficient will be calculated using a type-curve method (e.g., Theis, Jacob, or Hantush-Jacob). The choice of type-curve to employ for this calculation will depend on the type of confining layer above the main aquifer (i.e., leaky or non-leaky).

The extent of storage decrease and capture zone increase with groundwater withdrawal will be key concepts when realizing aquifer response to pumping. Once the hydrogeological model is developed, the process of numerically modelling groundwater flow can be initiated.

1.3.3 Build a steady-state groundwater flow numerical model of the study area

A numerical groundwater flow model is commonly used when assessing aquifer response to different stresses, such as the effect of climate, urbanization, or exploitation. Simulation of flow dynamics will further help conceptualize the system, including recharge and discharge zones as well as hydraulic connectivity between hydrogeological units (Freeze and Cherry, 1979). After the calibration of the numerical model, the model can be used to assess the effects of pumping on the groundwater system. These effects are changes in hydraulic head, storage, and fluxes to and from the boundaries of interest.

Of the many different numerical methods available to model groundwater flow, the finite element method is the preferred approach. The finite element method approximates the unknown function over the domain by dividing the larger system into smaller sections, which have the same parameter value within the sectional area, known as a finite element. The finite elements then ensemble into a larger system of equations that represent the entire domain. This method has some advantages over the finite difference method, especially the capability to represent discontinuities and irregular boundaries, as found in Quaternary deposits like the study area. Pandian et al. (2016) reviewed previous research where successful discretization of a complex Quaternary aquifer system and its flow dynamics was completed using the finite element method on the numerical simulator FEFLOW. Accordingly, the software, FEFLOW, is employed for this study to simulate groundwater flow. Greater detail on the application of FEFLOW for groundwater modelling is available in Diersch (2014). There are numerous additional examples of the successful use of FEFLOW to simulate groundwater flow (Lavigne et al., 2010; Pandian et al., 2016; Pétré et al., 2019; Rivard et al., 2014; Usman et al., 2018; Vižintin et al., 2018). Table 1.1 provides a brief explanation of some parameter and main equations to be solved at each cell of the model.

Table 1.1: Governing equations and variables to be used with the construction of the groundwater flow model in FEFLOW.

Equations and Parameters for the Groundwater Flow Model		
Hydraulic Gradient	Equation	$\frac{dh}{dL} = \frac{change\ in\ head\ (m)}{change\ in\ length}$
	Details	From static water level data, a contoured map will be created to determine the spatial hydraulic gradient.
Hydraulic Conductivity	Equation	$K = \frac{k\rho g}{\mu}$
	Details	Hydraulic conductivity (K) is the measure of ability of porous or fractured media to transmit water; constant of proportionality in Darcy's Law.
Storage coefficient (storativity)	Equation	$S = S_s * b$
	Details	The volume of water released from storage in a confined aquifer per unit surface area per unit decrease in the hydraulic head.
Specific Storage	Equation	$S_s = \rho g(\alpha + \varphi\beta)$
	Details	The volume of water that a unit volume of aquifer releases from storage under a unit decline in hydraulic head.
Leakage	Equation	$L = -K'_z * \left(\frac{h_{source} - h}{b'}\right)$
	Details	Used to represent a confining layer. Kz' = vertical hydraulic conductivity; b' = confining layer's thickness; h_{source} = head in the source reservoir on the other side of the confining layer
Aquifer Viewpoint	Equation	$\frac{\partial}{\partial x}\left(T_x \frac{\partial h}{\partial x}\right) + \frac{\partial}{\partial y}\left(T_y \frac{\partial h}{\partial x}\right) = S\frac{\partial h}{\partial t} - R + L$
	Details	T_x and T_y, or hydraulic conductivity multiplied by the aquifer's saturated thickness, is the transmissivity in the x and y direction. R is a source or sink term. L represents leakage through a confining bed.

The boundaries of the study area are delineated based on hydrological basin boundaries. In order to set up the model in FEFLOW, the total area of the region (27.6 km^2) must be divided into elements/cells. The cell size is to be determined based on geological surfaces representing the aquifers and aquitards. The elements are then refined where larger hydraulic gradients are expected such as along streams and pumping wells. The FE method creates an unstructured mesh in the x- and y- plane using triangular irregular networks (TINs) (Fig. 1.2). The TINs will be used to define different hydrogeological boundaries that correspond to different hydraulic conductivity zones. The model is then sliced into layers, which are created by grouping hydraulically similar and nearby cells together.

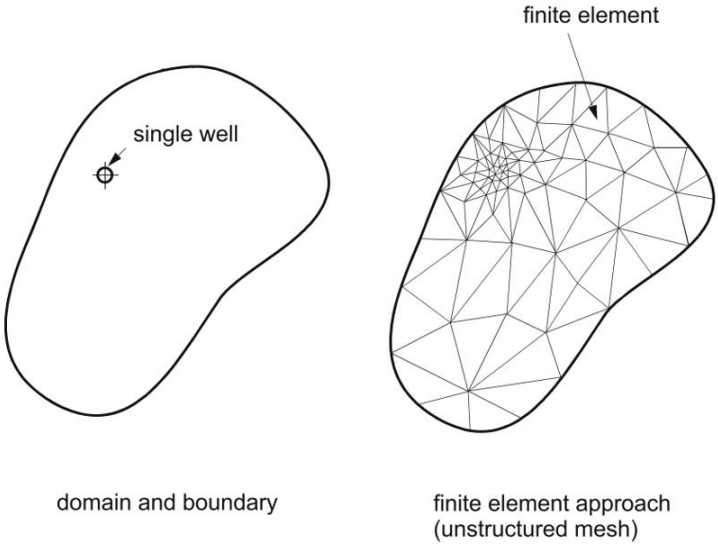

Figure 1.2: Example of a two-dimensional domain discretized by finite elements (Diersch, 2014).

1.4.3.2 Model Calibration

Model calibration is the process of manually or automatically adjusting parameters within their upper and lower limit such that when the model is run, it produces flow patterns and water levels of the groundwater system that reflect, as close as possible, the observations. Under steady-state conditions, the procedure typically relies heavily on the reproduction of measured water levels. Model performance must be independently verified.

The calibration parameters, hydraulic conductivity and recharge, have a range of possible values with upper and lower limits and are not independent parameters. The initial range of values of the calibration parameters are taken from the literature using sediment information from borehole logs. Manual calibration using piezometric water level is performed before automated calibration on a trial-and-error basis, to understand how the parameters affect the model. Doing so also reduces the

automated convergence time (Usman et al., 2018). In order to evaluate the model performance, observed and simulated values are statistically analysed using mean error and root mean square error (RMSE), which is applied to non-linear models. Another way to evaluate the model's performance is to check that the trend of observed and simulated head variation is more or less similar to the coefficient of determination (R^2) value for regression line.

Automated calibration is then performed using PEST, which adjusts hydraulic conductivity and recharge values when matching the model heads with observed heads (Vižintin et al., 2018). Once calibrated, each unit within the numerical model gets a unique hydraulic conductivity value that helps reproduce the general behaviour of the system.

1.4.3.4 Sensitivity Analysis

Uncertainty comes from many sources such as the data type and source, conceptual model, model structure, observations, boundary conditions, and model parameters. For example, rainfall and recharge can be highly uncertain due to variability. The uncertainty in the outcome of the model can be understood by a sensitivity analysis. A sensitivity analysis can be performed manually by multiplying the calibration parameters by different factors (Usman et al., 2018). When performing a sensitivity analysis, one parameter is changed while all others are held constant.

1.3.4 Analyse groundwater flow dynamics under different pumping scenarios.

Once a numerical model is built and calibrated, varying levels of pumping can be experimented with, under steady-state conditions, to simulate the system's response. This project will seek for the maximum level of exploitation such that the worst-case scenario is identified and accordingly avoided. While this model is run such that steady-state conditions are reached under different pumping scenarios, the time needed to reach such steady-state remains unknown. Nonetheless, the model is expected to provide important insights when identifying a potential range of sustainable management conditions for the aquifer system. Whether the model is good or not will be determined upon monitoring. Monitoring wells should be put in place to ensure that real-world observations are following closely what was simulated for the particular pumping rate. It should be noted that while the aquifer area is hydrogeologically conceptualized and the response to pumping is simulated, uncertainty remains.

1.4 Brief explanation of the structure of the thesis

This thesis is divided into four chapters. The first chapter is the introduction of the study. The next two chapters are the main research chapters of the thesis and are written in a format to facilitate their preparation for submission to scientific journals. Specifically, Chapter 2 describes the conceptual model, which utilizes the hydrostratigraphic surfaces developed by the GTK and couples it with hydraulic parameters to advance the conceptual understanding of the aquifer system. The third chapter describes the numerical groundwater flow model, which is used to investigate the effects of pumping, groundwater interaction across HSUs, and analyse the magnitude of flow and flow pathways to discharge areas. The fourth and last chapter concludes the study, explains the implication of the study, and suggests areas of future research.

1.5 Contributions

This study implements many approaches to achieve its overarching goal of providing an improved overall understanding of the Paloluoma BBV. Of these approaches, many are standard practises highly followed in the literature. For instance, the practise of building conceptual models followed by flow models to solve for hydrogeological topics/issues. Likewise, this study used two software, Leapfrog and FEFLOW, to form the structure of the conceptual 3D hydrogeological model and 3D groundwater flow model, respectively. Future studies can refer to the workflow conducted from this study to achieve their own hydrogeological model building goals.

While following some standard practises found throughout the literature is important, novel approaches pave new pathways and sometimes improve already well-established practices. Such novel approaches are constructed when faced with limitations that are not cited in the literature. For example, this study did not have historical data to validate the model against. Instead, this study applied synthetic wells of varying conditions to verify the groundwater flow model. Should future studies also lack historical data or other ways to validate their model, this approach may be adopted to verify and continue the study.

Another approach to investigating the groundwater system that this study adopted was to explore and quantify the flow between bedrock and sediment using internal transfer rate budget analyses. Previous understandings of the BBV did not consider bedrock to contribute much to the groundwater system. However, with new observations and results, bedrock appeared to play a larger role than expected. As such, an internal transfer rate budget analysis was performed to explore and quantify bedrock to sediment interaction. This is not a highly cited approach when investigating bedrock

to sediment interaction. Should future researchers find themselves in a similar position of speculating bedrock to play some type of role in the groundwater system, they can adopt this approach.

This study is unique in many ways. It is even unique in flow system across its study area. In other words, depending on where groundwater is being pumped in the study area, the flow system may alter altogether. Specifically, flow systems can alter from preferentially capture-type to overlying aquifers/bedrock-type flow systems. This study found both type of flow systems occurring within the same valley dependant on pumping location. This is an important discovery to the study as optimal pumping locations can be determined based on which flow system is least disruptive to the environment. Future research in or around this area or similar to this study, can also determine changes in flow systems during pumping to further develop their study.

Overall, this study will directly benefit the Towns of Kurikka and Vaasa, by supporting their freshwater demands. The flow model from this study can be used as a tool when making decisions around their freshwater resource. The results from this study can aid in the development of plans and policies to protect and distribute freshwater resources from the Paloluoma BBV.

Chapter 2

Three-Dimensional Hydrogeological Conceptual Model of the Paloluoma Buried Bedrock Valley in West Finland

2.1 Introduction

Groundwater is a critical resource for the Finnish population as 60% of drinking water usage is sourced from aquifers (Kløve et al., 2017). These aquifers vary in type ranging from fractured rocks, which host limited accessible water resources, to unconsolidated granular aquifers, which hold the greatest potential for water supply (Kurki et al., 2013). While these granular aquifers are attractive for groundwater abstraction purposes, high abstraction rates may still lead to unsustainable exploitation of aquifers because sustainability depends also on aquifer replenishment (i.e., recharge from precipitation). It is thus important to understand the groundwater system to assess the sustainability of its exploitation.

One of the first steps to achieve a comprehensive understanding of a groundwater flow system and determine the sustainability of different pumping scenarios is to develop a conceptual understanding of its different components (Kresic & Mikszewski, 2013; Rushton, 2003). The conceptual model of a groundwater system includes the identification of recharge and discharge areas, the definition of aquifer and aquitard units and their related hydraulic properties, the confining conditions of aquifer units, and the main groundwater flow pathways considering the connection and exchange between surface water and groundwater. Estimating hydraulic conductivity and recharge rates can also be achieved at this stage. The conceptual model also forms the basis for the development of a groundwater flow numerical model and its representative boundary conditions (see Chapter 3). A numerical model is critical for investigating the general behaviour of the groundwater system and its response to different pumping rates or changing recharge rates, for instance.

The main purpose of this chapter is to develop a conceptual understanding of the groundwater system within and around the Paloluoma Buried Bedrock Valley (BBV; Fig. 2.1). This system is important since it is targeted to supply water to the towns of Kurikka and Vaasa in Western Finland and possibly other nearby municipalities. While the Paloluoma BBV is recognized to host a productive aquifer system attributed to the geological structure of its subsurface and local weather, a conceptual hydrogeological understanding of the system has yet to be achieved.

Specifically, this chapter aims to develop a conceptual model of the Paloluoma BBV using conventional hydrogeological techniques and datasets such as pumping data, borehole data, and geophysical data. This is the first study in the region in which available geological and physical components are analysed within their hydrogeological context. The specific objectives for the conceptual study are to:

1. Define the watershed and the nature of its flow boundaries.
    - Assess overall groundwater flow pathway.
2. Develop a hydrostratigraphic model of the Paloluoma BBV.
3. Estimate the hydraulic conductivity of each hydrogeological unit.
4. Assess recharge to the granular aquifers and spatial flux across the surface of the Paloluoma BBV.

Historically, the Paloluoma BBV has had widespread artesian conditions, suggesting a promising future of groundwater availability. However, sustainable groundwater extraction cannot be confidently expected with the current understanding. This chapter thus advances the current understanding of the Paloluoma groundwater system. The conceptual model described in this chapter forms the basis for the numerical hydrogeological model, which is described and analysed in the following chapter.

2.2 Study Area

2.2.1 Physiography

The Paloluoma BBV study area is located to the west of the Town of Kurikka, which is currently receiving its drinking water supply from shallow aquifers providing groundwater. The valley spans an area of about 30 km^2 and is bounded by the catchment area of the Paloluoma stream, which runs down from the centre of the study area to its southeastern end where it meets and converges into the larger Kyrönjoki River system (Fig. 2.1).

The Kyrönjoki River spans a length of 225 km across west-central Finland and is fed by many small streams, like the Paloluoma stream. The study area is bounded between northern latitudes of 62º34’30” – 69º39’30” and eastern longitudes of 22º14’0” – 22º23’0”. Topographic highs of up to 190 m asl occur in the northern region, whereas the southern region is characterized by topographic lows at about 70 m asl. Most of the area’s land use is classified as agricultural and forested land.

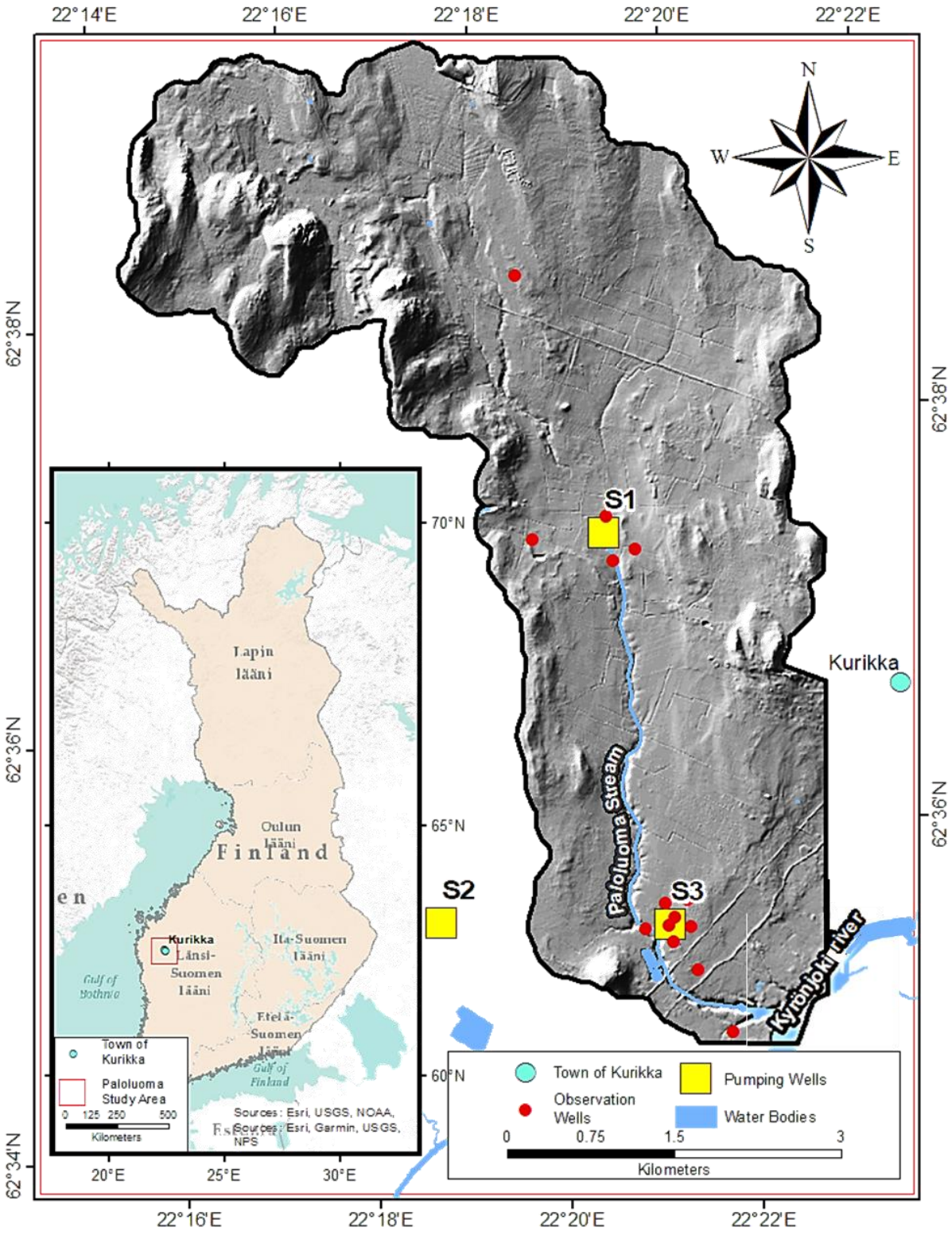

Figure 2.1: Location of the Paloluoma Valley directly west to the Town of Kurikka and physiography of its watershed. Pumping wells S1, S2 and S3 and observation wells are also shown on the map.

2.2.2 Climate

The Paloluoma BBV is located in a subarctic climate zone. The area experiences cold summers and there is no dry season (Dfc Köppen climate classification). Two weather stations (with opensource data made available by the Finnish Meteorological Institute) near the valley were selected to characterize the average monthly precipitation and temperature. Both stations are located in the same area but do not record every parameter during the same timespan. Precipitation data is retrieved from station Kauhajoki Kaupunki and Kauhajoki Kuja-Kokko from 1993-2008 and 2009-2019, respectively. Temperature data is retrieved from station Kauhajoki Kuja-Kokko from 1993-2019.

The average annual temperature and precipitation are 3.3 ^{o}C and 556 mm, respectively. During the winter months (December – March) temperature and precipitation levels average around -6 ^{o}C and 33 mm, respectively. During the summer months (June – August) temperature and precipitation levels average around 14 ^{o}C and 62 mm, respectively (Table 2.1). Figure 2.2 illustrates monthly weather conditions for the Paloluoma BBV area.

Table 2.1: Kurikka monthly weather averages (Source: Finnish Meteorological Institute).

	Jan	**Feb**	**Mar**	**Apr**	**May**	**Jun**	**Jul**	**Aug**	**Sept**	**Oct**	**Nov**	**Dec**
Average Temperature (^{o}C)	-7.8	-8.1	-3.8	2.3	8.4	13.5	15.4	13.7	9	4.2	-1.3	-5.6
Minimum Temperature (^{o}C)	-11.4	-12.2	-8.1	-2	2.6	7.7	10	8.7	4.8	1.2	-3.8	-8.8
Maximum Temperature (^{o}C)	-4.1	-4	0.5	6.6	14.2	19.3	20.9	18.8	13.3	7.2	1.2	-2.3
Precipitation (mm)	36	25	29	31	35	47	64	74	65	54	53	43

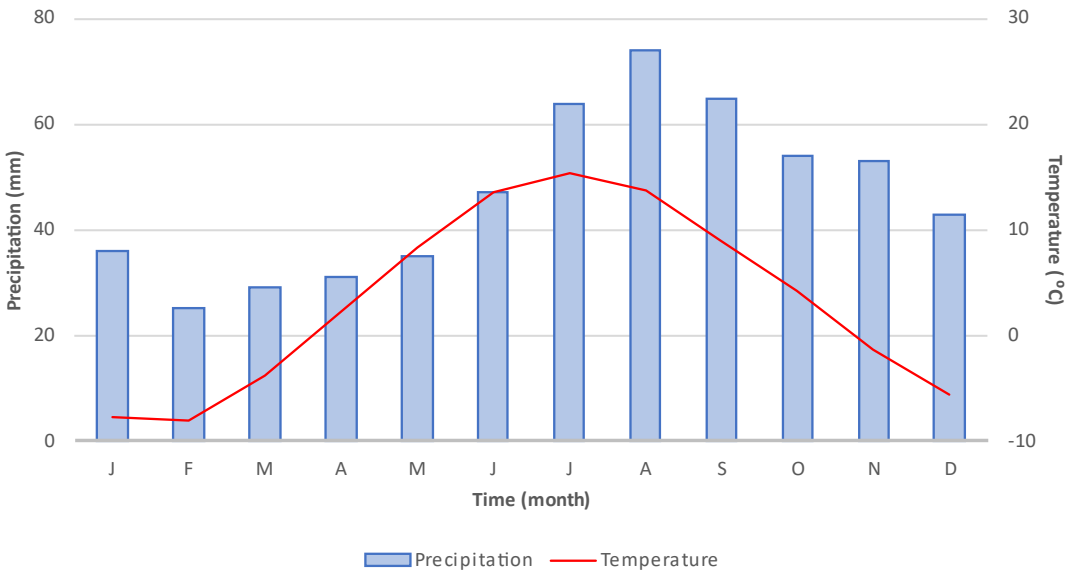

Figure 2.2: Average monthly precipitation and temperature. Data retrieved from Kauhajoki Kaupunki and Kauhajoki Kuja-Kokko Weather Stations.

2.2.3 Geology

The bedrock in the study area is characterized by porphyritic crystalline rocks that are part of the Central Finland Granitoid Complex (Nironen, 2005). Bedrock outcrops are prevalent in the topographic highs of the northwestern portion of the study area and are also present locally along the valley sides as well. Topographic lows are found at the southern end of the study area where the Paloluoma Stream meets the Kyrönjoki River. There, the structure of the bedrock valley opens up to the neighbouring eastern watershed, which significantly contributes to the flow and discharge of groundwater.

Bedrock in the study area is largely covered by more recent (Quaternary; last 2.6 Ma) unconsolidated sediments, especially in the valleys and other depressions. These sediments were deposited during the last glaciation as well as during deglaciation and post-glacial times. These include glacial sediments deposited by processes related to the Fennoscandian Ice Sheet (Punkari, 1997), as well as during deglaciation in proglacial environments (e.g. marine, lacustrine). Deglaciation patterns of the Fennoscandian Ice Sheet varied greatly throughout different regions due to variation in climate, geomorphology, and the type of ice margin (terrestrial or aquatic; (Stroeven et al., 2016). Prominent Fennoscandian features found around Finland include elongated ridges of ice-contact glaciofluvial gravel, sand and silt deposits, namely eskers, and ice-marginal formations (Punkari, 1997; Putkinen et

al., 2017). The specific area of interest is located at an interlobate zone (Fig. 2.3) where adjacent ice lobes merged.

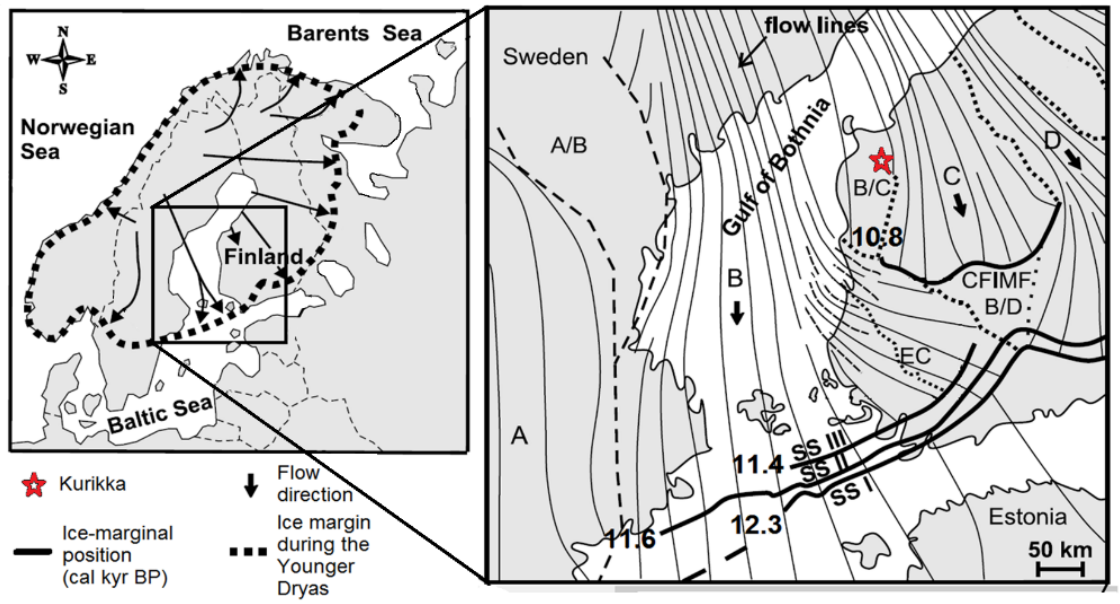

Figure 2.3: Main deglaciation features of southwestern Finland. Map shows ice lobes with flow lines. Letter symbols: (A) Middle Swedish lobe; (B) Baltic Sea lobe; (C) Nasijarvi-Jyvaskyla lobe; (D) Finnish Lake District lobe; (A/B-C/D) interlobe zone/passive ice; (SSI-III) Salpausselka ice-marginal formation; (CFIMF) Central Finland Ice-Marginal Formation; (EC) esker chain. Modified from Artimo et al., (2003) and Stroeven et al., (2016).

Accordingly, the surficial geology of the study area (Fig. 2.4) mainly results from deglaciation of the Fennoscandian Ice Sheet (Boulton et al., 2001). Putkinen et al. (2012) states that several retreat and advance phases of the ice margin in contact with water basins have created a succession of aquifers and aquitards along the Paloluoma BBV, forming a pressurized hydrogeological system. The aquifers are composed of relatively heterogeneous glaciofluvial sediments, which in the study area mostly range from fine sand to coarse gravel. Putkinen et al. continues to describe these aquifer layers to be interstratified with layers of till, which is a well-compacted poorly-sorted sediment (diamictons) of glacial origin (Dreimanis, 1989; Evans et al., 2006; Eyles and Eyles., 2010). Furthermore, Putkinen et al. states that this hydrostratigraphic sequence is buried in the valley and overlain by the lowest permeability aquitards, consisting mostly of silt and clay, which are related to glaciolacustrine and glaciomarine depositional environments. The latter occurred upon ice margin retreat because the area was glacio-isostatically depressed at the time. Glacio-isostatic rebound led to local regression of the sea

in the study area, which created a series of raised beaches and otherwise washed shorelines along the flanks of the local bedrock hills.

A closer look at the surficial geology map of the study area (Fig. 2.4) reveals important clues into the nature and distribution of sediments at the surface. Notably, the centre of the study area predominantly consists of silt and clay material forming a relatively flat plain (Fig. 2.5a), which is only incised by the Paloluoma Stream. The map (Fig. 2.4) also shows that the Paloluoma stream is incised into those silt and clay deposits. Due to the poor permeability characteristic of the stream bed and its surroundings, little to no connection is assumed between the surface stream and groundwater. The northwestern region includes most of the bedrock highs which have been affected by shoreline processes during the marine regressive phase. The surface of the bedrock hills indeed contains raised beaches and washed till which have created several linear ridges of cobbles and boulders (Fig. 2.5b). This northwestern region is thus considered a prominent recharge zone of the study area. South of this area, sandy gravel sediments abound (Fig. 2.5c).

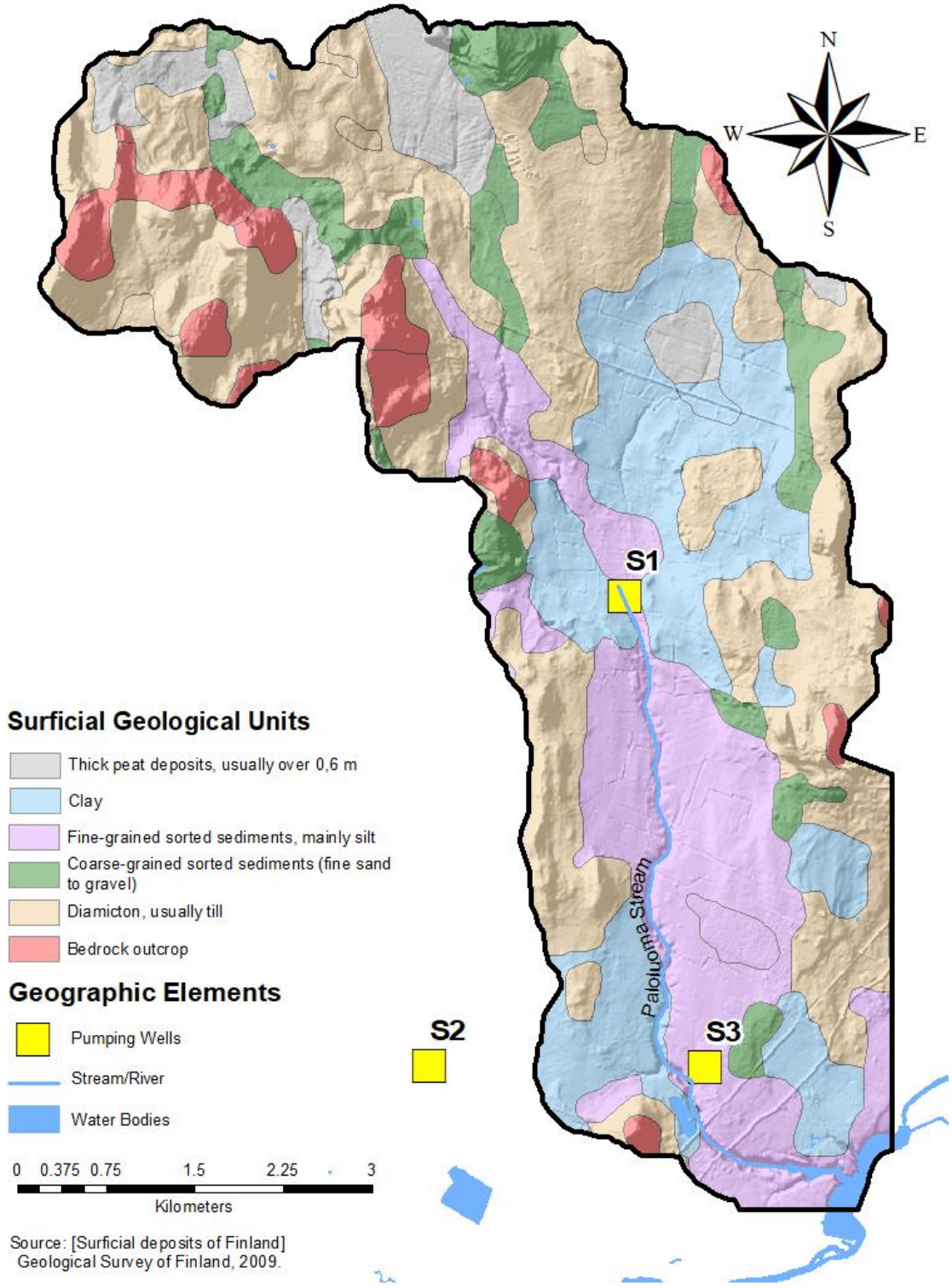

Figure 2.4: Surficial geological map of the Paloluoma Valley study area overlain on top of DEM hillshade model. The surface waterbody, Paloluoma Stream, runs north to south and discharges into the Kyrönjoki River located at the south end of the study area. Pumping wells Siivilä 1 (S1), Siivilä 2 (S2) and Siivilä 3 (S3) are shown on the map. Unit colours are based on the Finnish system for surficial geology.

Figure 2.5: a) Flat central region covered by clay-silt deposits. b) Large portion of the highland study area is predominantly covered with cobbles and boulders. c) Small scale steep sandy slope with low content of organic material. Tree roots and other organic materials are visible.

2.3 Methods

This chapter combines quantitative and qualitative methods in a single large-scale conceptual study. The general workflow for creating the Paloluoma BBV conceptual model (Fig. 2.6) follows current conceptual model building practises in the literature and investigates key components of the system using conventional hydrogeological techniques and datasets (Betancur et al., 2012; Enemark et al., 2019; Kresic & Mikszewski, 2013; Rivera, 2007). Specifically, pumping data, meteorological data, borehole data, and geophysical data all contribute to the building of the conceptual model. From these datasets, hydraulic parameters such as hydraulic conductivity and recharge rate can be estimated and provide a basis for the construction of the hydrostratigraphic model. The key components obtained from this conceptual study are an understanding of the aquifer behaviour, groundwater flow directions, flow boundaries, recharge zones, and the comprehensive hydrostratigraphic structure.

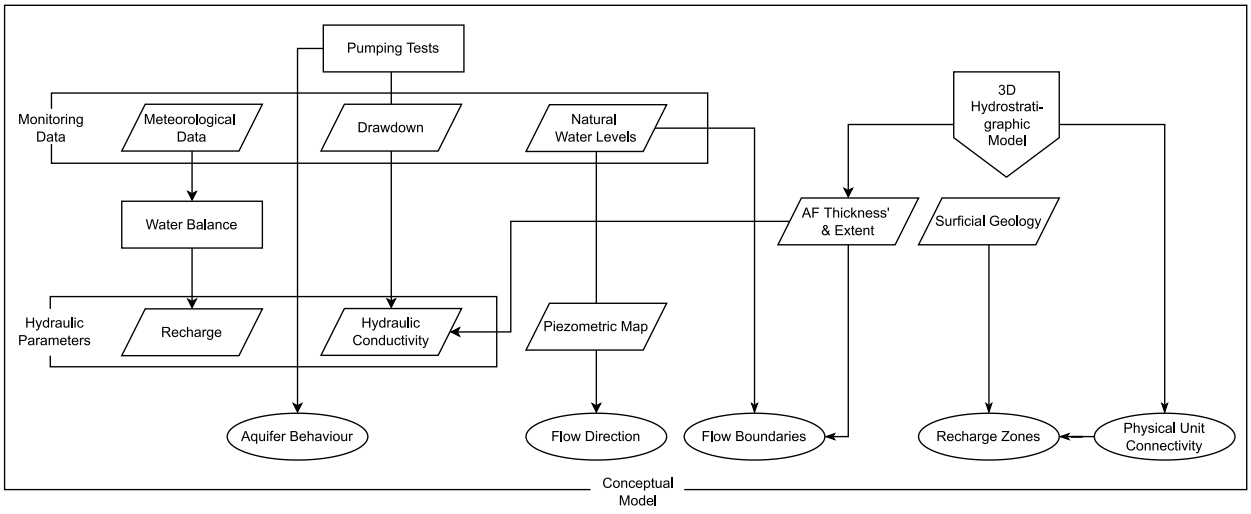

Figure 2.6: Simplified conceptual model flowchart for Paloluoma BBV.

2.3.1 Hydrogeology

2.3.1.1 Watershed Boundaries

The initial watershed boundary that was adopted from the GTK database was delineated according to the upstream area of the Paloluoma Stream. This boundary represents the division between neighbouring watersheds and hosts a deep buried bedrock valley. The northern boundary is characterized by topographic highs and the stream network's headwaters. The southern boundary is characterized by topographic lows and the outlet of the Paloluoma Stream into the larger Kyrönjoki River System. The southeastern boundary (represented in pink as an outflow in Figure 2.7) of the study area is of particular importance because as previously mentioned in the last section, the southern

opening of the buried bedrock valley significantly contributes to the flow and discharge of groundwater. This is because deeper aquifers are continuous and extend beyond the watershed area. Accordingly, the southeastern boundary must provide hydraulic continuity as this is the main subsurface exit for groundwater. An initial numerical model using hydrological boundaries could not be calibrated. As such, the southern boundary was extended to encompass the deeper aquifers to allow for the model to calibrate well. The extent of this exit boundary in terms of depth encompasses all Quaternary sediment material.

The main point for water entry into the steady-state groundwater system is from surficial recharge. Upon groundwater extraction from pumping, water may enter from the sides of the model, which is represented in green as an inflow boundary in Figure 2.7. The extent of this boundary reaches depths to encompass all Quaternary sediment material as well as the top layer of bedrock. A more detailed explanation of both inflow and outflow boundaries is further discussed in Chapter 3.

As mentioned in the previous section, the Paloluoma stream has little impact on overall discharge from the valley. This is due to the fact that the stream flows mostly if not entirely, on very fine-grained, low permeability material. Consequently, there is very limited connection between surface water and groundwater and, as such, the Paloluoma Stream is not considered as a significant boundary.

Figure 2.7 shows the watershed boundaries as described in this subsection as well as the piezometric contours under natural conditions. Water level data from quality observation wells were used to generate the groundwater level contours. These observation wells do not extend everywhere across the study area, especially towards the north. In other words, reliable observed water levels are not available beyond the extent of the interpolated contours. This map will be used to calibrate the simulated groundwater levels, which will be explored in Chapter 3.

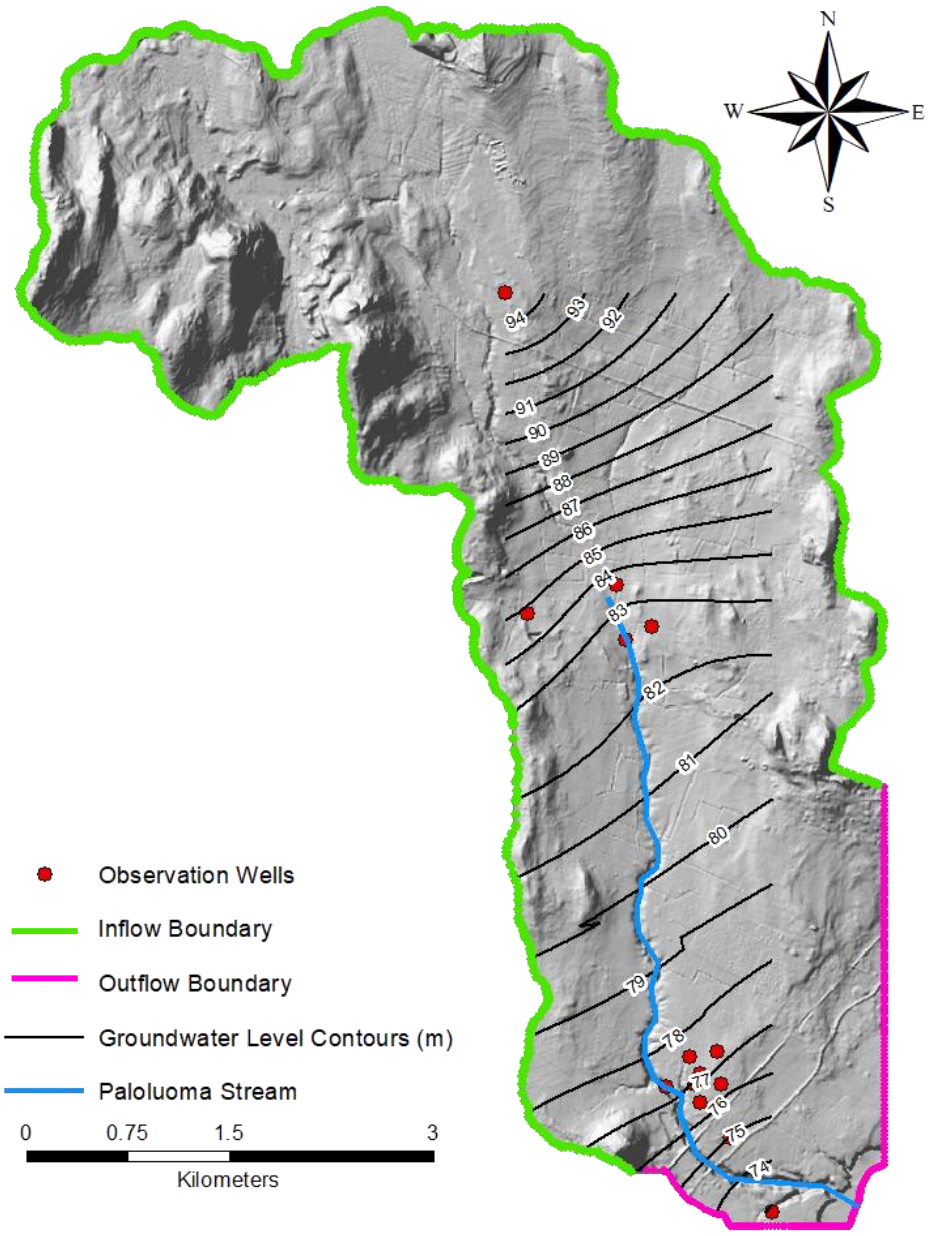

Figure 2.7: Map depicting groundwater levels (m asl). The general direction of groundwater is NW to SE. The pink boundary represents where topographic lows are found and is also where most of groundwater exits from the valley. At this edge, deep aquifers are continuous into the neighbouring eastern watershed. The green boundary represents where water can enter.

2.3.1.2 Hydrostratigraphic Units

Hydrostratigraphy is the classification of subsurface geological layers into laterally extensive units, which can be considered relatively consistent in terms of their hydraulic properties (Maxey, 1964). The stratigraphic framework which is used to define the hydrostratigraphic units (HSU) in the study area

was generated by the Geological Survey of Finland (GTK). The geological units were identified using data from 110 boreholes to bedrock, gravity surveys, and a preliminary 3D geological model built using cross-sections. Borehole data provided sediment type information. Figure 2.8 shows an example of one such borehole. One key procedure was the grouping of multiple geological layers to form one simplified HSU. This was done to focus on the thicker, laterally extensive units, and consisted mainly in eliminating the numerous thin lenses and interbeds of limited lateral extent from the HSU framework. For instance, a till unit containing a few thin interbeds of moderately sorted sand and gravel may form a single homogenous aquitard layer in the HSU framework. Similarly, a thick layer made up dominantly of sandy or gravelly sediment with a few lenses of poorly-sorted sediment or fine-grained sediment may be grouped together and classified as an aquifer. This simplification procedure is used to facilitate the correlation of HSUs across boreholes as most thin layers are discontinuous and thus not traceable from one borehole to the next. Despite these simplifications, the hydrostratigraphic model consists of 14 HSUs and bedrock. Each HSU is defined as a continuous layer of sediment type and hydraulic conductivity, which contrasts to adjacent HSUs located above and below, or laterally.

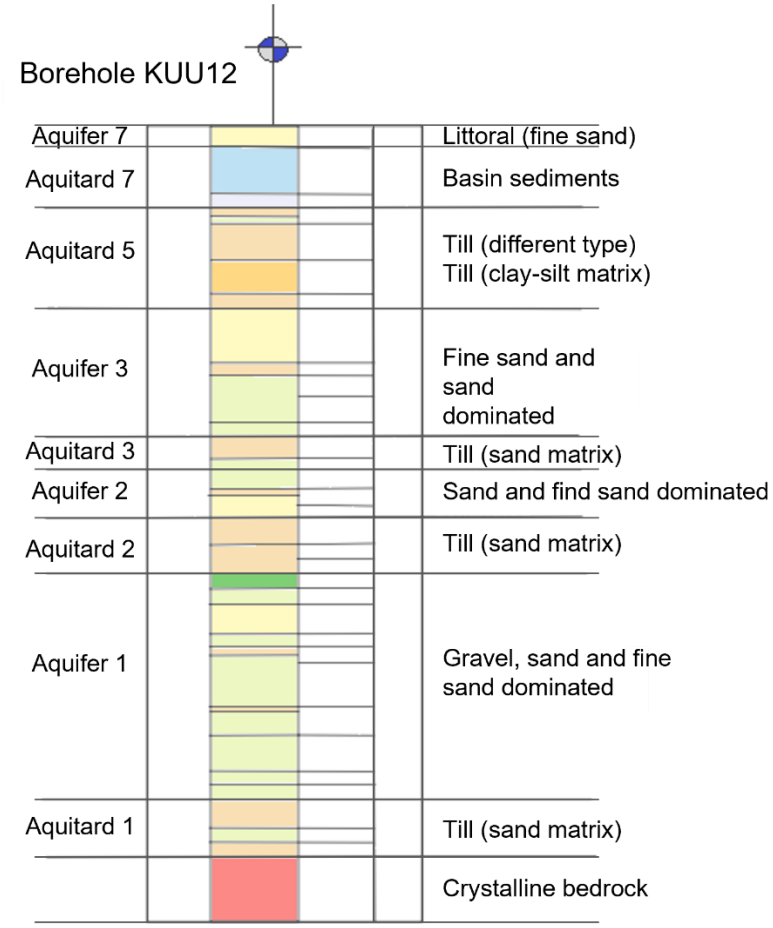

Figure 2.8: Example borehole log from KUU12 location within the Paloluoma valley.

With each unit given hydraulic significance, one bedrock unit, seven aquifer (AF 1-7), and seven aquitard (AT 1-7) units were identified for a total of fifteen HSUs (AF 1-7, AT 1-7, and bedrock) within the model domain. The depositional history of the area, which is controlled by deglaciation patterns, is such that each aquitard unit is subsequently followed by an aquifer unit. However, not all layers exist everywhere, and the thickness of each layer varies throughout the study area. Figure 2.9 shows the conceptual hydrostratigraphic distribution of Quaternary deposits at the Paloluoma BBV. Following the Finnish system of colours, aquifer units are represented in green and yellow, whereas aquitard units are represented in beige, blue, and purple. More details on each of the hydrostratigraphic units' sediment type and description are presented in table 2.2.

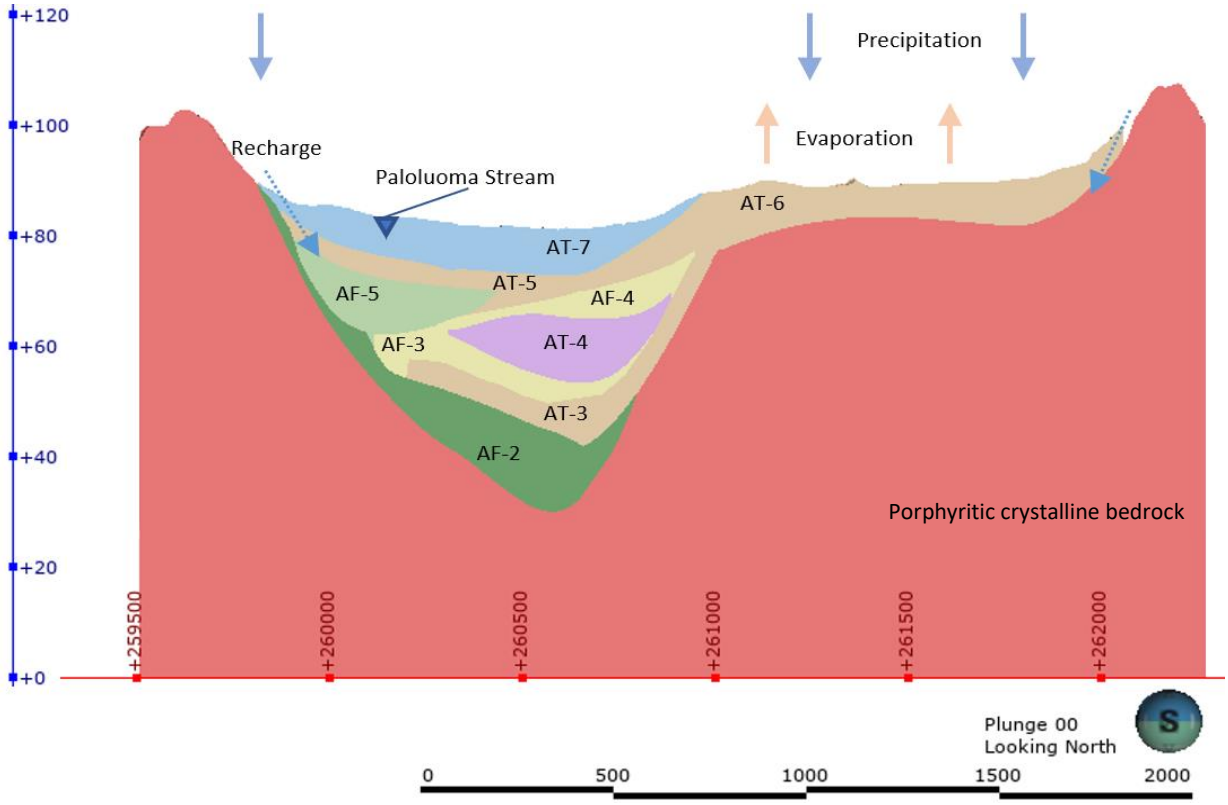

Figure 2.9: Conceptual cross-section of the Paloluoma buried valley. AF- and AT- refers to aquifer and aquitard, respectively. The numbers correspond to the aquifer and aquitard layer. The layers are described in Table 2.2. Vertical exaggeration: 15X.

Table 2.2: Summarized characteristics of the hydrogeological layers. Layers are listed in stratigraphic order. AF- and AT- refers to aquifer and aquitard, respectively. Sediment types in brackets are translated in Finnish notation.

Layer	*Sediment Type*	*Description and Interpretation*
AF-7	Cobbles	Very coarse-grained material, littoral (high energy)
AT-7	Clay (Sa)	Glaciomarine (deeper basinal sediment including clay and fine silt)
AF-6	Coarse Sand (Hk)	Glaciofluvial sediment
AT-6	Till (HkMr)	All types of tills, typically silt-rich at top, last ice advance
AF-5	Coarse Sand (Hk)	Coarse material, sometimes fine-sand
AT-5	Till (HkMr)	Poorly-sorted glacial sediment (diamicton)
AF-4	Fine Sand (HHk)	Coarse- and fine- grained sand from ice contact environment (glaciofluvial)
AT-4	Till (HkMr)	Poorly-sorted coarse material (diamicton)
AF-3	Fine Sand (HHk)	Well-sorted fine sand; proglacial basinal environment (subaqueous fan)
AT-3	Till (HkMr)	Extensive diamicton unit; poorly-sorted and matrix-supported
AF-2	Sandy Gravel (HkSr)	Dominantly coarse-grained (gravel) with minor finer grained material. Some till interlayers
AT-2	Till (HkMr)	Mostly sandy till (diamicton)
AF-1	Sandy Gravel (HkSr)	Coarse-grained (gravel) and sand dominant, some fine sand layers also present
AT-1	Till (HkMr)	The deepest, oldest till, very dense
ROCK	Bedrock (Kp)	Porphyritic crystalline rock

2.3.1.3 3D Hydrostratigraphic Model

Creating a hydrostratigraphic model is standard practise when building a groundwater flow model and analysing the flow system, especially at a regional scale (Bajc & Shirota, 2007; Meyer et al., 2014; Pasanen & Okkonen, 2017; Pétré et al., 2019; Ross et al., 2005; Usman et al., 2018). It is the foundation of the numerical flow model. As such, the quality and performance of the flow model largely depends on the hydrostratigraphic model, which depends on the quality and density/distribution of the data collected. With the stratigraphic framework developed by GTK, and hydraulic information available thus far, data processing and model building were the next steps of the study.

Tools such as geographic information systems and visualization and modelling software can be used to synthesize spatial information as well as interpreting processes (Betancur et al., 2012). The general 3D hydrostratigraphic model building methodology of the Paloluoma BBV is presented in figure 2.10. The hydrostratigraphic model building process was carried out using available data such as borehole logs, bedrock surface, DEM, HSU limits, and other information to compile the valley boundaries and subsurface. Cross-sections constructed in the preliminary model building stage were

used to verify internal consistency of the final three-dimensional geological model used as a basis for the numerical model (Fig. 2.11). The cross-section comparisons can be found in Appendix I.

Also, it is important to note that some consideration must be given when deciding between geological modelling software. Some geological modelling software are more compatible with certain numerical flow modelling tools than others. While knowing that the choice of software for flow modelling in Chapter 3 is FEFLOW (Diersch, 2014), Leapfrog® Geo (Seequent Limited) was chosen for hydrostratigraphic model building. Leapfrog has a built-in hydrogeology module that allows for seamless model exchange to and from FEFLOW. The seamless interaction between the two software allows for easy bridging between the hydrostratigraphic model and the flow model.

The hydrostratigraphic model contributes to an overall better understanding of the subsurface structure and visualization of connection between units. It is one part of the larger conceptual model. At this stage, the characterization of hydraulic parameters for each HSU is important. Integrating parameters such as hydraulic conductivity of aquifer and aquitard units, zones and magnitude of recharge, and overall geometry will produce and help support the required analyses of the flow model as presented in Chapter 3.

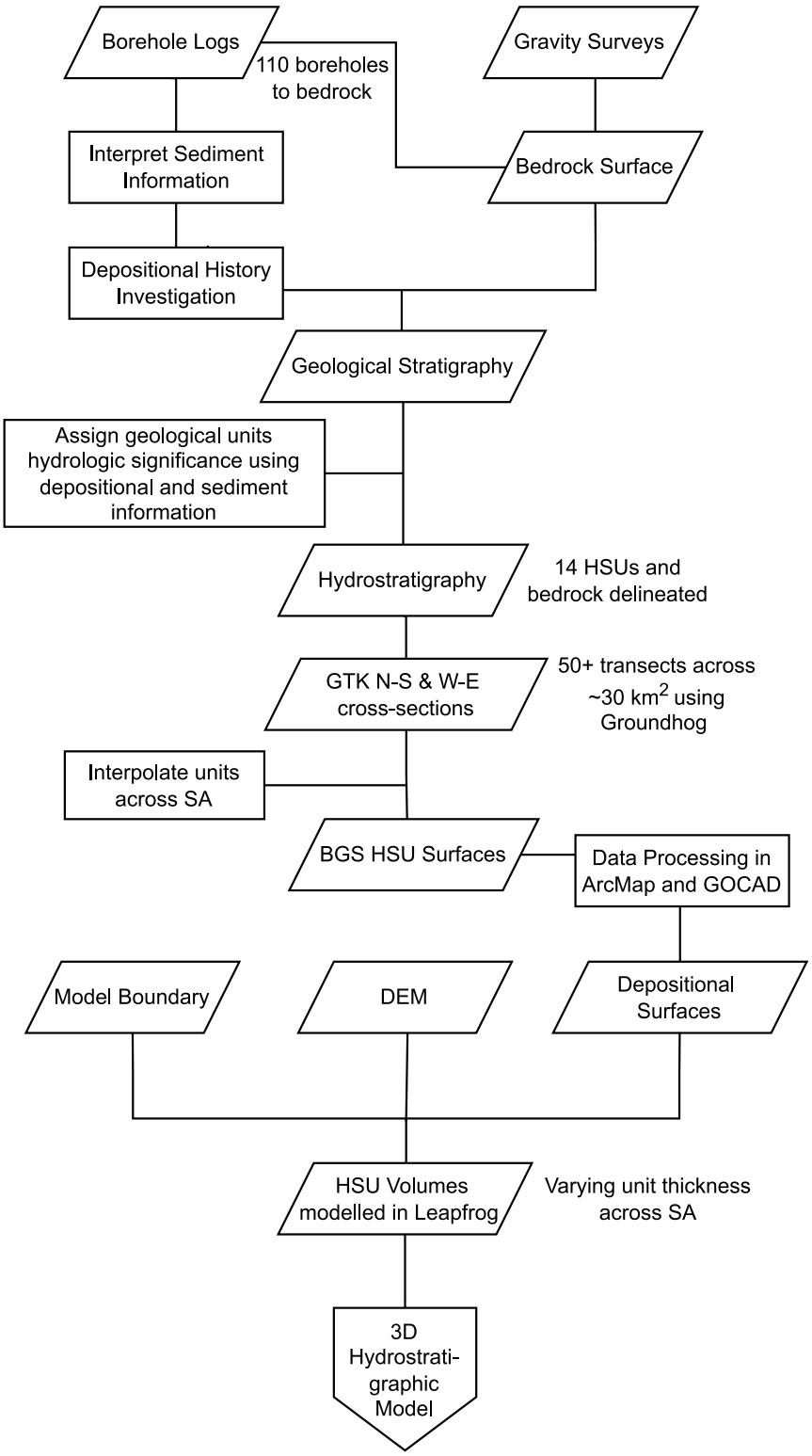

Figure 2.10: Paloluoma BBV 3D hydrostratigraphic model methodology chart. Abbreviations: GTK = Geological Survey of Finland, BGS = British Geological Survey, DEM = digital elevation model, SA = study area, HSU = hydrostratigraphic unit.

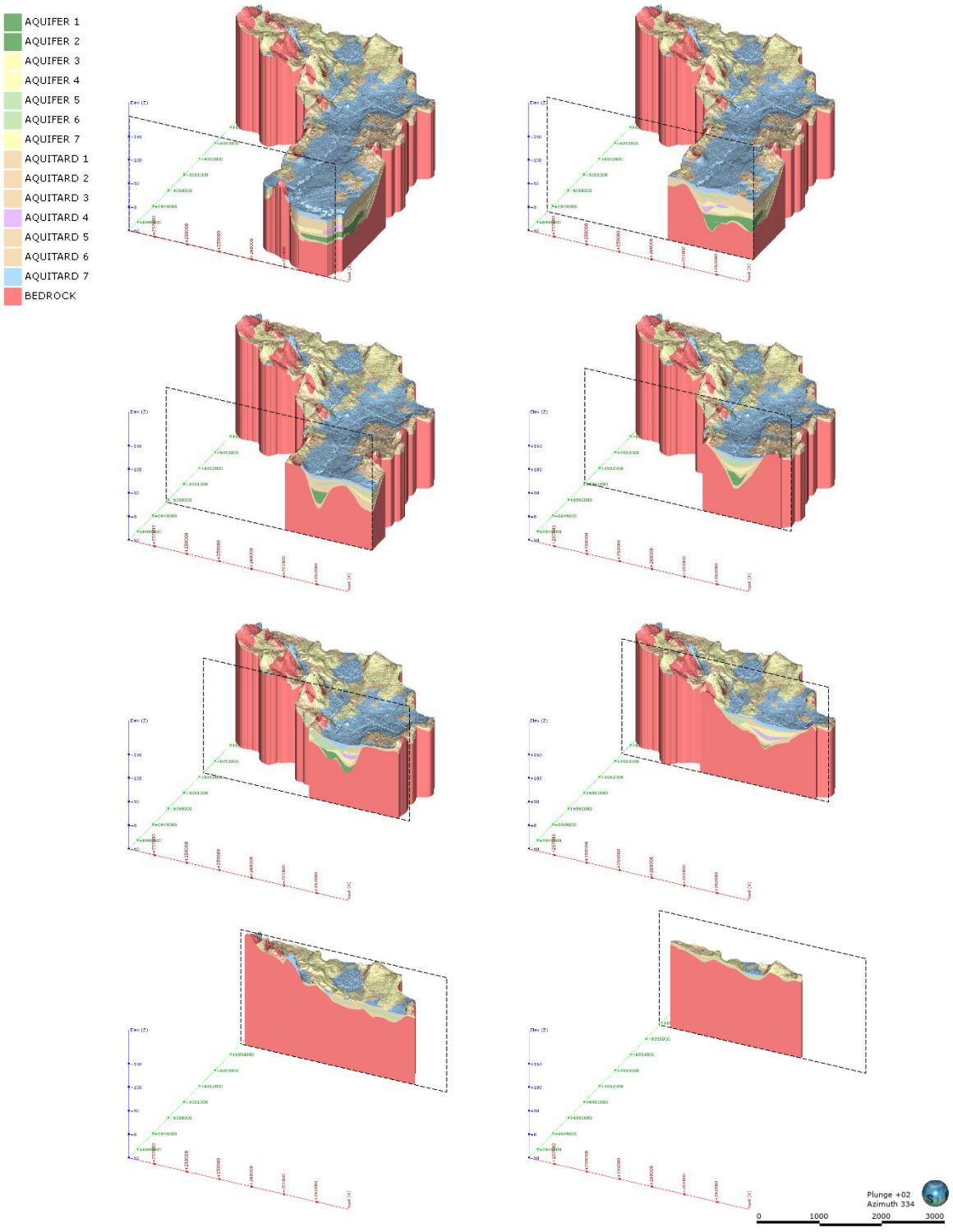

Figure 2.11: The 3D hydrostratigraphic model used to visualize the subsurface architecture of the Paloluoma Valley, which is the framework model of the groundwater flow numerical model developed and analysed in Chapter 3. Slices at intervals of every 1.2 km. Vertical exaggeration: 15X.

2.3.2 Hydraulics

2.3.2.1 Hydraulic conductivity from pumping tests

Pumping tests are an important part of any groundwater study. They provide essential information about the subsurface system such as the hydraulic characteristic of aquifers, yield, drawdown, and aquifer behaviour (Fetter, 2001; Freeze & Cherry, 1979; Kresic, 1997; Kruseman, 1994).

At the Paloluoma BBV, a series of long-term step drawdown tests were performed to assess the aquifer system response at varied rates of stress until the maximum pumping rate is achieved. Data from a 60-well monitoring network was recorded on an hourly basis over increments of 3-month periods for each pumping well. The two pumping wells within the study are named Siivilä 1 and Siivilä 3 and are located at the center and south end of the study area, respectively (cf. Figure 2.4). Pumping from Siivilä 1 occurred from December 17th, 2014 to March 18th, 2015 at varying rates. Pumping from Siivilä 3 occurred from August 16th, 2016 to November 25th, 2016 at varying pumping rates. The pumping schedule is shown in detail in Table 2.3.

Table 2.3: Pumping schedule with progressively increasing pumping rates for step-drawdown test for Siivilä 1 and Siivilä 3.

	Test	**Start Date**	**End Date**	**Days**	**Rate (m^3d^{-1})**
Siivilä 1	1	17.12.2014	7.1.2015	21	1621
	2	7.1.2015	5.2.2015	29	2100
	3	5.2.2015	6.3.2015	29	3166
	Test	**Start Date**	**End Date**	**Days**	**Rate (m^3d^{-1})**
Siivilä 3	1	16.8.2016	27.8.2016	11	1170
	2	27.8.2016	12.9.2016	14	1876
	3	12.9.2016	31.10.2016	49	2363

Pumping in a step drawdown fashion allows the impact of a range of pumping rates on the groundwater system to be analysed. After each step-test and once water levels were stabilized, the water level was recovered before continuing with the next step test (Fig. 2.12). These large-scale step-tests are analysed using conventional type-curve fitting methods to estimate transmissivity and storage information and ultimately hydraulic conductivity (Cooper & Jacob, 1946; Hantush, 1959; Theis, 1941). It is important to keep in mind the assumptions that go along with each type-curve method.

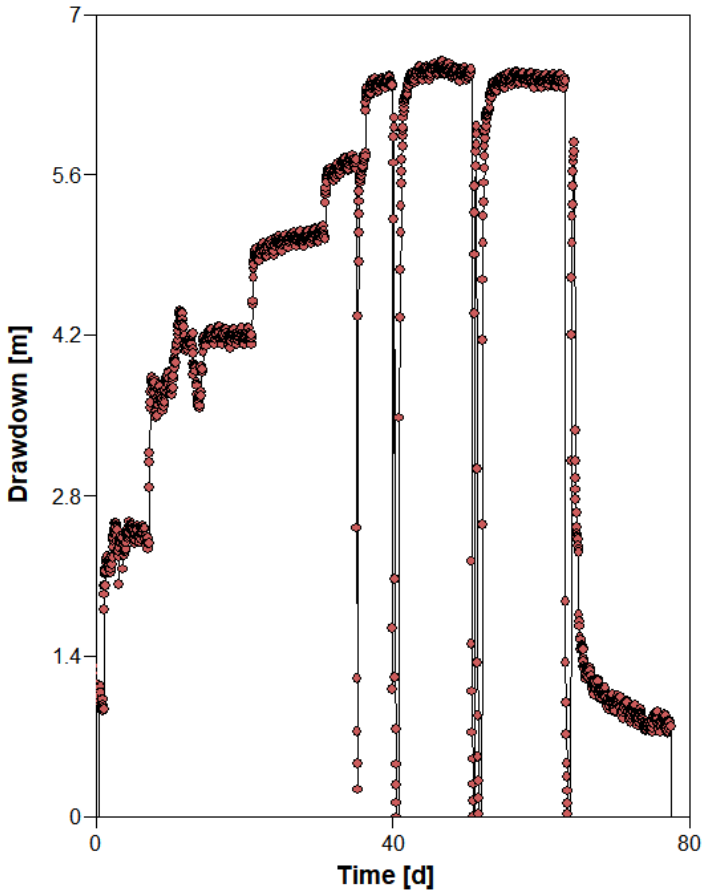

Figure 2.12: A series of step-drawdown pumping tests performed at Siivilä 1. Pumping is continued until water levels stabilize and recovery is reached before the next step-test.

Pumping test analysis began with an initial fit using the Cooper-Jacob solution and was followed by a Theis solution fit (Fig. 2.13) using the Cooper-Jacob transmissivity and storage (Cooper & Jacob, 1946; Theis, 1941). The Theis solution assumes that all the water is pumped from storage within the aquifer. Upon analysis, the Theis solution did not entirely fit the data, as observed in Figure 2.13. Instead, the data more accurately fit the Hantush solution, which assumes a leaky confined aquifer. This means that the aquifer of interest could possibly receive leakage across confining beds from other aquifers or other sources like bedrock fractures.

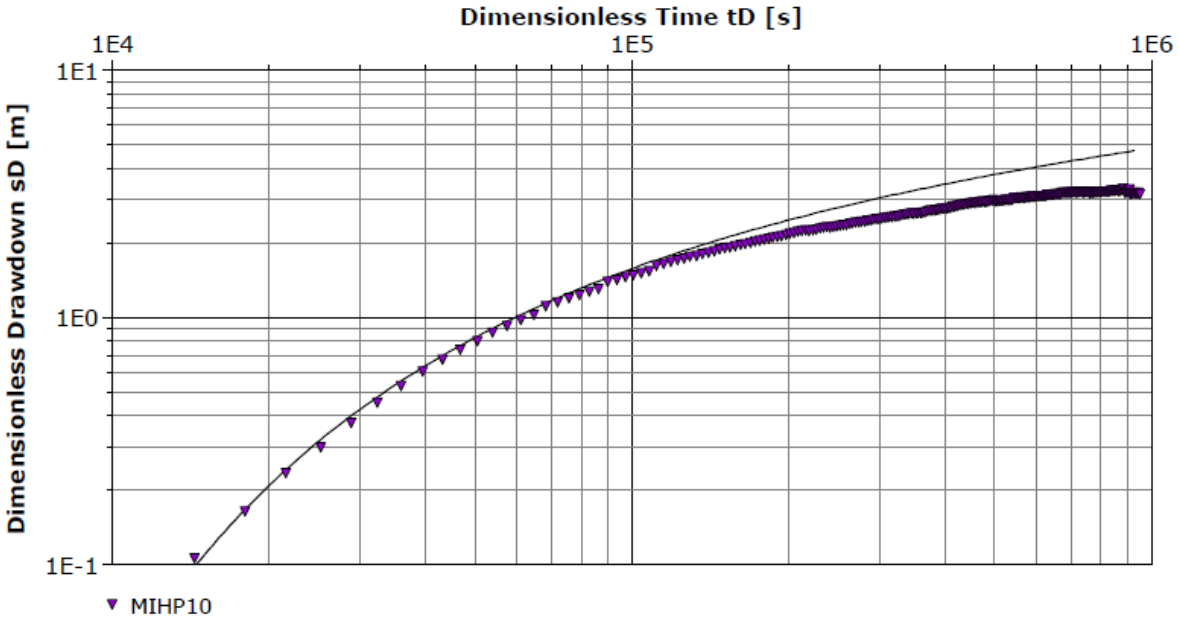

Figure 2.13: Drawdown period from observation well, MIHP 10, during pumping at Siivilä 3. Results show that the Theis solution (solid line) is not entirely matched with observed well data. Data suggests a leaky nature that better fits the Hantush solution.

2.3.2.2 Hydraulic conductivity based on sediment type

Another method to determine sediment-hydraulic characteristics of aquifers is through analysing the characteristics of sediments that affect their hydraulic conductivity, a technique referred to as hydrofacies characterization or analysis. The purpose of a hydrofacies analysis in this study is to determine the range of realistic hydraulic conductivities consistent with sediment characteristics such as grain size and overall sorting. This method was used to set minimum and maximum constraints for the hydraulic conductivities of the aquifers and aquitards at the time of calibration. The hydrofacies were determined by analysing data and descriptions from high-quality borehole logs and identifying primary, secondary, and tertiary sediments based on most common to least common sediments within each unit. The International Sediment System (ISO 14688-1:2002), in which the boreholes were described by, was rendered to the American Sedimentary System based on the Udden-Wentworth scale (Table 2.4). Using the Udden-Wentworth scale definition for the grain size of each sediment type, the conductivity values were then determined according to the American sedimentary materials (Domenico & Schwartz, 1990), which is commonly used when relating sediment type to hydraulic conductivity. The hydraulic conductivity of each HSU was constrained on the basis of their range of conductivity values from their

dominant sediment material (Freeze & Cherry, 1979). At the time of calibration to optimize the conductivity value, the minimum and maximum values will be valuable to refer to as limits.

Hydraulic conductivity analysis for bedrock and aquitard units was not available from pumping tests, thus they were solely estimated using their lithological information. As previously described, most aquitards within the Paloluoma BBV predominantly share the same sediment characteristics (till). Therefore, these aquitard units share the same hydraulic conductivity, which also helps simplify the model. In this chapter, bedrock hydraulic conductivity is initially also assumed to be isotropic. However, this is further explored and discussed in Chapter 3. Hydraulic conductivity estimates and constraints for each unit are presented in the next section.

Table 2.4: Summary of hydrofacies of the primary sediment types used to define the HSU framework. The Finnish International Sediment System (ISO 14688-1:2002) is translated to American Sediment System for relating conductivity information to sediment material. Sources: International System: ISO 14688-1:2002, American Sedimentary System based on Udden-Wentworth scale, K values according to American sedimentary materials: Domenico and Schwartz (1990) and Freeze and Cherry (1979).

Finnish (International) System			
Sediment	**Size**	**Symbol**	**Grain Size (mm)**
Gravel	Coarse Gravel		6-20
	Fine Gravel	SrHk, Sr	2-6
Sand	Coarse Sand	Hk, KeHk	0.6-2
	Fine Sand	HHk	0.2-0.6
Fine-Sand	Coarse Fine-Sand		0.06-0.2
	Fine Fine-Sand	Si	0.02-0.06
Silt	Coarse Silt		0.006-0.02
	Fine Silt	SaSi	0.002-0.006
Clay		Sa	<0.002
Till	Sandy Till	HkMr	
	Silty Sandy Till	SiHkMr	
	Silty Till	SiMr	
	Clay Till	SaSiMr	

American System		K (m/s)	
Sediment	**Grain size (mm)**	min	max
Gravel	2-64	3.00E-04	3.00E-02
Coarse Sand	0.5-2	9.00E-07	6.00E-03
Medium Sand	0.25-0.5	9.00E-07	5.00E-04
Fine Sand	0.0625-0.250	2.00E-07	2.00E-04
Silt	0.0039-0.0625	1.00E-09	2.00E-05
Clay	0.0039-0.00098	1.00E-11	4.70E-09
Till		1.00E-12	2.00E-06

2.3.3 Recharge

It is difficult to estimate groundwater recharge reliably using any one single method due to uncertainties and limitations of each method (Scanlon et al., 2002). Therefore, often recharge is estimated using multiple methods to cross-check the results and constrain the values obtained (Rivard et al., 2014). Accordingly, both a water balance and groundwater flux analysis are performed to estimate groundwater recharge of the Paloluoma BBV.

2.3.3.1 Water Balance Method

Performing a water balance is standard practise when estimating recharge (Healy, 2010; Lefebvre et al., 2011; Misstear et al., 2009; Rivard et al., 2014). For the purposes of this study, hydrometeorological data such as monthly precipitation and temperature were obtained from the Finnish Meteorological Institute [en.ilmatieteenlaitos.fi] over a 15-year period, which was collected from the nearby weather station, Kauhajoki Kuja-Kokko Weather Station. The water balance was conducted on a monthly basis, from 2004 to 2018.

According to the recharge definition where only water reaching the water table is considered as recharge, key parameters were identified to calculate total recharge and include runoff (*R*, mm, Eq. 1), infiltration (*Peff*, mm, Eq. 2), potential evapotranspiration (*ETP*, mm. Eq. 3) according to the Thornthwaite method (1944), soil humidity deficit (*D*, Eq. 6), real evapotranspiration (*ETR*, mm, Eq. 7), and readily available water in soil (*RAS*, mm).

Runoff was calculated according to the following Equation (1):

$$R = P_{acc} * Cr \quad (1)$$

Where, P_{acc} is accumulated precipitation in units of mm, which accounts for all winter precipitation available for spring thaw, as well as monthly summer precipitation; and *Cr* is the runoff coefficient.

Infiltration was calculated according to the following Equation (2):

$$P_{eff} = P_m - R \quad (2)$$

where, P_m (mm) is the monthly precipitation; *R* (mm) is runoff as described in Eq. 1.

Potential evapotranspiration according to the Thornthwaite method (1944) was calculated using the following equations (3) – (5):

$$ETP = 16 * F(\lambda) * \left(10 * \frac{Tm}{I}\right)^a \quad (3)$$

$$I \sum_{n=1}^{12} i \text{ where } i = \left(\frac{Tm}{5}\right)^{1.514} \quad (4)$$

$$a = (675 * 10^{-9} * I^3) - (771 * 10^{-7} * I^2) - (1792 * 10^{-5} * I) + 0.49239 \quad (5)$$

where *F(λ)* is the latitude-dependent correction factor accounting the number of days in the month and the actual number of hours of insolation; *I* is the annual heat index; *a* is a coefficient strictly proportional to *I*.

Soil humidity deficit was calculated according to the following Equation (6):

$$D = RAS_{i-1} + P_{eff} - ETP \quad (6)$$

Where, *RAS* is the readily available water in soil in units of mm and is dependent on *D* such that if *D* is greater than the RAS_{max} value, the *RAS* will be the RAS_{max} value. However, if *D* is less than the RAS_{max} value, then the *RAS* will be equal to *D*. Otherwise, if *D* is less than or equal to 0, the *RAS* value will be 0. Parameters *Peff*, which is infiltration, and *ETP*, which is potential evapotranspiration, are described in Equation (2) and (3), respectively.

Finally, using the definition where infiltration reaches the water table, recharge (ΔSg, mm) was calculated using the following Equation (7):

$$\Delta Sg = D - RAS \quad (7)$$

Where soil humidity deficit, *D*, and readily available water in soil, *RAS*, have been described in Equation (6).

2.3.3.2 Groundwater Flux

The groundwater flux method was also used to estimate total recharge over the study area as a means to provide additional support to the findings from the water balance method. Groundwater flux through the aquifer (Q_a, mm), is calculated using the following Equation (8):

$$Q_a = A_x * K * i \quad (8)$$

Where, A_x (m^2) is the cross-sectional area of flow and is a function of the valley width and aquifer thickness; *K* (ms^{-1}) is the hydraulic conductivity of the aquifer; *i* is the hydraulic gradient.

Recharge *(*ΔSg, mm) as a function of the groundwater flux through the aquifer (Q_a) and the recharge area (A_r, mm) can be calculated using the following Equation (9):

$$\Delta S_g = Q_a / A_r \quad (9)$$

Field observations were used to determine hydraulic gradient and subsurface information was used to determine aquifer thickness and hydraulic conductivity. Results of the total recharge rate from the groundwater flux method are presented in the following section.

2.3.3.3 Spatial Distribution

The total recharge rate, as estimated from the water balance and groundwater flux methods, was distributed over the entire study area according to surface permeability derived from surficial geology information. The surficial geology of the study area (Figure 2.4) is here given hydrogeological significance by categorizing all the units into only two categories: good permeability areas and poor permeability areas. For example, sandier areas as represented in green on the surficial geology map, are sorted sediments considered to be permeable. In contrast, clay and silt, which are represented in blue and purple, respectively, are fine-grained sediments that are less permeable. Dividing the study area into permeable and less permeable zones was determined by taking the 3D hydrogeological model and analysing aquifer unit locations on the surface. Figure 2.14 depicts the recharge zone map in accordance with surface unit permeability. These permeability areas were then assigned a proportion of the total recharge rate in which the area would allow inflow to occur. Permeable zones accounted for 80% of total recharge, whereas less permeable zones accounted for 20% of total recharge. Using the minimum and maximum recharge rates obtained from the water balance method, a maximum and minimum recharge rate was calculated for each type of permeability zone. This range of recharge is especially useful when calibrating the model (see Chapter 3).

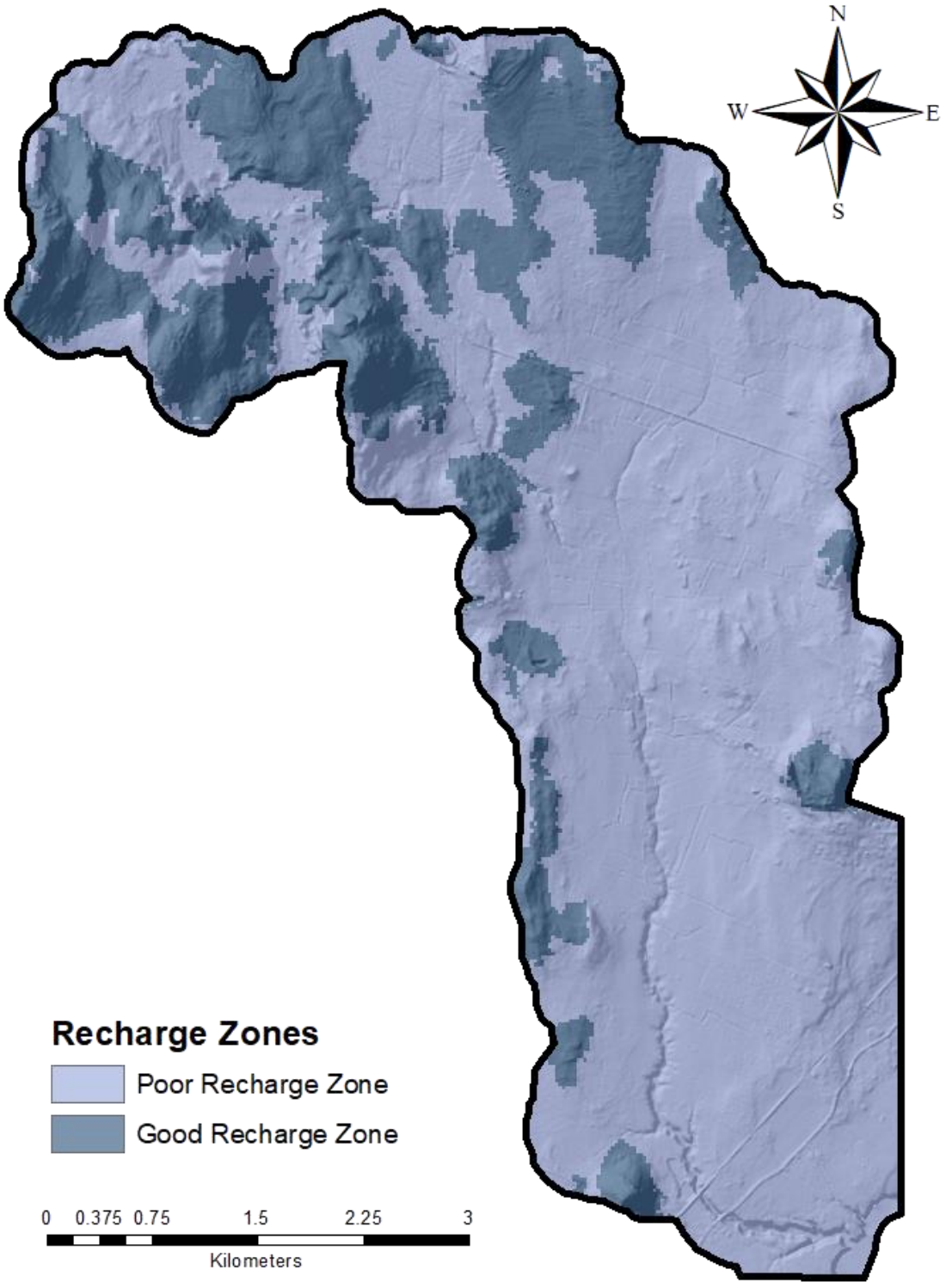

Figure 2.14: Map depicting good and poor recharge zones according to permeable and less permeable areas, respectively. Good recharge zones are predominantly found in the northern region of the study area.

2.4 Results

2.4.1. Hydraulics

From pumping tests, as described earlier, hydraulic conductivity values for aquifer units are of 10^{-4} to 10^{-3} orders of magnitude. Matched curve plots from pumping test analysis are included in Appendix II and III. Table 2.5 shows the exact hydraulic conductivity value obtained from pumping tests for each aquifer HSU as well as the range of hydraulic conductivity possible for the hydraulic unit corresponding to their dominant sediment material (cf. Table 2.4). Hydraulic conductivity analysis for aquitard units was not available from pumping tests, thus it is solely estimated using lithological information. Aquitards 1-7 are grouped together when considering hydraulic conductivity as most share the same sediment characteristics (till) except for the upper most glaciomarine aquitard (clay). Nonetheless, hydraulic conductivity for all aquitards falls closely within the range of values considered. Thus, aquitard units are assigned a hydraulic conductivity value of 2.0E-7 ms^{-1} with a range from 1.0E-12 ms^{-1} to 2.0E-06 ms^{-1}. Values from Table 2.5 are for conductivity in all x-, y-, z-directions as it is assumed the hydrofacies are isotropic. Bedrock hydraulic conductivity is initially also assumed to be isotropic at 2.0E-7 ms^{-1}. However, this is further explored and discussed in Chapter 3.

Table 2.5: Hydraulic conductivity value for each hydrogeological unit in the Paloluoma BBV system estimated using pumping tests (Value). Maximum and minimum hydraulic conductivity are estimated from hydrofacies descriptions. Hydraulic conductivity range for bedrock aquitards estimated from geological information.

HSU	**Hydraulic Conductivity (ms^{-1})**		
	Minimum	**Value**	**Maximum**
AF-7	1.0E-03	2.6E-03	1.0E-01
AF-6	9.0E-07	2.0E-03	6.0E-03
AF-5	9.0E-07	6.4E-04	6.0E-03
AF-4	9.0E-07	4.4E-04	5.0E-04
AF-3	9.0E-07	5.2E-04	5.0E-04
AF-2	3.0E-04	2.9E-04	3.0E-02
AF-1	3.0E-04	3.3E-04	3.0E-02
AT- 1-7	1.0E-12	2.0E-07	2.0E-06
BEDROCK	1.0E-12	2.0E-07	1.0E-05

2.4.2. Recharge

Recharge was estimated using two methods, the water balance method and the groundwater flux method. Analysis of the water balance method revealed the minimum total recharge rate, which was found to be approximately 35 mm/a, and the maximum total recharge rate, which was found to be approximately 150 mm/a. This range is applied as a parameter constraint for recharge during calibration. The average total recharge rate found over the 15-year period is approximately 80 mm/a. The varying rates of recharge have been depicted in Figure 2.15. Uncertainties in the water balance method include uncertainties in variables, particularly precipitation and temperature. Error in measurements could be from the type of data collection method employed. Sources of errors to consider when collecting precipitation include wind levels causing precipitation to not fall directly into the measuring instrument, which could cause data not to be registered accurately. High wind levels also contribute to evaporation, especially if the collected precipitation is at a standstill for long periods. High temperatures can also prompt evaporation and cold temperatures may cause frozen precipitation, which makes data collection more difficult.

The groundwater flux method, as described earlier, utilizes field observations to determine hydraulic gradient and subsurface information to determine aquifer thickness and hydraulic conductivity. Using this secondary method, the total recharge rate over the 30 km^2 study area was found to also be approximately 80 mm/a. These results from the groundwater flux method are thus consistent with the results from the water balance method.

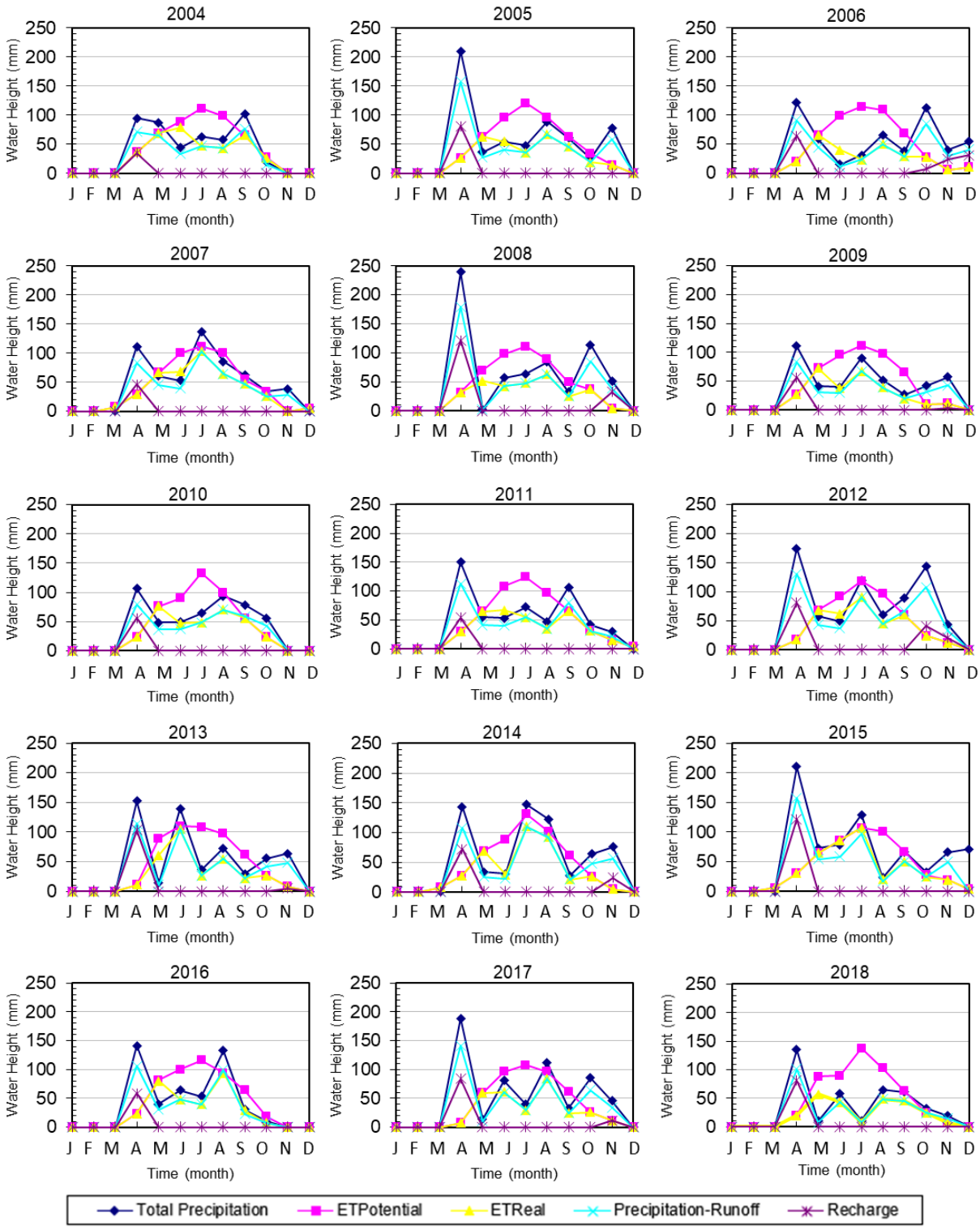

Figure 2.15: Water balance for Paloluoma Valley over a 15-year period (2004-2018). Plots show estimated recharge (mm) represented as the purple star.

2.5 Discussion

The foundation of model analysis is the conceptual model. The conceptual model emphasizes understanding the system before its analysis (Betancur et al., 2012; Bredehoeft, 2005; Rushton, 2003). It represents the hydrogeology and groundwater system required to create the desired flow model. Previous studies demonstrate the process of conceptual model building well (Bajc et al., 2018, 2014; Blackport et al., 2014; Meyer et al., 2014; Hendry et al., 1991; Pétré et al., 2016). In this section, the Paloluoma BBV conceptual model is summarized.

There is great interest surrounding sustainable extraction of the Paloluoma BBV groundwater resource. Prior to increased exploitation, hydrogeological conceptualization of the study area is required to improve the understanding of the system and provide useful quantitative analysis of the groundwater flow system. The conceptual model developed in this Chapter is an important part of the groundwater model building process. The conceptual model has characterized the hydrogeological boundaries, properties, and processes, which are crucial to our hydrogeological understanding of the system. Field investigations, data analysis, and model building have all greatly contributed to the conceptual model.

One of the main points resulting from the conceptual model is the general North to South direction of groundwater flow within the Paloluoma BBV. The main waterbody is the Paloluoma stream, which runs down the watershed area to reach the larger river system, the Kyrönjoki River, located at the south end of the study area. There is minimum interaction between surface water bodies and subsurface units. This is because surface water streams flow on relatively thick and continuous clay and silt deposits, which act as a barrier between surface and subsurface waters. This is found to be true in the central and southern regions of the study area. As for the northern region of the study area, there are small springs that are fed by groundwater.

Congruent with the topography, surficial geology, and field observations, the main recharge zones are found to be located in the north and northwestern regions of the study area. The northwest region of the study area has topographic highs, bedrock outcrops and surficial coarse-grained sediments, which are considered good recharge zones. The central and southern regions of the study area, where the surficial geology is predominantly clay and silt, are considered poor recharge zones.

A hydrogeological water balance, which is standardly used to determine recharge rates was applied for this study using hydrometeorological data from a nearby weather station, Kauhajoki Kuja-Kokko. Recharge rates were also estimated using the groundwater flux method to support findings from the first water balance method. Different data collection methods have different sources of error.

Therefore, it is important to verify output variables using multiple techniques. These simple recharge estimation methods resulted in an average recharge rate of approximately 80 mm/a. This pre-calibrated rate was spatially distributed accordingly across good and poor recharge zones within the study area.

Aquifer behaviour for the Paloluoma BBV can be understood through pumping tests. From pumping test analysis, a positive boundary limit was identified. This positive boundary limit suggests that the aquifer that was being pumped, is recharging or receiving water outside of storage. As such, the observed drawdown closely matched the Hantush solution, which gives us important information that the aquifers are of a leaky confined nature. This leaky flow behaviour into the aquifers can be partially explained using the geological model. It is suspected that there could be an external source outside of storage in which exploited aquifers are receiving replenishment. Such external sources could be from bedrock fractures providing recharge to the aquifers, or other aquifers leaking across interbedded aquitards. Analysing the hydrostratigraphic model, partial flow pathways between aquifers can be interpreted to be present on account of direct vertical unit connectivity in the central region of the study area between aquifers two and five. This suggests that flow from shallow aquifers to deep aquifers is possible. Further exploration of the study area using geophysical instruments has also led to the identification of permeable structures within the bedrock (pers. Comm, Timo Ruskeeniemi, GTK, February 1st, 2021 at 10:30 a.m. EST), which supports earlier suspicions and could also greatly contribute to the leaky flow behaviour found during pumping test analysis.

Creating a hydrostratigraphic model (Fig. 2.11) using subsurface geological information is standard practise when building a flow model, especially at a regional scale (Bajc & Shirota, 2007; Meyer et al., 2014; Pasanen & Okkonen, 2017; Pétré et al., 2019; Ross et al., 2005; Usman et al., 2018). The hydrostratigraphic model contributes to an overall better understanding of the subsurface structure and visualization of connection between units. The structure of the bedrock valley and Quaternary sediments is also useful when analysing modelling results. Since the flow model is heavily dependant on the hydrostratigraphic model, any changes that are made to the hydrostratigraphic model, must be reflected on the flow model. With constant updates from both the structure of the hydrostratigraphic model, as well as updates from the post-run flow model requiring improvements, there is considerable interplay between the hydrostratigraphic model and flow model. As such, hydrologically important areas of the model that were not initially appreciated, have been integrated leading to important improvements to both the conceptual understanding of the system and the flow model itself.

2.6 Conclusion

The purpose of this study was to develop a conceptual model of the Paloluoma BBV. This was successfully accomplished through evaluating watershed and flow boundaries, developing a hydrostratigraphic model of the Paloluoma BBV, and assessing recharge to the granular aquifers and spatial flux across the surface of the Paloluoma BBV. The comprehensive approach that is used in this study to build a conceptual model for the Paloluoma BBV can be applied to characterization and quantification studies of other similar regional aquifers. Being the first study of its kind in the region, future research around this region can be supported with this study.

With the current conceptual understanding, important questions about the function of the system persist. For example, what are the flow dynamics under natural conditions, what are the changes to flow dynamics under pumping conditions, where and how far does drawdown extend, and how does the system react with varying pumping scenarios? These questions and additional investigations can be explored using the numerical model that accompanies the 3D hydrogeological model. This leads us into the significant characteristics of the flow model, which are discussed in the next chapter.

Chapter 3

Numerical Groundwater Modelling of the Paloluoma Buried Bedrock Valley in West Finland

3.1 Introduction

The Paloluoma Buried Bedrock Valley (BBV) contains granular aquifers that have been targeted to supply drinking water to the surrounding population (Putkinen et al., 2015, 2018). Currently, production wells are used for drinking water purposes for the Town of Kurikka. Other nearby municipalities have expressed interest in exploiting the same aquifer to supply for their own, much larger towns. With the increased demand, the response of the aquifer under varying and increased pumping scenarios and changes to the dynamic of the aquifer system must be analysed thoroughly to ensure sustainable management of the resource.

Prior to increased groundwater abstraction, safe long-term sustainable pumping rates must be determined. Otherwise, as historically observed, the system and surrounding environment may experience detrimental effects (Konikow & Kendy, 2005; Sophocleous, 2010; Vélez-Nicolás et al., 2020). In order to determine safe rates of groundwater abstraction, a good understanding of the groundwater system is required. This includes an overall conceptual understanding of key components of the system such as the hydrostratigraphic sequence, recharge and discharge areas, aquifer behaviour, and flow dynamics. These key components have been explored in the previous chapter, Chapter 2 – Conceptual Model. This chapter describes the constructed groundwater flow model and uses the conceptual model to further the investigation and understanding of the groundwater system. Specifically, the flow model investigates flow dynamics under natural and pumping conditions, hydraulic response to pumping events, drawdown distribution, and changes in fluxes. These results are then used to define the conditions required for sustainable groundwater extraction.

Through the development of the flow model, important uncertainties will likely be identified about the characterization of the Paloluoma BBV. Additional gaps in knowledge may be highlighted, especially since this is the first quantitative study of its kind in this region. Future field investigations could be carried out to reduce the main uncertainties. With an improved understanding of the Paloluoma BBV groundwater flow system, which is heavily depended on for drinking water, sustainable

water management can be implemented. As such, the nearby municipality of Kurikka will be able to ensure the long-term protection of its freshwater resource.

3.1.1 Study Area

The Paloluoma BBV watershed has an areal extent of 30 km^2 and is located west of the Town of Kurikka in West Finland. Its watershed boundaries are governed by the upstream area of the Paloluoma Stream. This region exhibits a subarctic climate and is classified as Dfc (D: continental, f: without dry season, c: cold summer) in accordance with the Köppen-Geiger climate classification system (Peel et al., 2007). The average annual temperature and precipitation levels are 3.3 ^{o}C and 556 mm, respectively. The topography includes hills and valleys with elevation ranging from 190 m asl in the northern area, where there are bedrock outcrops, to about 70 m asl in the southern area. The southern area is characterized by the union of the Paloluoma Stream, which flows down the center of the study area, and the Kyrönjoki River, which spans a length of approximately 225 km across west-central Finland.

As per the glaciation history of the area, the advance and retreat of the Fennoscandian Ice Sheet has created a succession of heterogenous aquifer and aquitard layers confined underneath a thick glaciomarine aquitard along the Paloluoma BBV, forming a semi-confined to confined pressurized hydrogeological system. The subsurface system is complicated in its geology and has been extensively mapped using borehole logging and geophysical techniques carried out by the Geological Survey of Finland (GTK; Putkinen et al., 2012, 2015, 2018). The hydrostratigraphic sequence of the study area follows a consecutive aquitard/aquifer pattern up to the surface. A total of seven aquitards and seven aquifers are delineated within the Paloluoma BBV (cf. Chapter 2, Fig. 2.10 and Table 2.2). The aquifers are dominantly composed of sandy gravel sediments with some silt interbeds whereas the aquitards are dominantly composed of till material, except for the uppermost thick glaciomarine fine-grained unit. The bedrock in this area is characterized by porphyritic crystalline rocks that are part of the Central Finland Granitoid Complex (Nironen, 2017). Bedrock outcrops are prevalent in the topographic highs in the northwestern part of the study area and are also found along the sides of the valley.

The surficial geology of the study area has been described in Chapter 2 (cf. Sect. 2.2). The centre of the study area is predominantly silt and clay material forming a relatively flat plain (cf. Chap. 2, Fig. 2.3), which is only incised by the Paloluoma Stream. Due to the low permeability of the stream bed and its surroundings, little to no connection is assumed between the surface stream and groundwater. The northwestern part of the BBV includes most of the bedrock highs which have been affected by the shoreline processes during the marine regressive phase. The surface of the bedrock hills contains raised

beaches and washed till which have created several linear ridges of cobbles and boulders (cf. Chap. 2, Fig. 2.5). This NW region is thus considered a prominent recharge zone of the study area. South of this area, sandy gravel sediments abound (cf. Chap. 2, Fig. 2.5).

3.1.2 Conceptual Model

The geology of the Paloluoma BBV results in a complicated hydrostratigraphy and intricate groundwater system. The stratigraphic framework which is used to define the hydrostratigraphic units (HSU) was characterized by the Geological Survey of Finland (GTK). The geological units were identified using data from 110 boreholes to bedrock and a preliminary 3D geological model built via cross-sections. Borehole data provided sediment type and grain size information and were used to amalgamate groups of geological units to define hydrostratigraphic units. Boreholes were also used as control points for the gravity surveys to define the bedrock surface. Cross-sections oriented N-S and W-E across the study area provided a detailed understanding of the stratigraphy. A total of 55 cross-sections with a maximum of 350 m spacing between each transect was produced. Spacing between transects was reduced where more detail about the subsurface was required. The geological units that arose from the borehole data and cross-sections were then assigned hydraulic significance to define hydrostratigraphic units (HSU). As a result, seven aquifers (AF 1-7), seven aquitards (AT 1-7), for a total of 14 HSUs and one bedrock unit, were delineated within the geological model (cf. Chap. 2, Table 2.2).

With these cross-sections, units were interpolated across the area to form bounding surfaces for each HSU. Top surfaces were used as the contact points for the digital depositional surfaces and acted as the top and bottom boundaries of the hydrostratigraphic unit volumes. Once the HSU volumes were compiled in stratigraphic order, analysis of the 3D subsurface structure began. Upon analysis, it was found that most HSU layers are discontinuous and have variable thickness throughout the study area. This variability is the result of the depositional and erosional history of the area, which reflects the glacial and deglacial processes. Another characteristic of the resulting stratigraphy is that each aquitard unit is overlain by an aquifer unit (cf. Chap. 2, Table 2.2).

The estimation of recharge conditions is imperative to a functioning groundwater model. It is difficult to estimate groundwater recharge reliably using any single method due to uncertainties and limitations of each method (Scanlon et al., 2002). Therefore, often recharge is estimated using multiple methods in order to cross-check the results and constrain the values obtained (Rivard et al., 2014). Accordingly, both a water balance and groundwater flux analysis were performed to estimate groundwater recharge of the Paloluoma BBV (cf. Chap. 2, Sect. 2.3.3).

The water balance method yielded a minimum total recharge rate estimate of 35 mm/a, and a maximum total recharge rate estimate of 150 mm/a. The average total recharge rate found over the 15-year period was approximately 80 mm/a. The groundwater flux method was also used to estimate total recharge over the study area as a means to provide additional support to the findings from the water balance method. The estimate of total recharge was obtained by assuming that the influx of groundwater is solely from surficial recharge. Definitions and equations used to carry out the estimation of total recharge are detailed in Chapter 2. The total recharge rate over the 30 km^2 study area was found to be approximately 80 mm/a. These results from the groundwater flux method coincide with the results from the water balance method.

This total recharge rate was spatially distributed over the entire study area according to surface permeability. The surficial geology of the study area is given hydrogeological significance and is coupled to permeable and less permeable areas (cf. Chap. 2, Fig. 2.14). Permeable areas account for 80% of total recharge whereas poorly permeable areas account for 20% of total recharge. Using the minimum and maximum recharge rates obtained from the water balance method, a maximum and minimum recharge rate was calculated for each type of permeability zone for the purpose of model calibration.

The conceptual model as developed and described in detail in Chapter 2, is the basis of the numerical groundwater flow model. The conceptual model is an amalgamation of key properties and processes that represent the dynamics of the groundwater system, which are summarized in figure 3.1. The conceptual model illustrates that groundwater inflow into the system occurs from surface recharge under natural conditions but that inflow can also occur across watershed boundaries under pumping conditions. Groundwater outflow takes place at the lower end of the valley through deep aquifers spanning across the intersection of the Paloluoma Stream and Kyrönjoki River. Within the system, groundwater preferentially flows through granular aquifers within the valley but also through the underlying fractured rock whose hydraulic conductivity is reduced with depth below the bedrock surface.

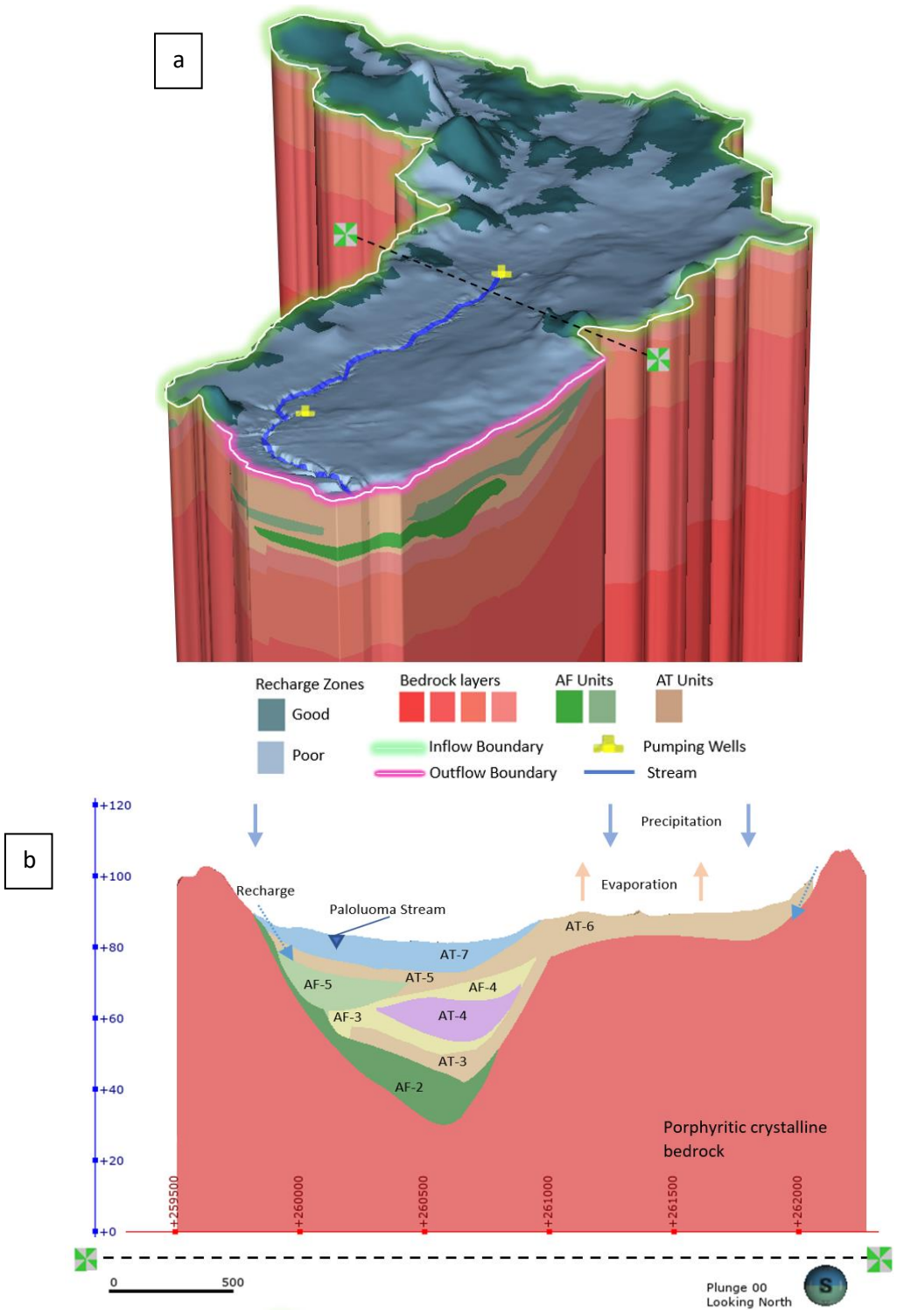

Figure 3.1: a) Conceptual Model with surface boundaries, recharge zones, visible HSUs and bedrock layers. Transect running across the centre of the study area. b) Cross-section of the Paloluoma buried valley. AF- and AT- refers to aquifer and aquitard, respective respectively. The numbers correspond to the aquifer and aquitard layer. Vertical exaggeration: 15X.

3.2 Methods

The Paloluoma BBV numerical flow model is based on the previously developed 3D hydrostratigraphic conceptual model. The subsurface structure and all properties are identically represented in the flow model relative to the hydrostratigraphic model. As such, the flow model is constrained by the 3D hydrostratigraphic model, which has its own set of uncertainties and assumptions that must also be considered for the flow model. For the purpose of this study, simulations were done to represent natural conditions as well as three groundwater exploitation scenarios. The model under natural conditions is calibrated to simulate field conditions. The calibrated model is then used to simulate pumping conditions from pumping tests. Finally, a maximum pumping scenario is simulated to assess the impact on the Paloluoma BBV.

3.2.1 Boundary and Extent

The model's boundary is defined by the watershed area as described in Sect. 3.3.1. This watershed is one of many sub-basin areas that make up the larger watershed of the Kyrönjoki River system. The south-eastern boundary of the study area is of particular importance as at great depths, groundwater flow is continuous beyond the boundary line due to deep aquifer extents. As such, the south-eastern boundary, which accounts for the intersection between the Paloluoma Stream and the Kyrönjoki River (cf. Chapter 2, Fig. 2.1), as well as the deep aquifers which are continuous beyond the boundary, is considered to be an area where groundwater can exit the basin.

3.2.2 Numerical Grid

3.2.2.1 2D Mesh

The Paloluoma valley groundwater flow model is structured using a finite element numerical grid and code (FEFLOW) to simulate groundwater flow dynamics. The finite element grid was generated with a 2D supermesh, which is the framework of all basic geometric information required by the FEFLOW algorithm (DHI-WASY, 2016). The supermesh uses the same outline of the model area and boundaries as described in the conceptual and hydrogeological model. The first step in the grid generation process is to create a 2D irregular triangular mesh in the xy-directions (Fig. 3.2). This type of structure allows grid refinement only where it is needed, such as in areas of high hydraulic gradient, while keeping the grid 'coarse' elsewhere for efficient computer processing. The reference mesh structure is then copied and extended in the z-direction to fit the top of all the units of the hydrostratigraphic model.

The supermesh elements must also undergo an auxiliary parameter check to ensure mesh quality and minimal errors at the time of simulation. One such property check includes correcting for Delaunay-violating triangles by manually adjusting triangle finite elements to reduce large angles that may lead to model instabilities.

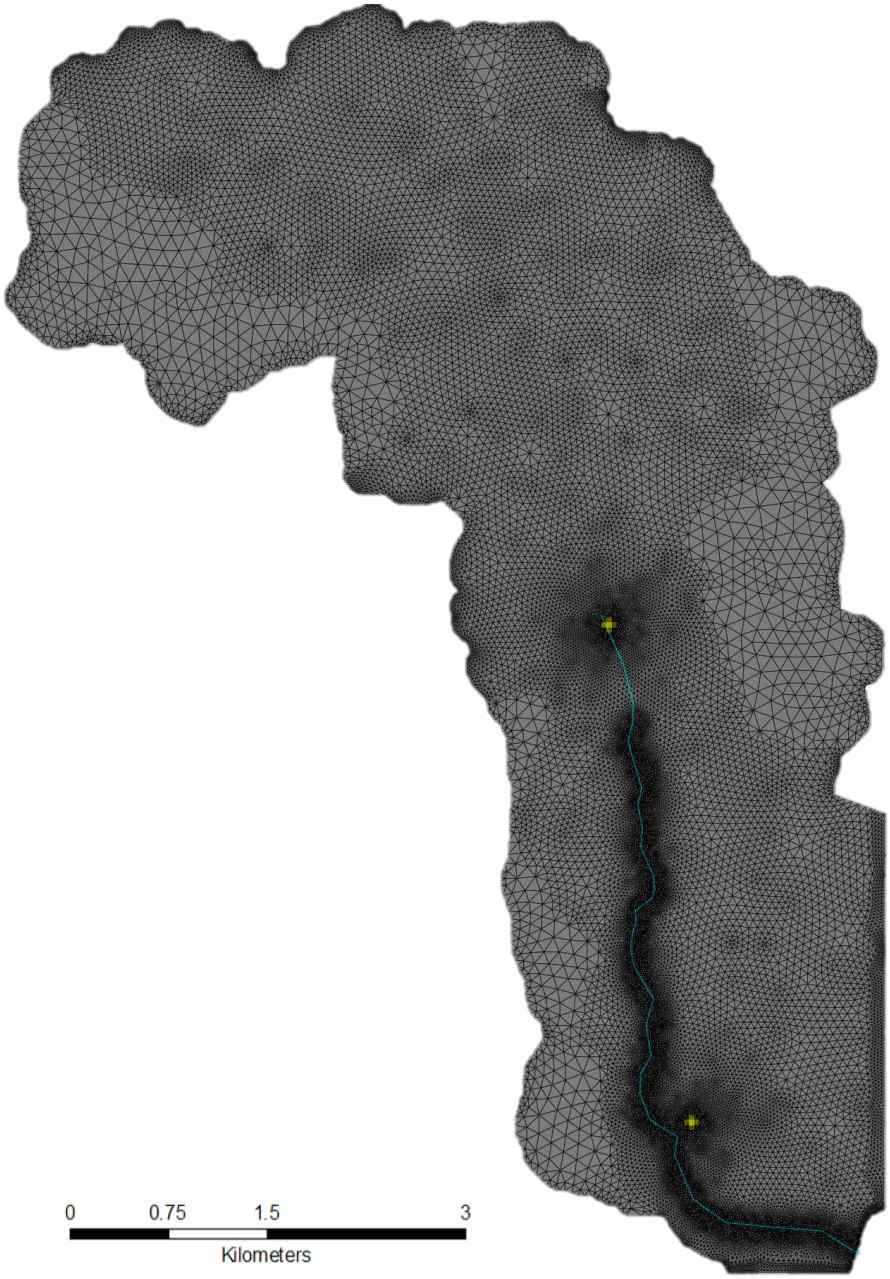

Figure 3.2: 2D finite element mesh of Paloluoma BBV. Mesh is refined where high hydraulic gradients are higher, specifically around pumping wells, streams, and aquifer areas.

3.2.2.2 3D Layer Configuration

The model is constructed as a layer-based model and maps all hydrogeological structures within the 3D subsurface model domain. The triangles of the 2D supermesh described in the previous section are extruded vertically (z-direction) to form prismatic elements whose lengths vary according to hydrostratigraphic unit thickness. This is a type of semi-regular grid (i.e., irregular in the xy- directions and regular in the z-direction). It is important that the 3D hydrogeological model, which is the basis of the 3D flow model, is meshed properly such that there are no overlaps or intersections of hydraulic units. Changes and improvements to either the 2D mesh or the 3D hydrogeological model itself, leads to an iterative process when creating the 3D layered mesh until the resulting mesh fulfills the requirements of the project. The 3D layered mesh is then further delineated into sub-layers per hydrogeological unit.

As water flows through the Paloluoma BBV model domain, it will come across different types of material with varying permeabilities, especially attributed to the valley's complex geology. The transition from a low permeable unit to a high permeable unit can cause numerical error as the transition may be too abrupt depending on the magnitude of contrasting permeabilities or conductivities. More specifically, flow in and flow out of cells when the hydraulic conductivity gradient is too high, can cause major flow changes that are difficult to compute and also lead to errors in the model. Additional discretization by adding layers within each unit to help compute the contrast in properties across adjacent layers was applied to mitigate such issues. This resulting 3D layered model (Fig. 3.3a) ensures the transition between low permeability/flow (LOW K) and high permeability/flow (HIGH K) is stable.

Furthermore, the internal layers within each unit are set to be continuous and parallel/conformable to each other; i.e., no unconformities such as one layer truncating the structure of an underlying layer. Since the thicknesses of units vary laterally, the layers within them also vary proportionally in order to remain parallel and conformable to the underlying and overlying bounding surfaces. One fundamental problem with layer-based models is that all layers are continuous across the entire domain, even if they are discontinuous. Therefore, where hydraulic units thin or pinch out in the model, the layers within the unit are assigned a minimum thickness that is just greater than zero until it reaches the next area of the model where the unit occurs again. A minimum distance of 0.3 m between slices ensures that the layers are still continuous everywhere in the model while honouring the stratigraphy of the valley as best as possible, albeit without real discontinuities. The Quaternary sediments and bedrock unit are highlighted in figures 3.3b and c, respectively. While the vertical (z) distance of aligned nodes (collocated nodes in the xy-plane of reference) of the internal unit layers is

constant relative to each other in each aquifer and aquitard unit of the unconsolidated sediment portion of the model, it increases with depth in the bedrock unit (Fig. 3.9d). This is because flow is limited in the deeper bedrock and additional layers are unnecessary. This gradual increase in thickness of bedrock layers with depth also follows a gradual decrease of hydraulic conductivity. Deeper layers are less permeable and are thus assigned lower hydraulic conductivity values than the conductivity found at the surface of bedrock. The exact conductivity value for each bedrock layer is explored during calibration of the model and will be further discussed in section 3.4.4.

In total, there are 66 layers (i.e., 67 slices) within the 15-unit model with 10 layers making up the bedrock unit and 56 layers making up the Quaternary sediments. Each layer is composed of 70 196 elements and each slice has 35 776 nodes. This totals to 4 632 926 elements and 2 396 992 nodes within the model. An array of cross-sections across the study area for the 3D constructed model in FEFLOW is presented in figure 3.4. The cross-sections show how the model layers represent the spatially varying thicknesses of the hydrostratigraphic units as well as the development of the valley structure as you move from North to South. In addition, cross-section 7 (XS 7) from figure 3.4 presents the continuous deep aquifers extending beyond the Paloluoma valley and across sub-basins.

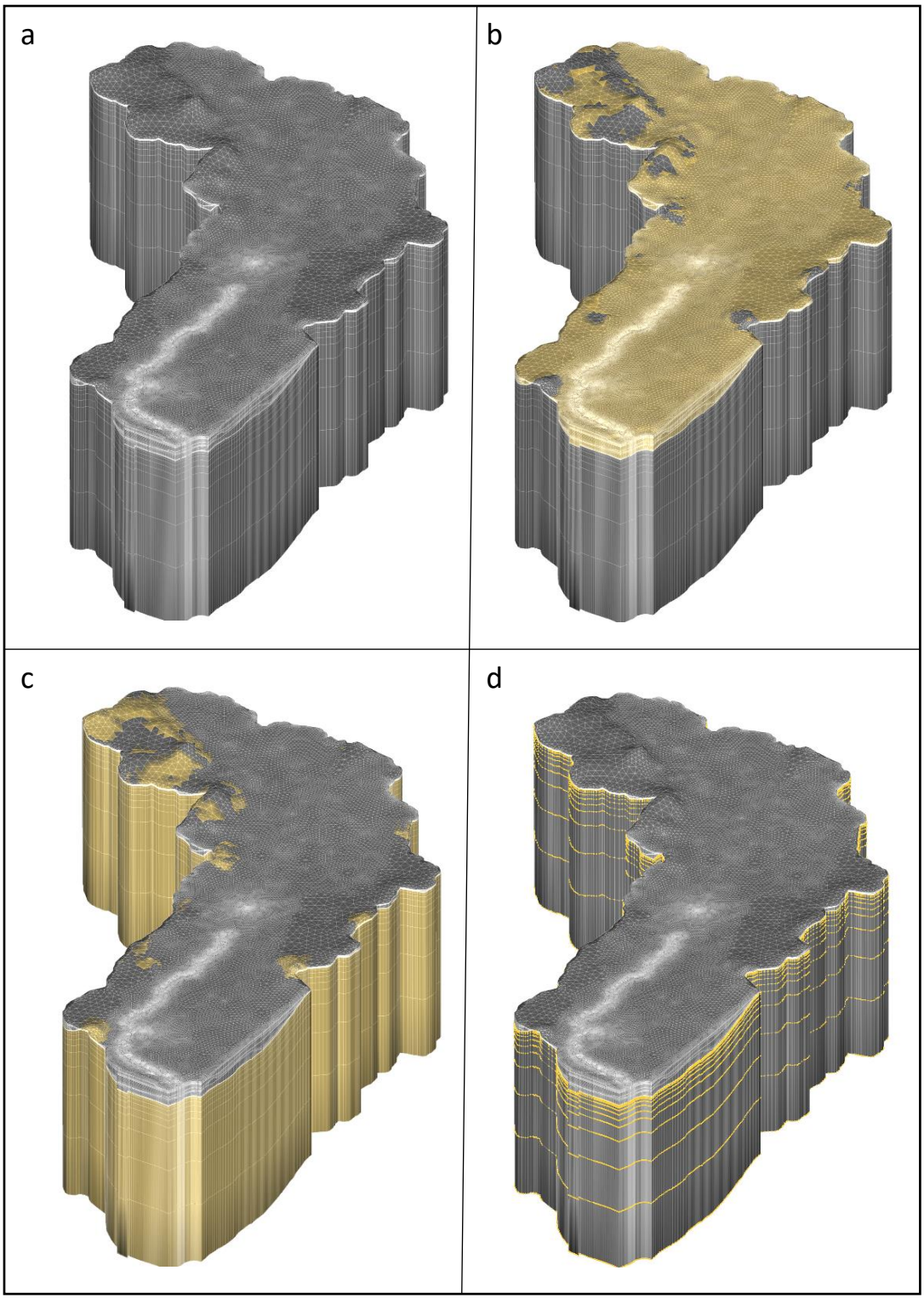

Figure 3.3: Numerical grid. a) 3D discretized layered model. b) Sediment units composed of aquifer and aquitard layers highlighted. c) Bedrock units composed of 10 layers highlighted. d) Bedrock slices highlighted.

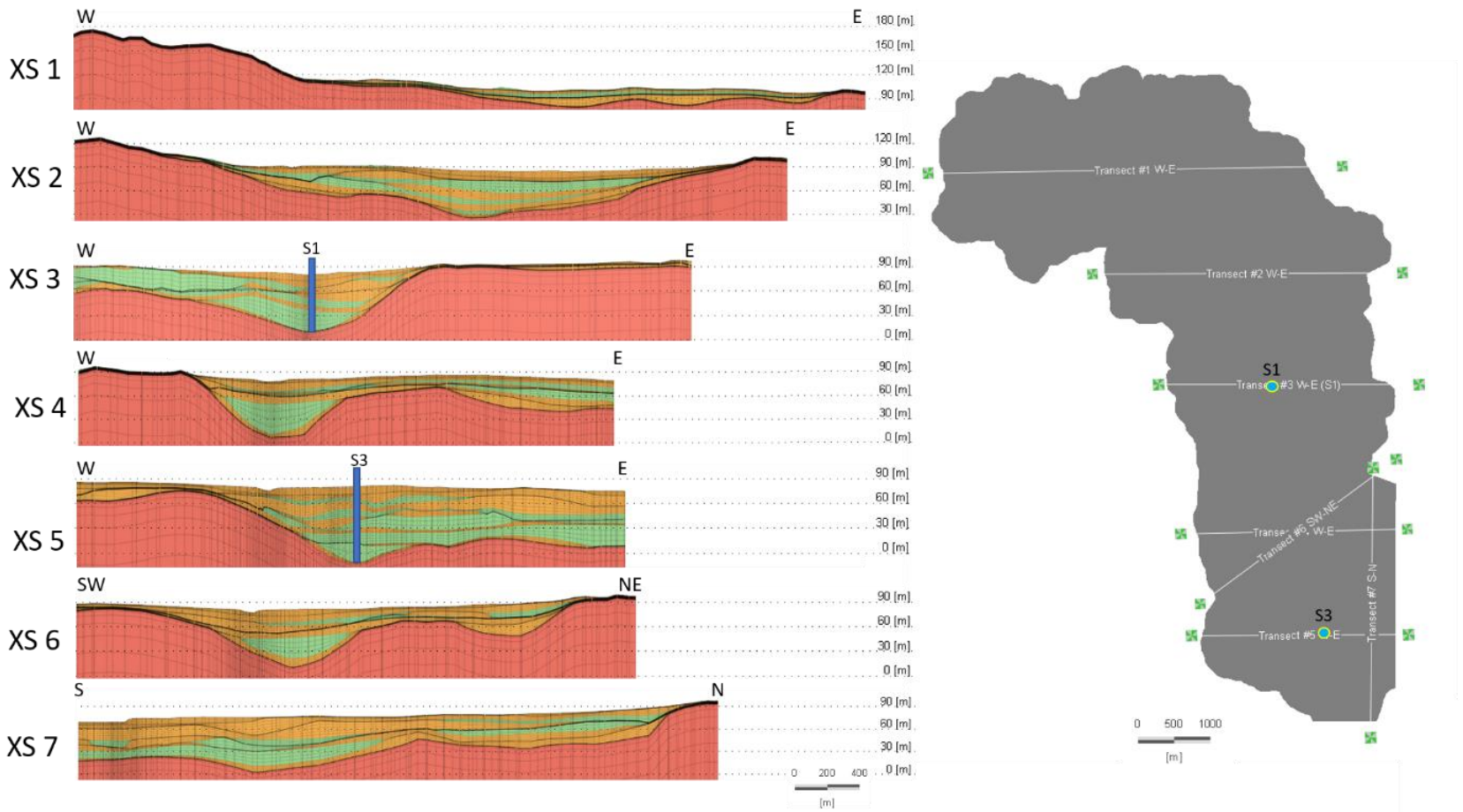

Figure 3.4: Cross-sections from the FEFLOW groundwater flow model. Aquifers are depicted in green, aquitards are orange, and bedrock is pink. Cross-sections do not show the entire bedrock thickness represented in the flow model (see fig. 3.3). Vertical exaggeration: 5X.

3.2.3 Model Conditions

The Paloluoma BBV groundwater flow model is set up as a fully saturated and confined aquifer system. For the purpose of this study, a steady-state model is developed to simulate flow processes and aquifer behaviour. While steady-state conditions in groundwater systems do not represent the response to climatic variations, they do represent long-term "average" conditions. Hence, a steady-state model is nonetheless an important step in all modelling studies (Luoma, 2012; Meyer et al., 2014; Pandian et al., 2016; Pétré et al., 2019). In this study, the steady-state model is used to calibrate hydraulic parameters, perform a sensitivity analysis, and simulate the response to potential pumping conditions.

It is also important to specify the boundary conditions of the model. The inflow and outflow boundaries are described in detail in Chapter 2 - Conceptual Model and also shown in figure 3.1a. The outflow boundary found along the south perimeter of the study area is assigned a 1st-type (constant head) boundary condition with a fixed hydraulic head value of 72 m, which is applied at every node along this boundary. The value of 72 m was obtained by averaging the topographic level at these end locations. Topographic levels at the south and southeast end ranged from 68 – 82 masl. This 1st-type boundary condition is extended in the z-direction to encompass the entire depth of Quaternary sediments including aquifer and aquitard units (~8 m – ~70 m thickness; slice 1 – 56). For the initial steady-state model, a no-flow boundary condition was applied along the majority of the remaining watershed perimeter. The model was later improved to account for water entering through the sides of the model under pumping conditions. For this reason, a 3rd-type (fluid-transfer) boundary condition at the very surface of the remaining perimeter of the watershed was applied to the steady-state model and extended down the depth of the sediment units similarly as the first type boundary condition was, and included 17 m into bedrock as well (slice 1 – 60). Bedrock was also included into the boundary condition to reflect our current hypothesis that bedrock fractures contribute to water inflow. However, unlike the first type boundary condition assignment, the 3rd type boundary condition values were not averaged from topographic levels; instead, hydraulic head levels from the initial steady-state model under natural conditions were applied at the respective nodes along this boundary. A minimum flow-rate constraint of 0 m was assigned along with the 3rd-type boundary to prevent outflow from this boundary. Everything outside of these specified boundaries has a no-flow boundary condition.

There are two pumping wells within the study area, Siivilä 1 and Siivilä 3. Siivilä 2 is just outside the study area within a separate watershed and is not considered for this study. Pumping tests for each well were conducted over approximately 3-month periods and progressively increased in pumping rate.

Siivilä 1 pumping occurred from December 17th, 2014, to March 18th, 2015, at varying rates. Siivilä 3 pumping occurred from August 16th, 2016, to November 25th, 2016, at varying pumping rates. The pumping schedule is shown in detail in Table 3.1.

Table 3.1. Pumping schedule with progressively increasing pumping rates for long-term pumping tests for Siivilä 1 and Siivilä 3. Progressively larger pumping rates were maintained for periods (stages) of about 2 to 7 weeks.

	Test	**Start Date**	**End Date**	**Days**	**Rate (m^3d^{-1})**
Siivilä 1	1	17.12.2014	7.1.2015	21	1621
	2	7.1.2015	5.2.2015	29	2100
	3	5.2.2015	6.3.2015	29	3166
	Test	**Start Date**	**End Date**	**Days**	**Rate (m^3d^{-1})**
Siivilä 3	1	16.8.2016	27.8.2016	11	1170
	2	27.8.2016	12.9.2016	14	1876
	3	12.9.2016	31.10.2016	49	2363

In order to reproduce field pumping conditions, the groundwater flow model was run to simulate pumping resulting from the final and greatest pumping rate at both Siivilä 1 and Siivilä 3 pumping wells. During the pumping tests, water levels remained stable near the end of all pumping stages, both in the pumped well and observation wells. Numerical modelling could thus be done under steady-state conditions to represent the drawdowns observed near the end of the final pumping stage.

To model the impact of the Paloluoma BBV, four simulation programs were chosen as follows: (Program 1) baseline case under natural conditions, (Program 2) current pumping conditions at one of the pumping wells, (Program 3) current pumping conditions at the other pumping well, and (Program 4) maximum pumping at both wells. All four programs are under steady-state saturated conditions and have an assigned first type boundary condition applied at the discharge area. Table 3.2 describes the variable conditions between the four programs. For the first program, the model was run without pumping to simulate natural conditions. Two areas of exploitation were introduced for the other scenarios. These exploitation areas are represented by pumping wells, Siivilä 1 (S1) and Siivilä 3 (S3). A rate budget analysis of the model domain was conducted to understand how water is flowing in and out of the system under both natural and pumping conditions. Finally, a maximum pumping scenario was simulated where both pumping wells were active and pumping at a realistic maximum pumping rate (S1 = 3000 m^3d^{-1} and S3 = 2500 m^3d^{-1}), which the pumping wells will likely be pumped at for future use.

Table 3.2: Simulation programs and their associated varying conditions.

PROGRAM	PUMPING WELL(S)	ACTIVE BOUNDARY CONDITION(S)
1	N/A	1st – type along discharge area
2	Siivilä 1	1st – type along discharge area and 3rd – type along remaining watershed perimeter
3	Siivilä 3	
4	Siivilä 1 and 3	

3.2.4 Model Calibration

3.2.4.1 Observation Points

Observation data from real and synthetic observation wells were used to calibrate the model. Figure 3.5 illustrates the location of a total of 58 observation wells. Of the 58 observation wells, there are 20 real observation wells and 38 synthetic observation wells. Table 3.3 describes how the observation wells were grouped. A portion of the real observation wells (11) provided quality water level information monitored every 15 minutes over a period of several months before, during, and after pumping. As for the remaining nine real observation wells and 38 synthetic observation wells, hydraulic head levels were not available, thus topographic elevations were used as the reference level. The 13 remaining real observation wells are artesian. When calibrating the model, this group of observation wells were inspected to ensure that simulated head values were above ground.

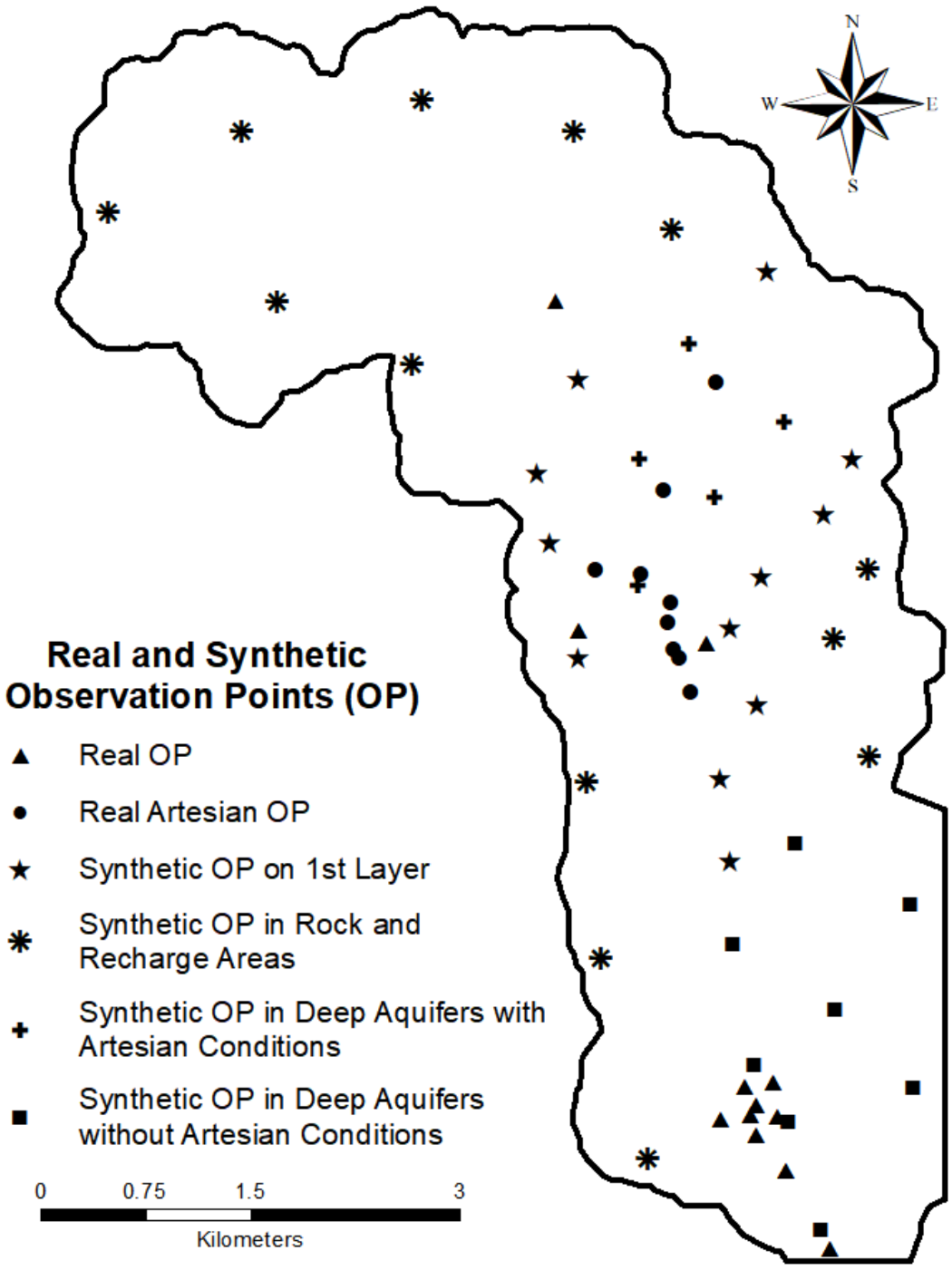

Figure 3.5: Real and synthetic observation points across the study area.

Table 3.3. Real and Synthetic Observation Points described in terms of target purposes for model calibration.

OBSERVATION POINTS	COUNT	PURPOSE DESCRIPTION
Real Observation Points	11	Quality observation wells. Targeted such that simulated heads fall on observed water levels
Real Artesian Observation Points (Overflowing Wells)	9	Observation wells displaying artesian conditions. Targeted such that simulated heads fall above ground level
Synthetic Observation Points on First Model Layer	12	Topographic levels used as reference. Targeted such that simulated heads fall on or below ground level
Synthetic Observation Points on Bedrock Outcrops and Recharge Areas	13	Topographic levels used as reference. Targeted such that simulated heads fall below ground level
Synthetic Observation Points in Deep Aquifer with Artesian Conditions	5	Topographic levels used as reference. Targeted such that simulated heads fall above ground level
Synthetic Observation Points in Deep Aquifer without Artesian Conditions	8	Topographic levels used as reference. Targeted such that simulated heads fall on or below ground level

As for the synthetic wells, the 38 synthetic wells were grouped into four categories, which included, (1) wells on the first layer, (2) artesian wells in deep aquifers, (3) non-artesian wells in deep aquifers, and (4) wells in recharge areas. These wells were used to calibrate the model. Synthetic observation wells on the first layer targeted areas that produce head values equal or close to topographic levels. The purpose of the synthetic observation wells in deep aquifers was to target areas where artesian conditions are known to be present (evidently with the real artesian observation wells) and produce head values that exceeded the topographic level. The third synthetic observation well category, non-artesian wells in deep aquifers, were targeted to represent areas where head levels were below topographic levels. Finally, the fourth synthetic observation well category, wells in recharge areas, represent areas that typically have water levels lower than topographic levels as they are found in areas with raised hills (no actual observation wells were available in these areas).

3.2.4.2 Calibration

To achieve a well-calibrated model, two techniques are typically employed; (1) the manual trial-and-error adjustment of parameters and (2) automated parameter estimation (Anderson & Woessner, 1992). While trial-and-error calibration is highly influenced by the modeller's experience, it is still recommended and is the preferred method as the modeller develops a better understanding of the impact of model assumptions and design. While performing this type of calibration, which involves

numerous changes of model parameters, the modeller is able to determine which parameters the model is most sensitive to. As a result, through manual calibration, the sensitivity analysis part of the modelling effort is already engaged and can be quantified alongside, or immediately after.

For this study, the model was first manually calibrated on a trial-and-error basis in order to get a feel for the model's response. First, an interval of hydrologically acceptable upper and lower limits for each parameter was determined. Next, each parameter was adjusted while holding all other parameters constant. Through this process, it is also determined how intensely each parameter affects the model results. From calibrating the model, it became very apparent that the parameters were highly interdependent and the model highly nonlinear.

The parameters calibrated for this model include recharge and hydraulic conductivity. The interval of hydrologically acceptable upper and lower limits for total recharge is from 35 mm/a to 150 mm/a. This range was determined by the water balance method over a 15-year period. The interval of hydrologically acceptable upper and lower limits for hydraulic conductivity for each HSU was determined using sediment material descriptions. Both methods are described in detail in chapter 2. The first phase of model calibration for this study was to visually fit simulated values to observed heads on plots. Using the categorized observation points as previously described in this section, we are able to visualize how changes to each parameter affect the model results. Manual calibration was an iterative process and was performed until a good fit was achieved for each group of observation points.

The model was then run under automatic calibration to further optimize the model. Automatic calibration approaches may be direct or indirect. For the direct approach, unknown parameters are dependent variables and heads are independent variables. Head values are only known at observation points; therefore, it is necessary to make estimates everywhere else in the grid, usually by kriging interpolation. The indirect approach checks the head solution and systematically adjusts parameters in order to minimize the objective function (Anderson & Woessner, 1992). With the indirect approach, a statistical framework is applied, in which errors in heads and parameters are quantified. For this study, automatic calibration was performed with FePEST, a graphical program within FEFLOW that utilizes the PEST algorithm (Doherty, 2005) in the background.

3.2.4.2.1 Calibration Quality

It is recommended that statistical analyses for hydrological models include a combination of evaluating graphical results, absolute value error statistics (i.e. root mean square error), and normalized goodness-of-fit statistics (i.e. Nash Sutcliffe Efficiency index; Ritter and Muñoz-Carpena, 2012). Hence, a good graphical match between observed and simulated heads for the Paloluoma BBV observation points was followed by evaluating the root mean square error (RMSE) and the Nash-Sutcliffe efficiency (NSE) index.

RMSE is the standard deviation of the residuals (prediction errors) and provides information on how well data is concentrated around the reference line (Eq. 1).

$$RMSE = \sqrt{\frac{\sum_{i=1}^{N}(x_i - \hat{x}_i)^2}{N}} \quad (1)$$

where, i is the hydraulic head variable, N is the total number of points, x_i is the observed head, and $\hat{x}_i$ is the simulated head.

The NSE is a normalized statistic that determines the relative magnitude of the residual variance compared to the measured data variance (Nash & Sutcliffe, 1970). It indicates how well the plot of observed versus simulated data fits the 1:1 line. When the NSE = 1, it corresponds to a perfect match of the model to the observed data. When the NSE = 0, indicates that the model predictions are as accurate as the mean of the observed data (Eq. 2).

$$NSE = 1 - \frac{\sum_{i=1}^{N}(x_i - \hat{x}_i)^2}{\sum_{i=1}^{N}(x_i - \bar{x}_i)^2} \quad (2)$$

where, $\bar{x}_i$ is the mean of the observed head.

Both objective functions were determined for each set of observation points as they had their own target conditions regarding the reference line. For observation points in categories that are not meant to be in alignment with the reference line (i.e., above or below the reference line depending on category), an additional trendline was created. In order to still use RMSE and NSE as a check for these groups in the model, a trendline of the observation points from the base case model was developed and head values were extrapolated. The extrapolated head values were ~5 meters above or below the topographic level depending on the synthetic observation point category. Using this technique was necessary as there were not enough real observation points to calibrate the model effectively. The ROP

was given more weight when considering how well the model is calibrated. In order to relate both the RMSE and NSE when establishing model efficiency, the number of times (n_t; Eq. 3) that the observations variability is greater than the mean error can be estimated. Ritter and Muñoz-Carpena (2013) published figure 3.6, which depicts the relationship between the NSE and model mean error relative to the spread of observations.

$$n_t = \frac{SD}{RMSE} - 1 \tag{3}$$

where SD is the standard deviation, which represents the variability of the observation points.

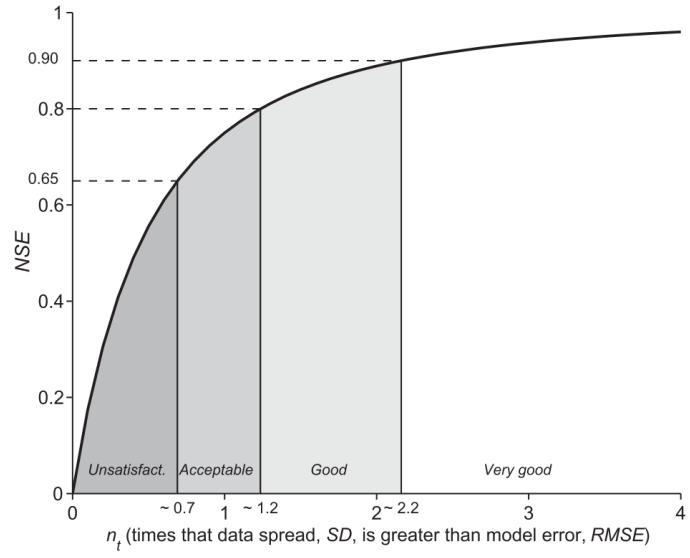

Figure 3.6: Relationship between goodness-of-fit statistic, NSE, and number of times, n_t , that the observations variability (SD) is greater than the mean error (RMSE). Source: Ritter and Muñoz-Carpena (2013).

3.2.4.3 Parameter Sensitivity Analysis

A sensitivity analysis was performed for the Paloluoma BBV groundwater flow model. The final calibrated results for each parameter are used as the reference model during the sensitivity analysis. Recharge, hydraulic conductivity for bedrock, bedrock anisotropy, and hydraulic conductivity for hydrostratigraphic units were analysed to determine how each affects the model.

In order to evaluate the model sensitivity to changes in recharge value, the model was run holding all parameters constant but recharge (R). The final calibrated model is used as the base case model (R = 50 mm/a) and compared to a model where R is halved (R = 25 mm/a), and to another model

where R is doubled (R = 100 mm/a). Sensitivity to anisotropy of hydraulic conductivity (ratio between horizontal K and vertical K) for bedrock was also analysed. The base case model has an anisotropy of bedrock K of 1000. For the sensitivity analysis, bedrock conductivity anisotropy was set to 100 and 500, respectively. In addition, model sensitivity to hydraulic conductivity was evaluated. Hydraulic conductivity for bedrock was changed by one order of magnitude in both directions (increase and decrease) while holding all other parameters constant. Finally, sensitivity to hydraulic conductivity for aquifers and aquitards was analysed. Hydraulic conductivity for all HSU were divided by two for the X Model and multiplied by two for the Y Model. These changes to the HSU were conducted in all directions to maintain isotropy. Table 3.4 summarizes the changes for each model (X and Y) for each parameter.

Table 3.4. Features/parameters modified during sensitivity analysis.

Feature	**Modifications**
Recharge	Change recharge to (1) half the value (X Model) and (2) double the value (Y Model) from the Base Case Model.
Bedrock K Anisotropy	Change bedrock anisotropy to (1; X Model) 100 and (2; Y Model) 500.
Bedrock Hydraulic Conductivity	Decrease (X Model) and increase (Y Model) bedrock hydraulic conductivity value from base case model by one order of magnitude in both horizontal and vertical directions.
AF & AT Hydraulic Conductivity	Change HSU hydraulic conductivity value to (1) half the value (X Model) and (2) double the value (Y Model) from the Base Case Model in both horizontal and vertical directions.

3.3 Results

3.3.1 Under Natural Conditions

3.3.1.1 Calibration and Sensitivity Analysis

Table 3.5 depicts the calibrated recharge results. Hydraulic conductivity for each HSU was also calibrated as presented in table 3.6. Hydraulic conductivity for aquifers and aquitards were kept isotropic from the beginning of modelling stages and were kept isotropic based on the fact that simulated heads fit well with observed heads. However, hydraulic conductivity for bedrock in the vertical direction does not equal the hydraulic conductivity in the horizontal direction. Table 3.7 depicts how conductivity changed with depth and with increasing bedrock layer thickness.

Table 3.5. Initial and calibrated recharge value for entire model domain and distinguished permeable and less permeable areas. Lower and upper limits as calculated from methods described in Chapter 2.

	% of Total Recharge	Lower Limit (mm/a)	Initial Value (mm/a)	Upper Limit (mm/a)	Final Value (mm/a)
Total Recharge Area	100	35	80	150	50
Permeable Areas	80	105	241	452	150
Less Permeable Areas	20	10	22	40	14

Table 3.6. Initial and calibrated hydraulic conductivity (K) for aquifer and aquitard units. Lower and upper limits as calculated from methods described in Chapter 2. AF=aquifer and AT=aquitard.

Hydraulic Unit	Lower Limit (ms^{-1})	Initial K Value (ms^{-1})	Upper Limit (ms^{-1})	Final K Value (ms^{-1})
AF-7	1.00E-03	2.59E-03	1.00E-01	2.54E-03
AF-6	9.00E-07	2.03E-03	6.00E-03	2.31E-03
AF-5	9.00E-07	6.44E-04	6.00E-03	4.03E-04
AF-4	9.00E-07	4.38E-04	5.00E-04	4.21E-04
AF-3	9.00E-07	5.15E-04	5.00E-04	1.63E-04
AF-2	3.00E-04	2.94E-04	3.00E-02	5.79E-04
AF-1	3.00E-04	3.33E-04	3.00E-02	4.44E-04
AT- 1-7	1.00E-12	2.00E-07	2.00E-06	2.0E-07

Table 3.7: Initial hydraulic conductivity (isotropic $K_h = K_v$) and calibrated horizontal hydraulic conductivity (K_h) and vertical hydraulic conductivity (K_v) for bedrock layers. Lower and upper limits estimated from method described in Chapter 2.

Bedrock Layer	Thickness (m)	Lower Limit (ms^{-1})	Initial Value ($K_h = K_v$; ms^{-1})	Upper Limit (ms^{-1})	Final K_h Value (ms^{-1})	Final K_v Value (ms^{-1})	Initial Anisotropy	Final Anisotropy
Top Layer	17	1.00E-12	2.00E-07	1.00E-05	1.00E-05	1.0E-08	1	1000
Second Layer	60	1.00E-12	2.00E-07	1.00E-05	2.50E-06	2.5E-09	1	1000
Third Layer	150	1.00E-12	2.00E-07	1.00E-05	5.00E-07	5.0E-10	1	1000
Bottom Layer	300	1.00E-12	2.00E-07	1.00E-05	2.50E-07	2.5E-10	1	1000

Figure 3.7 depicts the final plots for the calibrated model for each categorized set of observation points. Since the reference values for all but the 'Real Observation Points' (ROP) category are topographic levels rather than head levels, simulated points are targeted to fall above, below, or on the reference line depending on its category. The ROP category is the most reliable category used to calibrate the model as it represents quality head values as observed in the field. As such, calibration results are statistically analysed using the ROP category values.

This graphical match between observed and simulated heads for the Paloluoma BBV observation points was followed by evaluating objective functions for error and goodness-of-fit statistics. Referring to figure 3.6, which depicts the relationship between NSE and n_t to determine the quality of the model, the calibrated Paloluoma BBV groundwater flow model falls on the boundary between a 'Good' and a 'Very Good' calibration based on the resultant NSE of 0.89 and n_t of 2.2 from the ROP group.

It is important to note that calibrated models are not unique in the sense that any combination of parameter values may produce similar, good objective functions but based on the information and an understanding that the hydrogeologist has. In other words, the combination is subjectively the best based on the available data, honouring certain constraints, and the overall knowledge of the system.

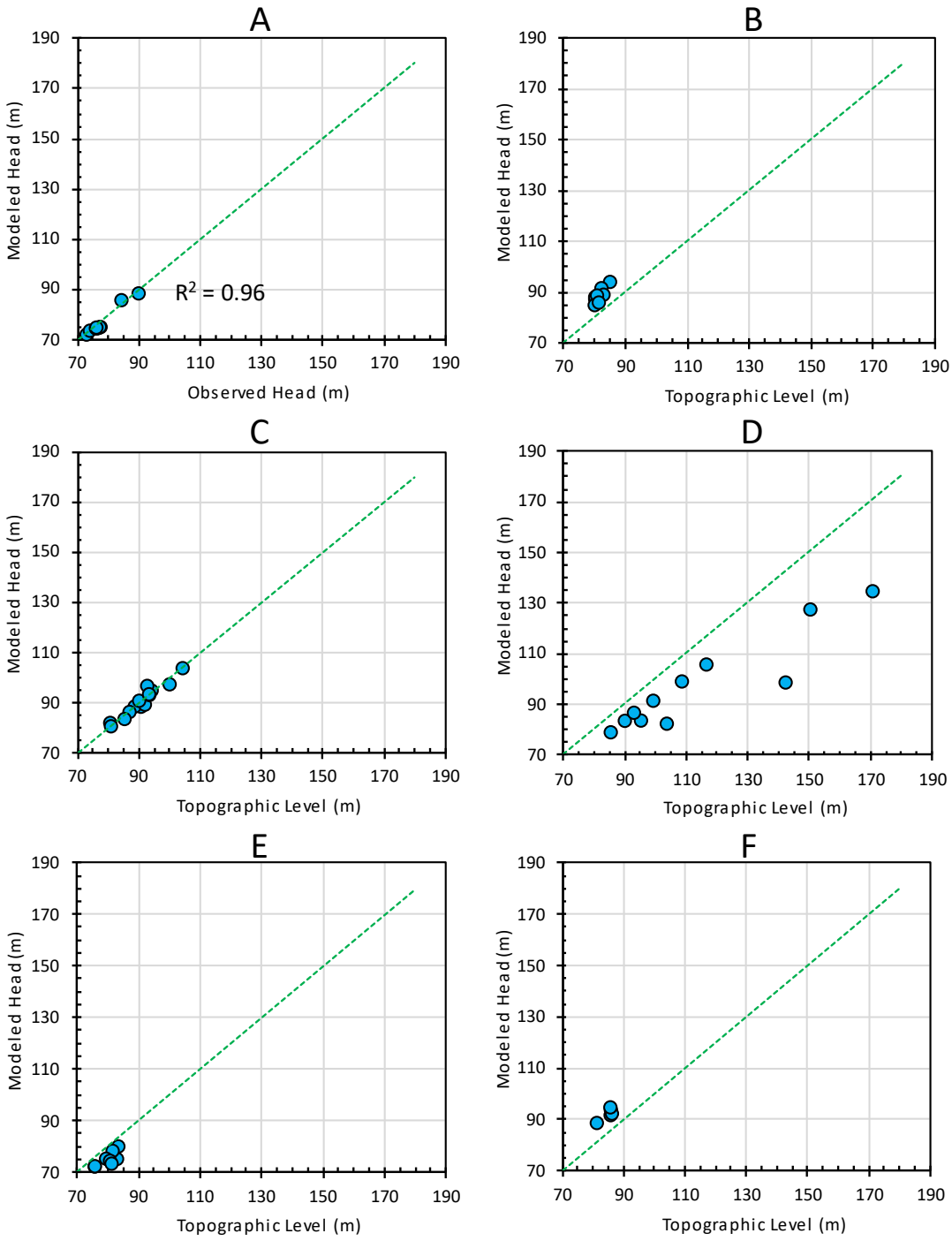

Figure 3.7: Calibrated model results for each group of observation points. Group (A): real observation points. (B): real artesian observation points i.e., overflow wells. (C): synthetic observation points on the first layer. (D): synthetic observation points in recharge areas. (E): synthetic observation points in deep aquifers without artesian conditions. (F): synthetic observation points in deep aquifers with artesian conditions

For the parameter sensitivity analysis, table 3.8 presents objective function results for each type of model (X, Y, and base case) and each feature modification. This table is plotted on figure 3.8. The presented objective functions, RMSE and NSE are from the ROP group.

Table 3.8. Objective function results for each type of model and feature modification during sensitivity analysis

	Recharge		Bedrock Anisotropy		Bedrock Conductivity		HSU Conductivity	
	RMSE	NSE	RMSE	NSE	RMSE	NSE	RMSE	NSE
X Model	3.99	0.27	1.63	0.88	1.57	0.89	3.74	0.36
Base Case Model	1.56	0.89	1.57	0.89	1.56	0.89	1.56	0.89
Y Model	7.40	-∞	1.56	0.89	4.03	0.25	3.77	0.35

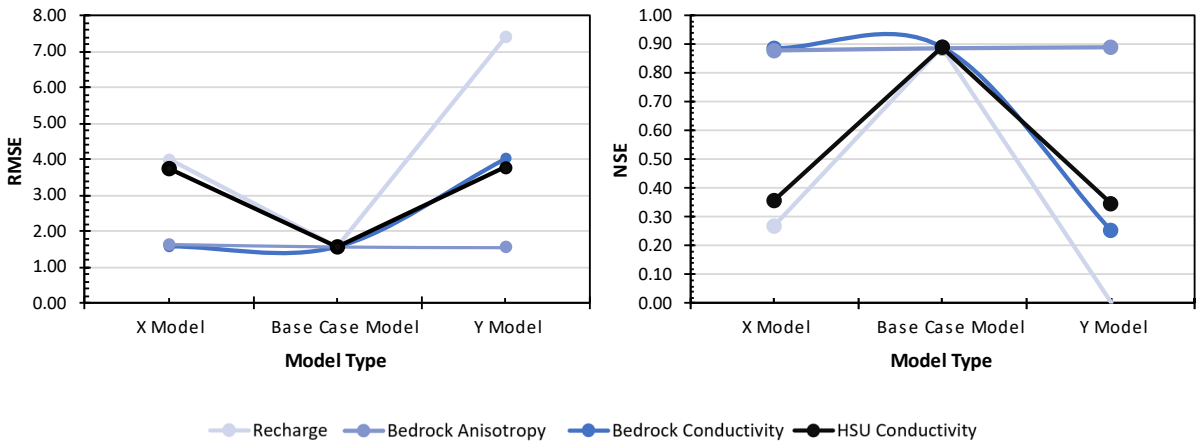

Figure 3.8: Objective function (RMSE and NSE) plot results for each type of model (X Model, Base Case Model, Y Model) and feature modification (recharge, bedrock anisotropy, bedrock conductivity, and HSU conductivity) during sensitivity analysis.

3.3.1.2 Particle Tracking

Forward particle tracking was used to track the journey of rain droplets at recharge areas, through the model until reaching a discharge point. Figure 3.9a illustrates the journey of water particles from the northern region of the study area, which is characterized as a recharge area, through the saturated groundwater flow system. This figure shows the fate of recharge in a spatial context, flow patterns within the aquifers, discharge locations, and advective residence times. In order to see the path travelled by the particle, an aerial view of forward particle tracking is complemented with a west-facing 3D view (Fig. 3.9b). Aquifer 5 and aquifer 2, which are the aquifers with the greatest lateral extent, are highlighted in another 3D view (Fig. 3.9c). From these figures, we can see that water that begins at the recharge area, travels throughout the saturated model, and is discharged at the south end of the model. We can also see that the particle pathway moves along aquifer 5 (shallow aquifer) until a certain point, after which the path deepens to move along aquifer 2 (deep aquifer). Furthermore, average advective residence times increase as the particle path progresses and deepens. Under natural conditions, the chosen nodes to initiate forward tracking presents pathways taking up to ~550 years to reach the discharge area.

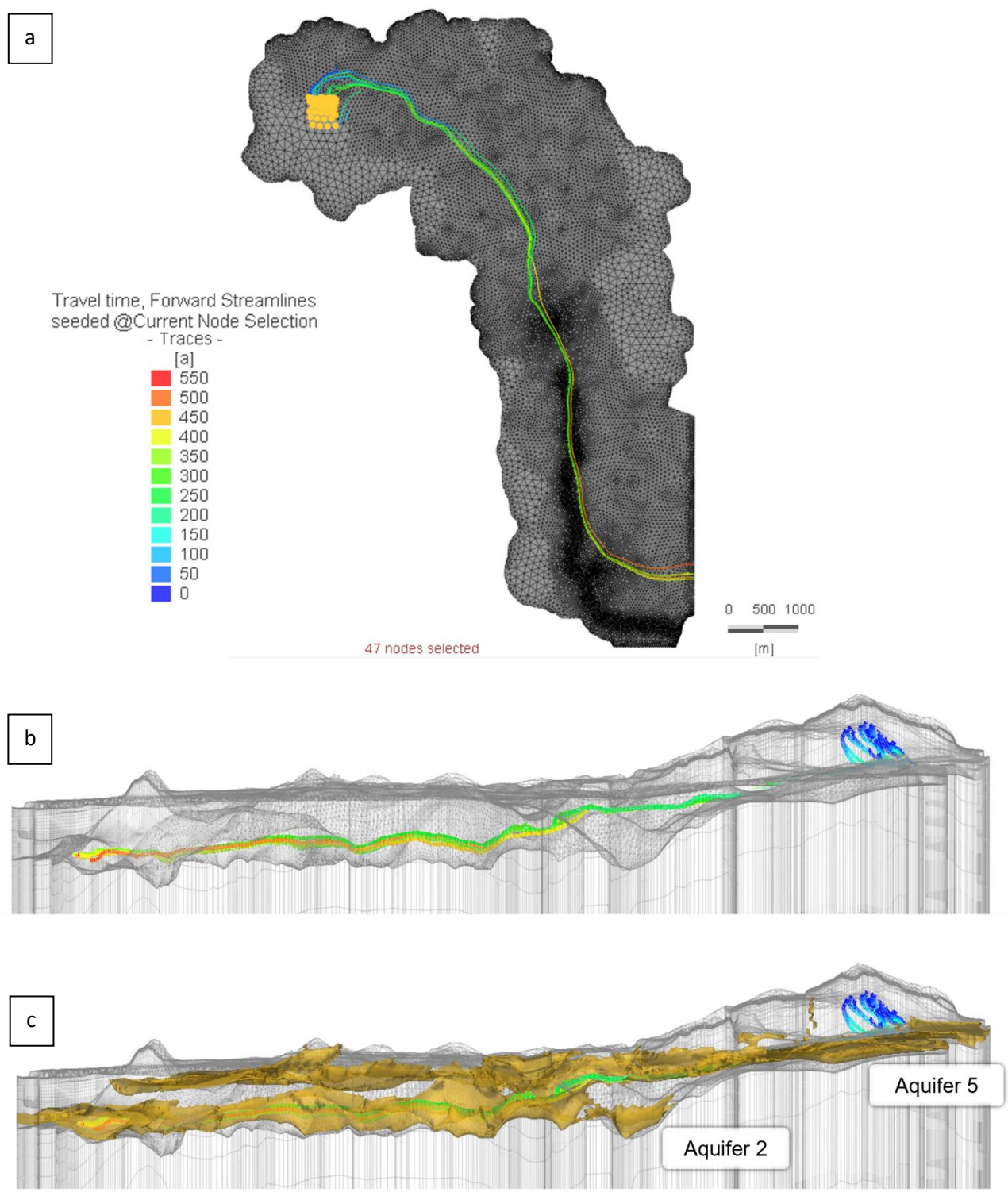

Figure 3.9: a) Forward particle tracking from recharge to discharge locations. Aerial view. b) 3D view of same particle tracking. West facing. c) 3D view of same particle tracking with the shallow aquifer, aquifer 5, and the deep aquifer, aquifer 2, highlighted West facing. Vertical exaggeration 10X.

3.3.2 Under Pumping Conditions

Simulated drawdowns are representative of observations. Appendix IV presents wells monitored during pumping at Siivilä 1 (KUU19, KUU21, KUU22, and KUU23B) and their drawdown and recovery over the pumping test periods. Appendix IV presents wells monitored during pumping at Siivilä 3 (MIHP3, MIHP6, MIHP9, MIHP10, MIHP12) and their drawdown over the last pumping test period. For clarity purposes, recovery data is not displayed for S3 as only one pumping period is presented. During pumping, all observation wells were not monitored, and so observed drawdown data is limited to about half a kilometer away from the pumping wells.

3.3.2.1 Siivilä 1 Pumping Conditions

Figure 3.10a depicts the drawdown at Siivilä 1 with a pumping rate of 3166 m^3d^{-1}. Drawdown is seen to extend to a depth of eight meters at Siivilä 1. The direction of drawdown away from Siivilä 1 is skewed towards the north and west ends of the watershed. The direction of drawdown may be explained through the subsurface architecture of the valley. Siivilä 1 is pumping from aquifer 2 and along this location, the valley opens up to the western neighbouring watershed (figure 3.10b), which may explain the extension of drawdown in the western direction. Aquifer 2 from which Siivilä 1 is pumping from has the greatest contiguous extent across the study area, which may also contribute to the greater drawdown extent. There is also an aquitard directly above aquifer 2, which could be contributing water via leakage as well as inflow from bedrock and granular aquifers through the watershed boundary, based on the pumping test analysis (Section 2.3.2). This is because pumping induces a vertical gradient, which the overlying units respond to by producing a downward flux into the confined aquifer that is being pumped. Also, the drawdowns reach the watershed boundary, which induce inflow from outside the watershed through the permeable sediments and bedrock found at the boundary. Therefore, the watershed boundary had to be represented by a 3rd type boundary condition in the model.

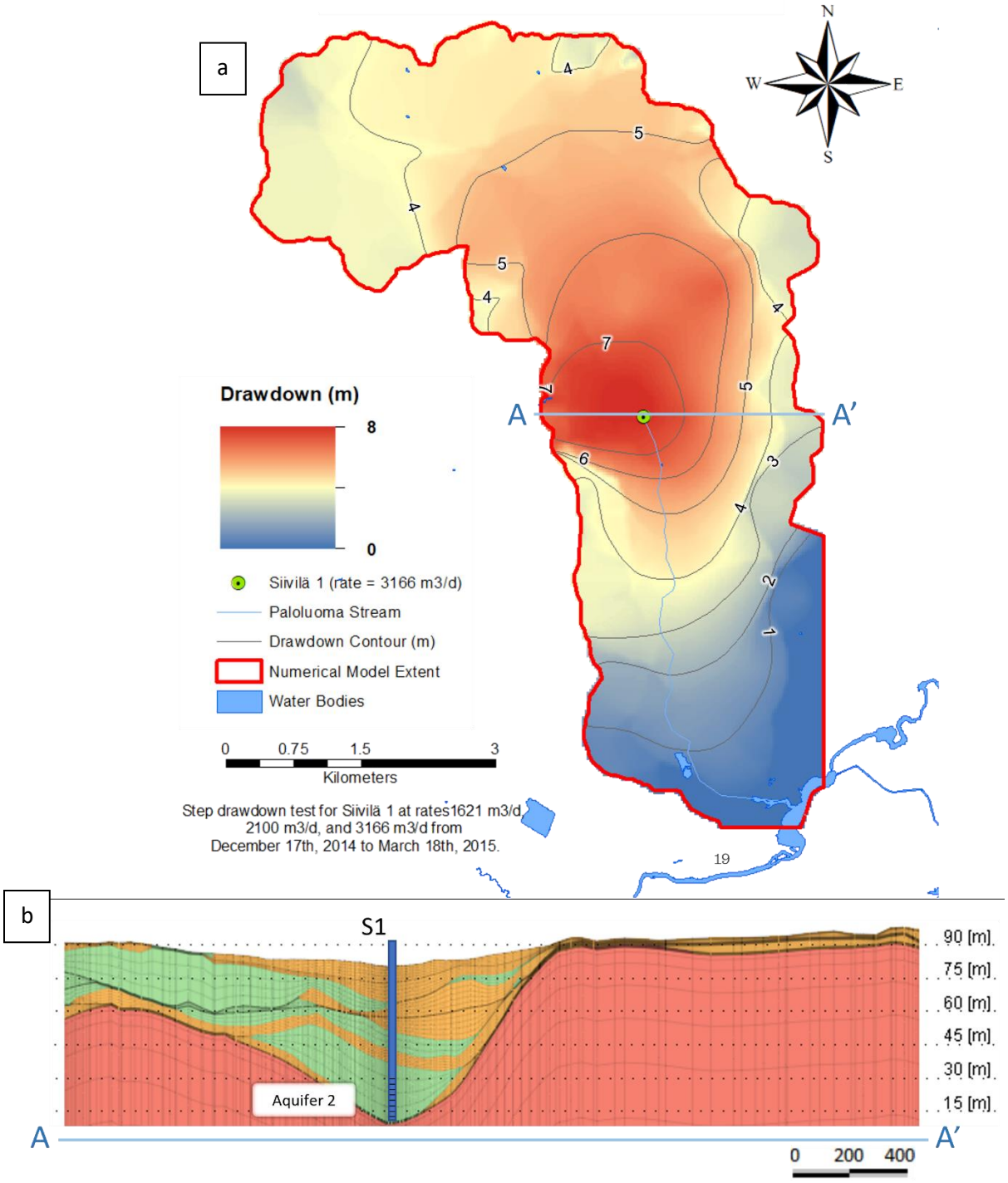

Figure 3.10: a) Simulated steady-state drawdown at Siivilä 1 at a pumping rate of 3166 m3d-1. Transect taken along pumping well location (A – A'). b) Cross-section depicting subsurface structure at Siivilä 1. Vertical exaggeration: 8X.

3.3.2.2 Siivilä 3 Pumping Conditions

Pumping test conditions at Siivilä 3 were also simulated with the groundwater flow model. The greatest pumping rate (2363 m^3d^{-1}) from the long-term pumping test performed at Siivilä 3 was used to simulate drawdown in the groundwater flow model. Comparatively, the test done with Siivilä 3 used a lower pumping rate than what was used for Siivilä 1. Figure 3.11a depicts the simulated drawdown distribution from Siivilä 3. A maximum drawdown of approximately 4.5 m was obtained at Siivilä 3. A west-east cross-section taken from where S3 is located shows the subsurface structure and that pumping is occurring from aquifer 1 (figure 3.11b).

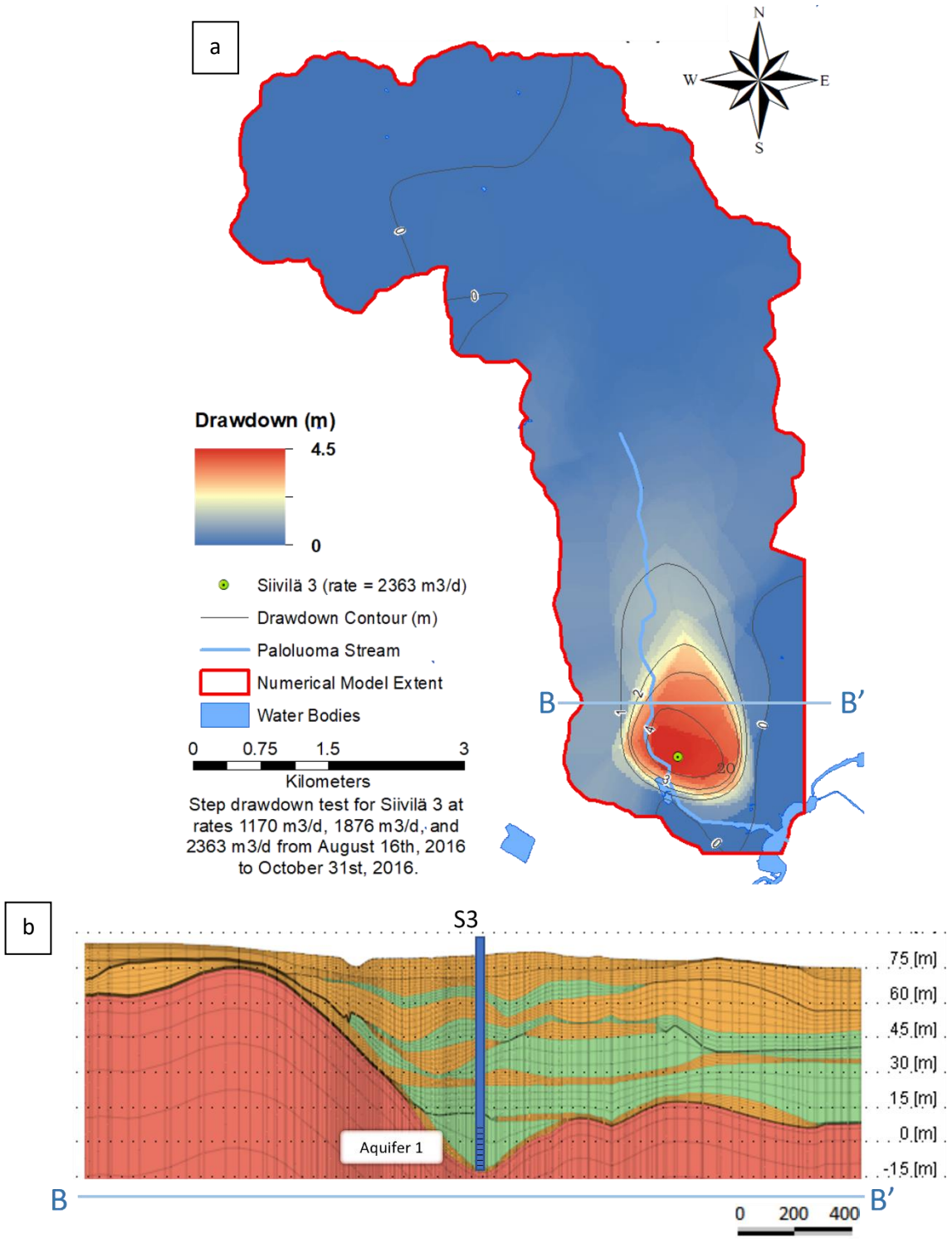

Figure 3.11: a) Simulated steady-state drawdown at Siivilä 3 at a pumping rate of 2363 m3d-1. Transect taken along pumping well location (B – B'). b) Cross-section depicting subsurface structure at Siivilä 3. Vertical exaggeration: 8X.

3.3.2.3 Maximum Pumping Conditions

The groundwater flow model was also used to explore the behaviour of the flow system under a maximum realistic pumping scenario. In this scenario, both S1 and S3 are active and pumping at a rate that is realistically the maximum pumping rate that the system will be exploited at for future use. The maximum realistic pumping scenario was defined by the Geological Survey of Finland and the Kurikan Vesihuolto Oy (Kurikka Water Company). Siivilä 1 and Siivilä 3 are assigned to simultaneously pump at a maximum realistic pumping rate of 3000 m^3d^{-1} and 2500 m^3d^{-1}, respectively. Figure 3.12a presents the drawdown distribution for the simulated maximum exploitation scenario. This figure is supplemented by the cross-sections at both S1 (figure 3.12b) and S3 (figure 3.12c) with the potentiometric surface under natural conditions and pumping condition comparisons. These results show that the maximum drawdown could be up to 7.5 m at the center of the watershed (at S1). This would mean that the potentiometric surface, represented by the blue dashed line, would drop from ~ 85 m to 77.5m at this location. Where S3 is located, a drawdown of approximately 4 m was simulated, which would mean that the potentiometric surface would drop from ~75 m to 71 m at this location. With this maximum level of exploitation, drawdown is extended quite far north but remains shallow relative to the depth of the valley.

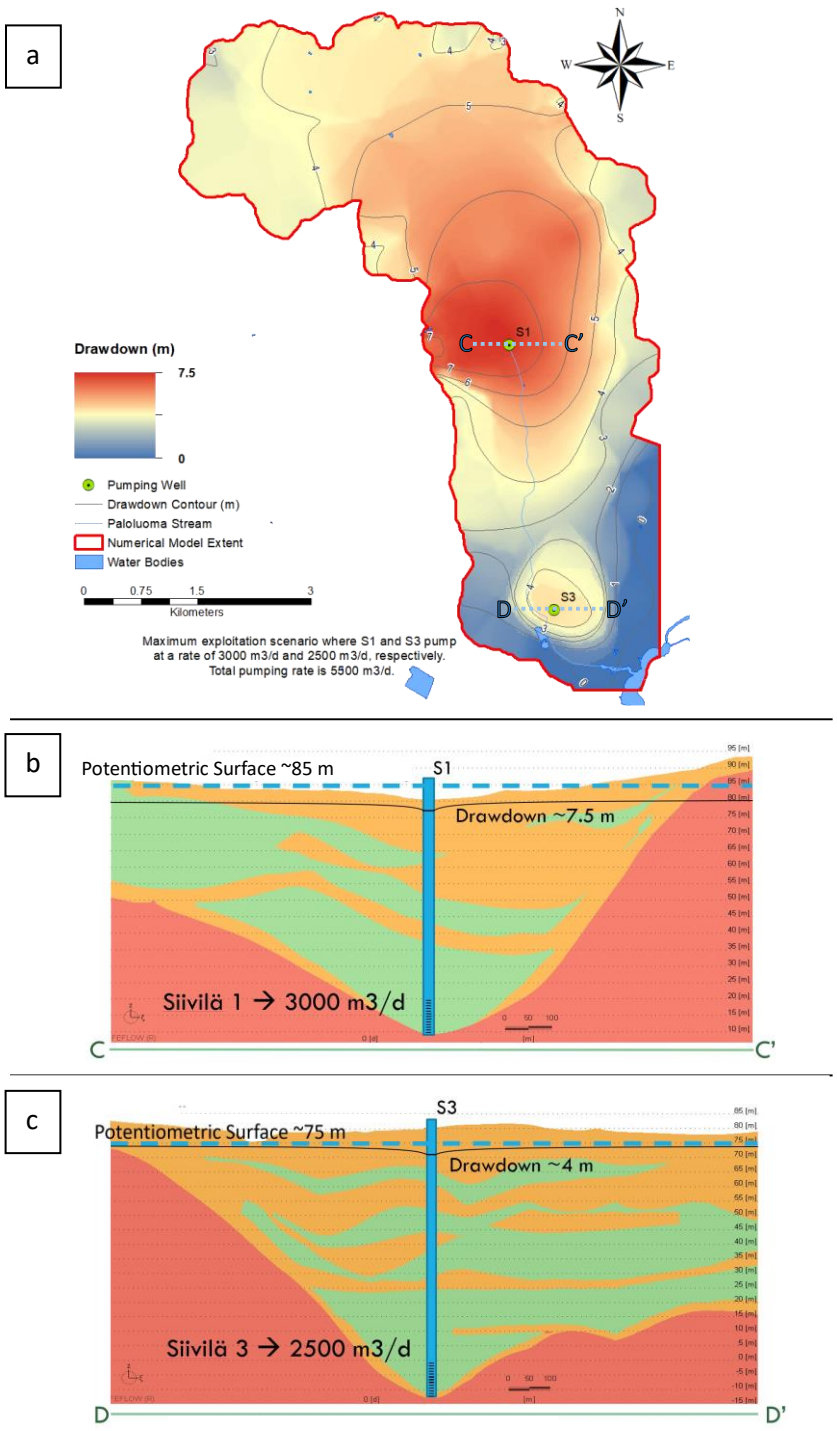

Figure 3.12: Maximum realistic groundwater extraction scenario. a) Plan view of simulated steady-state drawdown at both Siivilä 1 and Siivilä 3 at pumping rates of 3000 m3d-1 and 2500 m3d-1, respectively. Transects taken along pumping well locations (C – C' and D – D'). Cross-sections depicting the subsurface structure and potentiometric surface at b) Siivilä 1 and c) Siivilä 3. Vertical exaggeration: 8X.

3.3.3 Rate Budgets

In order to understand the inner workings of the flow model, we can look at the flux budget. Specifically, we can compare the flux at boundaries and specific locations of interest like recharge and discharge areas. The boundaries and areas of interest for flux budget analysis are presented in table 3.9 and include: (1) surficial recharge area, (2) the south outflow boundary (SB), which extends the entire depth of Quaternary sediments (~8 m - ~70 m thickness; slice 1 – 56), (3) the perimeter boundary (PB), which extends the entire depth of the Quaternary sediments as well as the top 17 m of bedrock (slice 1 – 60), (4) pumping, and (5) overall domain. The SB and PB are also described in section 3.2.3.

Results under natural conditions show that the system is in equilibrium where an outflux of ~3700 m^3d^{-1} is balanced by an influx of ~ 3700 m^3d^{-1}. Total outflux is occurring at the SB where the Paloluoma stream meets the Kyrönjoki River and deep aquifers extend to the neighbouring watershed. The majority of the outflux at this boundary is from the deep aquifers acting as a conduit beyond the Paloluoma BBV watershed. Total influx is solely attributed to recharge across the surface of the model domain. There is no flux at the PB, which encompasses the remaining surrounding perimeter of the watershed. There is a difference of just 1 m^3d^{-1} between flux in and flux out, which is an indication of a good numerical solution of the model.

Table 3.9 also depicts the flux budget for the model under pumping conditions for Siivilä 1. With pumping, the PB is "activated" and now an influx of ~2556 m^3d^{-1} of water is entering the system through this boundary. Compared to the model under natural conditions, the SB is allowing for less flux out to the system (~3072 m^3d^{-1}). Surficial recharge contribution remains at a total of ~3682 m^3d^{-1} as this is a fixed imposed rate. The combined increase of flux in from the PB and decrease of flux out from the SB facilitates pumping from the study area. The model reaches equilibrium at ~6237 m^3d^{-1}.

Aquifer 1 is the deepest aquifer from the Paloluoma BBV and S3 is pumping from the thickest portion of this aquifer. Looking at the rate budget table again, surficial recharge remains unchanged and contributes a flux into the model domain of ~ 3682 m^3d^{-1}. The PB contributes a relatively modest ~474 m^3d^{-1} as a flux into the model. However, the main change to the rate budget is that there is much less flux out of the SB (~1792 m^3d^{-1}) compared to the model under natural conditions as well as during S1 pumping. This means that water that would have been exiting the SB under natural conditions is now being intercepted by extraction from S3. Moreover, the fact that there is a decrease in flux out from the SB while S3 is pumping, verifies that the deep aquifers are the major contributors to the flux out of the system. Compared to pumping at S1, pumping at S3 does not rely as much on receiving water from the

outer boundaries of the study area (PB) due to the decreased flux out of the SB. The model reaches equilibrium at ~4155 m^3d^{-1}.

Finally, the rate budget table also depicts the results for the model under a maximum pumping scenario. Surficial recharge is fixed to contribute a flux in of ~3682 m^3d^{-1} and pumping from S1 and S3 at a rate of 3000 $m^3d^{-1}$and 2500 m^3d^{-1}, respectively, contributes an overall flux out of 5500 m^3d^{-1}.

Quantifying changes to the rate budget during varied groundwater exploitation scenarios is important to understand how the Paloluoma BBV flow system behaves in response to stress. Figure 3.13 presents a bar plot comparing rate budgets for the model under natural conditions and the three pumping programs/scenarios. The model under the maximum pumping scenario reacts as a combination of both flux dynamics from the previous pumping scenarios. Specifically, just as the S1-only model, a large portion of the total flux in was attributed from the PB while the SB only slightly contributed to the total flux out. The maximum pumping model exhibits this dynamic but at a greater rate such that water is being pulled into the system from the PB at a rate of ~2829 m^3d^{-1}. Compared to the S3-only model, the maximum pumping scenario also exhibited a decrease in flux out of the SB due to water exiting through pumping instead, while the PB only slightly increased. Overall, this maximum pumping scenario takes advantage of both the SB and PB in order to support pumping at the desired rate. The model reaches equilibrium at ~6511 m^3d^{-1}.

Table 3.9: Rate Budget for groundwater flow model under four scenarios as follows: natural conditions, S1-only conditions, S3-only conditions, and a maximum pumping scenario which includes S1 and S3 pumping at a rate of 3000 m^3d^{-1} and 2500 m^3d^{-1}, respectively.

Rate Budget (m^3d^{-1})

	Natural Conditions		Siivilä 1 Pumping Conditions		Siivilä 3 Pumping Conditions		Maximum Pumping Scenario	
	IN	**OUT**	**IN**	**OUT**	**IN**	**OUT**	**IN**	**OUT**
Surficial Recharge	3681.9	0	3681.9	0	3681.9	0	3681.9	0
South Boundary (SB)	0	3680.9	0	3071.6	0	1791.8	0	1010.6
Perimeter Boundary (PB)	0	0	2555.5	0	473.6	0	2828.6	0
Pumping Rate	0	0	0	3166	0	2363	0	5500
Entire Domain	3681.9	3680.9	6237.4	6237.6	4155.5	4154.8	6510.5	6510.6

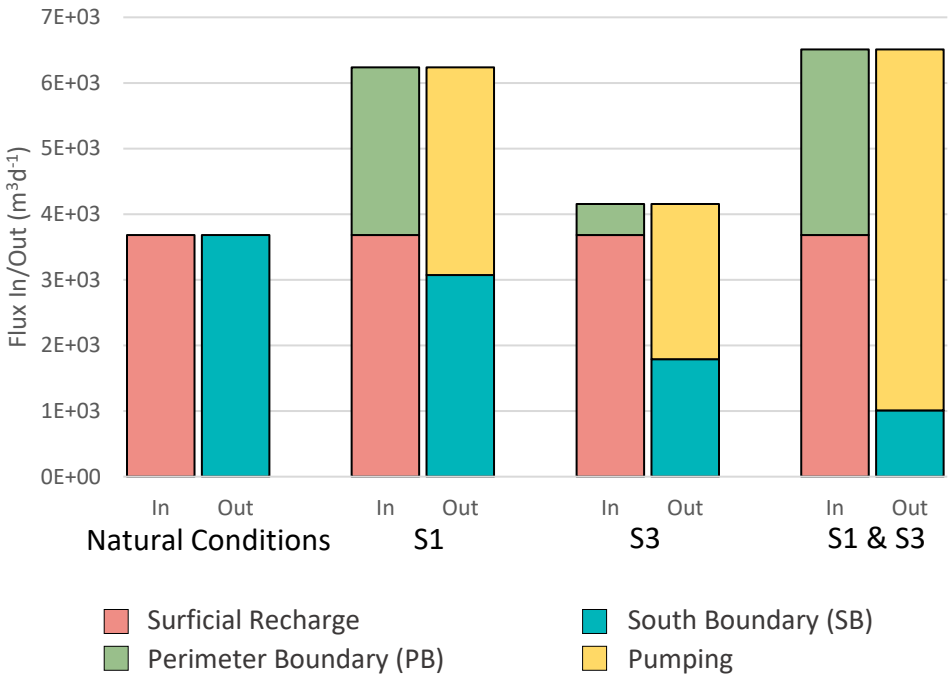

Figure 3.13: Bar plot of simulated groundwater flux budget comparisons under natural conditions and pumping conditions. Pumping conditions include the S1-only pumping model, S3-only pumping model, and the simultaneous S1 and S3 maximum pumping model.

3.3.4 Bedrock Contribution

To further understand the Paloluoma groundwater system, the potential interaction between bedrock and sediments was explored. The interaction between bedrock and sediment can be analysed by performing an internal transfer budget analysis at the bedrock-sediment interface. Figure 3.14 illustrates the internal transfer between bedrock and sediment rate budget under natural conditions and pumping conditions at S1 and S3. The same boundaries from the previous rate budget analyses are observed and include the recharge boundary at the surface of the model, the South Boundary (SB), the Perimeter Boundary (PB), and the pumping boundary. In addition, a fifth boundary is observed and illustrates the boundary between bedrock and sediment in purple in figure 3.14.

Beginning with the bedrock budget under natural conditions, a large portion of total flux into the system involves an internal transfer from sediment to bedrock. For total flux out, bedrock to sediment transfer accounts for 100%. Furthermore, total flux out, which consists only of bedrock to sediment internal transfer, is greater than total flux in.

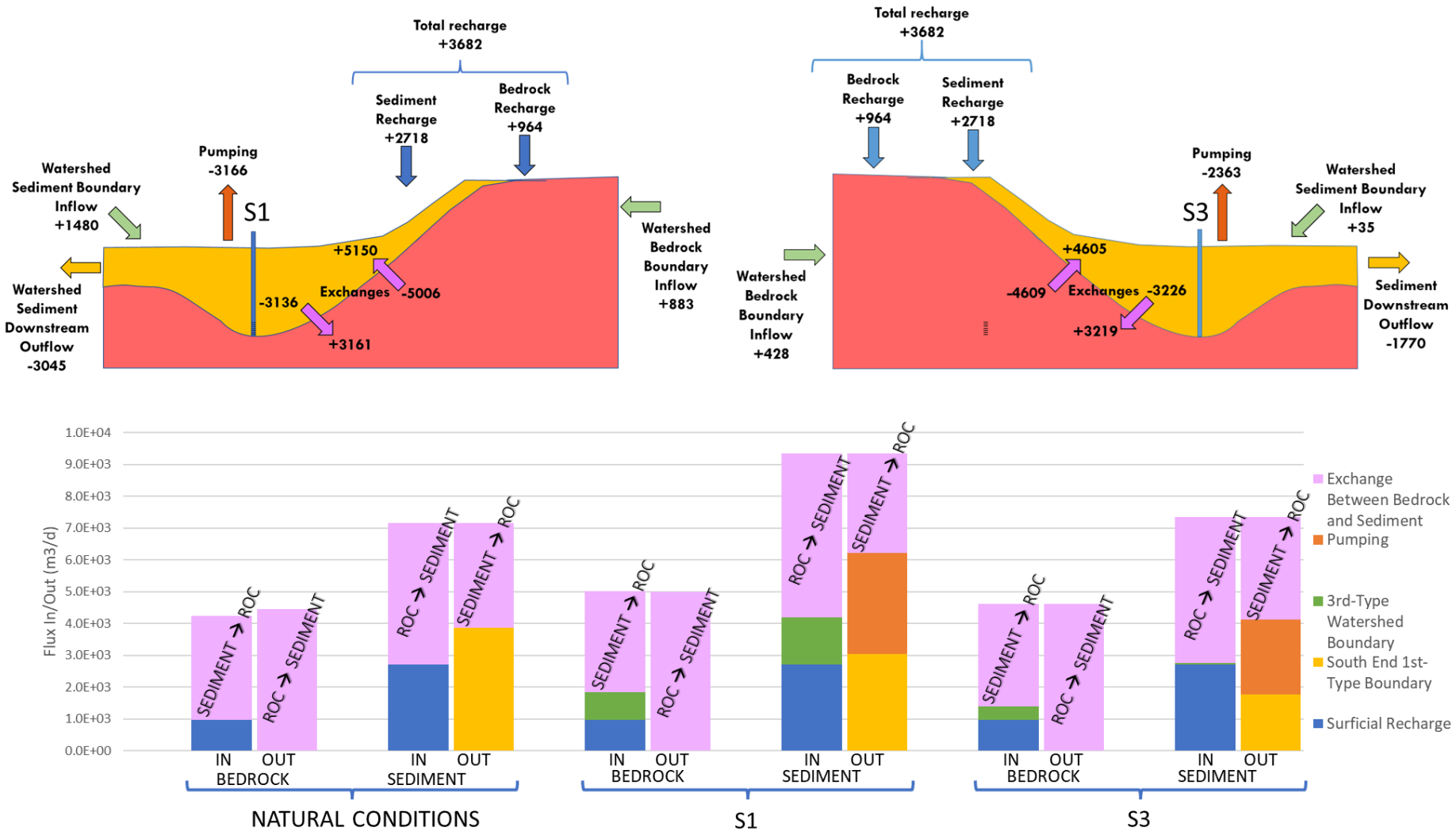

Figure 3.14: Paloluoma valley water balance for the simulation under S1-only (top left) and S3-only (top right) pumping conditions. Explicitly observing bedrock (ROC) to sediment internal transfer budget.

During the pumping cases, flow dynamics are similar. Figure 3.14 presents the flux rates at S1-only and S3-only conditions. For S1-only and S3-only pumping, the ratio between bedrock to sediment internal transfer remains consistent. There is not much variability. However, during S1-only pumping, more water is being pulled from bedrock than is being pulled during S3-only pumping. This is likely because S1 is pumping at a greater rate than S3 but also further supports the interpretation that pumping from S1 is supported by bedrock fractures or overlying units.

3.4 Discussion and Conclusion

The groundwater flow model developed to investigate the Paloluoma BBV hydrogeologic system is based on the current conceptual understanding of both the subsurface geology and hydrogeology of the study area. It is important to recognize that it is a simplification of reality with some parts of the model domain being more uncertain than others. The flow model is intended to be a tool for quantifying the valley's groundwater resources and to identify where more data may be needed. As there are simplifications, there are also assumptions that go along with the model that need to be considered when applying it as a tool. For instance, the hydrostratigraphic model, which the flow model is based on, has its own uncertainties that are now tied to the flow model as well. The main uncertainties are related to the geometry, thickness, and extent of the units in-between data (Anderson & Woessner, 1992; Refsgaard et al., 2012). These uncertainties are true for any geological or hydrostratigraphic model and are not unique to the Paloluoma BBV model. The hydrostratigraphic model was built using a deterministic approach, which is a good approach to ensure the model is geologically consistent; however, uncertainty is difficult to quantify with this approach (Bianchi et al., 2021).

One of the model uncertainties stems from the distribution and density of available data. For example, there is limited water level data in the north part of the study area. This leads to making assumptions about the water table in this area. Due to this constraint in available hydraulic head data in some areas, the approach to calibrate the model using synthetic observation points was favoured. The use of synthetic observation points to verify the model and also make meaningful predictions is not uncommon where data are sparse, but should also be considered for bias when analysing results of the model (Haworth et al., 2018; Limaye et al., 2006; Nair & Indu, 2020). Another point to consider is that the set of calibrated parameters produced from this study provides an optimal solution in regard to the objective functions (RMSE and NSE). However, a different set of parameters may give results that may

also be plausible. This is an ongoing problem related to the non-uniqueness issue in building models (Abbaspour, 2005).

From the three pumping conditions explored, pumping at Siivilä 3 produced the least drawdown both in terms of depth and extent. In addition to the fact that S3 was pumping at a lower rate than S1, the geology and subsurface structure at this location contributes to the lower drawdown. This is because S3 is pumping from the deepest aquifer in the valley, whereas S1 is pumping from a location with more nearby connectivity between aquifer units. Specifically, aquifer 2 that is pumped by S1 is more extensive laterally and perhaps more connected with other aquifers, i.e., less isolated, which means that it receives water from overlying/connected aquifers than deeper, more isolated aquifers (like aquifer 1 that is pumped by S3). This situation leads to greater and more laterally extensive drawdown during pumping at S1.

Another important difference relates to the source of the water between S1 and S3. From rate budget analyses, we have come to understand that at S1, there is likely contribution from upper aquifers, and/or the underlying bedrock, when pumping aquifer 2. In contrast, water extracted from S3 during pumping comes mainly from captured discharge that would have otherwise flowed out of the system in the absence of pumping, which is illustrated by the SB exhibiting a drastic drop in flux out during S3 pumping.

Furthermore, seeing how inflow and outflow compares between bedrock and sediment has further improved our understanding of the flow dynamics of the Paloluoma valley. However, geochemical analyses suggest minimal contribution from bedrock to sediment (Kietäväinen, 2015). Nonetheless, this bedrock rate budget analysis was still performed based on new suspicions of bedrock contribution. With these results and previous results from pumping data, there is a strong case to further explore bedrock structure.

Moreover, the system appears capable, based on rate budget analyses, to adapt to varying exploitation rates and ultimately reach equilibrium. However, the effects of the change in potentiometric surface on the local ecosystem is unknown as it is beyond the scope of this study. Future research may explore effects to surface water bodies in the northern region as well as possible effects on the biodiversity in the region.

It is in the best interest of the nearby municipalities to protect this resource as there may be detrimental environmental and socio-economic consequences if overexploited. As such, an improved

understanding of the aquifer system was required to make good decisions surrounding the use of the valley's groundwater resource. Being the first study of its kind in this region, this model provides the first step towards gaining a better understanding of the Paloluoma BBV hydrogeologic system. The resultant groundwater flow model can be used as a useful tool to manage the Paloluoma BBV's freshwater resource. Based on this initial model and the series of modelling experiments presented herein, the system under natural conditions limits inflow solely from recharge and outflow solely from the south end boundary. Furthermore, a sustainable rate of pumping could be achieved if limited to reasonable rates that bring the system to equilibrium. Nonetheless, modelling shows that such pumping at S1 would draw water from the adjacent valley to the west, therefore impacting an area that extends beyond the model domain considered in this study. It would thus be important to expand the model domain to include the other buried valleys around the Paloluoma BBV. It would also be important to reduce uncertainty by adding wells across the recharge area to the north, as well as by investigating the hydrogeology of the underlying bedrock unit. Future monitoring of the area during planned pumping should also be conducted to see how the real drawdown develops and to study how it may impact the ecosystem. Overall, management of the groundwater system is now aided with the groundwater flow model, which should be useful in guiding decisions and policies surrounding the use of this groundwater resource until new data from further studies, new modelling, and monitoring become available.

Chapter 4

Conclusion

This chapter first summarizes the key findings and contributions from each chapter of the thesis. Then, the important uncertainties and limitations of the flow model are described. Afterward, the findings from this study are placed into the broader context of previous studies. Finally, the main implications of this study are stated, and recommendations are made about potential future work.

4.1 Summary of Key Findings

The key findings of the Paloluoma BBV study are related to the characterization of the aquifer system, the conceptual model that was developed to represent the system, and the groundwater flow model aiming to provide a quantitative understanding of the system. The steps taken for each part of this study followed conventional flow model building practises that are commonly applied in the literature.

The characterization of the Paloluoma BBV aquifer system relied on methods such as water balances and pumping test analyses that were used to estimate hydraulic parameters such as groundwater recharge and hydraulic conductivity, respectively. In addition to estimating hydraulic parameters, hydrostratigraphic analysis and building of the 3D subsurface structure were also conducted. The initial stratigraphy of the valley was given hydraulic significance to build a series of aquifers and aquitards that shape the 3D hydrostratigraphic model. The 3D hydrostratigraphic model coupled with the estimated hydraulic parameters were used to construct the hydrogeological conceptual model of the aquifer system. The conceptual model is the foundation of the groundwater flow model as it is an amalgamation of key processes and parameters of the Paloluoma BBV groundwater system. The flow model is a valuable tool used to simulate the BBV environment and explore the aquifer's response to varying pumping rates in detail as well as to help identify long-term sustainable extraction rates.

The geological setting of the Paloluoma BBV was introduced in Chapter 1. In summary, the study area is a confined buried bedrock valley overlain with Quaternary sediment deposits that host a productive aquifer system. The area underwent a successive series of ice margin oscillations of the Fennoscandian Ice sheet, as it lies in an interlobate zone where adjacent ice lobes interacted. As a result of the complex glacial history of the study area, sediments accumulated in the subsurface of the valley

are highly complex in their interstratification. The complicated internal structure produces a sediment assemblage such that several coarse sand and gravel deposits are interbedded with matrix-rich till sheets and fine-grained units (e.g., glaciomarine). The surface of the valley is also quite variable from one end of the study area to the other end, which has an important control over the spatial distribution of recharge. The center of the study area is characterized predominantly by clay and silt deposits, which record relatively short-lived marine inundation and retreat phases. The northern highland region of the area is characterized by raised beach ridges, which represent the net effect of both the eustatic sea level rise and isostatic rebound (Sutcliffe et al., 2000). Erosional events have resulted in bedrock outcrops at topographic highs. As a result of these events, a variety of hydrofacies having distinct hydraulic properties were delineated and described in detail in Chapter 2. This work was performed as part of building the conceptual model.

From Chapter 2, which explored the conceptual model, an improved conceptual understanding of the Paloluoma BBV was achieved, especially with respect to hydraulic parameters, processes, and hydrostratigraphy. With respect to hydraulic parameters, multiple conventional methods based on the literature were used to estimate hydraulic conductivity and recharge. Specifically, sediment information from borehole logs, pumping test analyses, and hydrostratigraphic geometry were used to estimate hydraulic conductivity. As well, the water balance method, groundwater flux method, surficial geological information, and hydrostratigraphic structure were used to estimate recharge and the extent of recharge zones. From the results of these methods, additional information such as aquifer behaviour and hydraulic boundaries of the system were interpreted. Specifically, pumping test analyses indicated that the Paloluoma BBV aquifer behaves in a leaky fashion and that a positive boundary limit is present. This suggests that the aquifer units may be receiving groundwater from another source. The hydrostratigraphic unit geometry and structure information was solved through the construction of the 3D hydrostratigraphic model. The 3D hydrostratigraphic model presents the subsurface structure of the Paloluoma BBV. There is a total of seven aquitards stratigraphically alternating with seven aquifers. Processes and information that were interpreted based on the hydrostratigraphic model include preferential flow pathways, boundaries, and notable aquifer features.

The conceptual model from chapter 2 offers key findings, which are summarized in this paragraph. Groundwater flow direction was found to generally occur from north to south. There was minimum groundwater interaction between surface water bodies and subsurface units due to thick and continuous fine-grained deposits in the south and central region of the study area (including areas that

underlain the Paloluoma Stream), which act as a barrier. However, small springs in the north are fed by groundwater. Accordingly, since the central and south regions are dominated with fine-grained deposits, these areas are considered poor recharge zones. On the contrary, the north and northwestern region of the study area, where topographic highs area observed and coarse-grained sediments dominate, good recharge zones were inferred. Recharge rates determined through a water balance and the groundwater flux method were estimated to be approximately 80 mm/a. From these methods, a possible range of 35 mm/a to 150 mm/a depending on the year, was determined for recharge. Pumping tests indicated that the aquifer behaves in a confined and leaky nature. Local flow pathways between aquifers can be interpreted to be present on account of direct vertical unit connectivity in the central region of the study area between aquifers two and five. This suggests that flow from shallow aquifers to deep aquifers is possible. Further exploration of the study area using geophysical methods has also led to the identification of permeable structures within the bedrock which supports earlier suspicions and could also greatly contribute to the leaky flow behaviour found during pumping test analysis. Being the first study of its kind in the region, future research around the region can be supported with this study. Assembling the interpretations and results from each of these methods, developed the Paloluoma BBV conceptual model.

In Chapter 3, the constructed conceptual model was used to build the numerical flow model, which was critical to obtain a quantitative understanding of the Paloluoma BBV hydrogeological system. To this end, four simulation goals/scenarios were addressed: (1) produce steady-state stabilized conditions, (2) verify the model with field pumping observations, (3) understand where water is coming from and going to, and (4) explore what could be the future maximum sustainable pumping scenario. Also, from the construction of the flow model to the exploration of pumping scenarios, this chapter detailed the workflow at each step. The flow model was constructed with the conceptual model as its foundation. Thus, both models share the same characteristics, extent, and boundaries. The flow model is structured using a finite element numerical grid and code to simulate groundwater flow dynamics. The finite element grid was generated with a 2D supermesh, which is the framework of all basic geometric information the flow modelling software, FEFLOW, algorithm requires (Diersch, 2014). The 2D mesh is extended in the z-direction and in the process, triangular elements become triangular prisms, which model layers are comprised of. There are a total of 66 layers that compose the 15-unit model. The total number of nodes and elements that make up the model is 2 396 992 and 4 632 926, respectively. Once constructed, the flow model is calibrated to verify its reliability to simulate field conditions. Successful model calibration then allows the exploration of the system under various pumping scenarios. Of these

scenarios, a maximum realistic pumping scenario is studied to model the effect that such a level of exploitation has on the Paloluoma BBV groundwater system. These scenarios are studied and quantified using rate budgets at specific boundaries of interest. The change and comparison between scenarios at each boundary provide insight into how key areas of the model react to varying pumping rates. With this knowledge, previous understandings of the system are improved. Specifically, understandings of groundwater flow dynamics, connections between recharge and discharge areas, and aquifer response to pumping are improved. In conclusion, the groundwater flow model can be used as a useful tool for quantifying the valley's groundwater resources and exploring varying pumping scenarios. Once quantified, the nearby Town of Kurikka and Vaasa will have the proper tools to make effective decisions surrounding the sustainability of their groundwater resource system. It is in the best interest of the nearby municipalities to protect this resource as there may be detrimental environmental and socio-economic consequences if overexploited. These consequences are explained in a later section.

In summary, key findings from chapter 3 include flow dynamics under natural conditions showing particle pathways travelling from shallow to deep aquifers across the model domain to discharge areas, which are dominated by deeper aquifers that extend across sub-basins. Flow dynamics under pumping conditions were quite different and varied depending on pumping location. The source of water for production well, Siivilä 1, is likely contributed from upper aquifers or underlying bedrock when pumping from aquifer 2. Drawdowns induced by pumping at Siivilä 1 reach the watershed boundary and thus capture groundwater coming from outside of the Paloluoma BBV system. The source of groundwater at production well, Siivilä 3, which is pumping from aquifer 1, mainly comes from captured discharge that would have otherwise flowed out of the system in the absence of pumping. The maximum pumping scenario that was explored utilized both source areas for water for ultimate extraction. Also from rate budget analyses, interaction at the bedrock and sediment interface showed quite significant activity, enough to recommend further research about bedrock structure in the area. The maximum pumping scenario (5500 m^3d^{-1}) was found to be sustainable in terms of groundwater availability but it draws groundwater from outside of the watershed and reduces outflow out of the watershed. Groundwater production in the valley thus has impacts outside of the watershed that will need to be considered if other production wells are operated in adjacent watersheds.

4.2 Uncertainties and Limitations

Uncertainties and limitations of the Paloluoma BBV model must also be considered. After all, the groundwater flow model developed of the Paloluoma BBV is a simplification of reality. As there are

simplifications, there are assumptions that go along with the model that need to be considered when applying it as a tool. For instance, the hydrostratigraphic model, which the flow model is based on, has its own uncertainties that are now tied to the flow model as well. Such uncertainties include errors in the geometry, thickness, and extent of the units (Anderson & Woessner, 1992; Refsgaard et al., 2012). These uncertainties are true for any geological or hydrostratigraphic model and are not unique to the Paloluoma BBV model.

One of the model limitations is sourced from the available data at hand for the project. For example, there is limited data for water level in the north part of the study area, which required assumptions about the water table and recharge in this area which is quite important for groundwater renewal in the aquifer system. Due to the limited availability of hydraulic head data in some areas, the approach to calibrate the model using synthetic observation points was necessary and effective. The use of synthetic observation points to verify a model and also make meaningful predictions is not uncommon where data is sparse, but should also be considered for bias when analysing results of the model (Haworth et al., 2018; Limaye et al., 2006; Nair & Indu, 2020). Another area of uncertainty includes the presence of bedrock fractures. Suspicion of the presence of bedrock fractures is heightened and may play a larger role in the groundwater system than initially suspected. Another point to consider is that while the set of calibrated parameters produced from this study provides an optimal solution in regard to the objective functions (RMSE and NSE), a different set of parameters may provide just as good of results. This is an ongoing problem related to the non-uniqueness issue present during model building (Abbaspour, 2005). Moreover, the flow model was designed based on the current hydrometeorological and hydrogeological conditions of the region. If these conditions were to change or improved data was acquired from additional fieldwork, the flow model would require updating to continue to effectively represent the study site. As a result of the model-building process and analysis of the flow model results, more questions or uncertainties have been identified. That is to say, more detailed gaps in the knowledge of the system have been distinguished. For example, questions about the hydrogeological characteristics of the northern region of the study area including water levels under natural conditions and pumping conditions, as well as questions about the significance of the role that the bedrock-sediment interface plays, which in turn raises questions about the structure of bedrock. These gaps are a good starting point to address for the next stage of research.

4.3 Comparing Previous Studies to the Paloluoma BBV

Previous studies that have investigated aquifer systems via groundwater modelling that have set the standard when exploring sustainable groundwater extraction are compared and contrasted to the Paloluoma BBV in this section. These studies share a common goal as this study, which is to develop an improved understanding of an aquifer system. They utilize state-of-the-art flow modelling processes that are now commonly used and documented in the literature that will guide pumping and management plans. Examples of such studies include research on the aquifer system of Southwestern Quebec and the Waterloo Moraine. It should be noted that these studies while sharing the same goal as this thesis, were conducted by larger teams over several years. For context, it is useful to again specify that the Paloluoma BBV study is the first study of its kind in the region.

Beginning with the aquifer system of SW Quebec, Savard et al. (2013) produced a study that encompassed multiple sites including the Chatham quarry, St-Eustache quarry, Saint-Benoît, Saint-Janvier and Sainte-Anne-des-Plaines within its 1500 km^2 study area. The aquifer system is predominantly hosted at the interface of the fractured sedimentary rocks and the directly overlying layer of glaciofluvial Quaternary sediments. The glaciofluvial Quaternary sediments layer is thin in comparison to its overlying till and proglacial fine-grained layers that provide semi-confined to confined conditions, especially along buried valleys. There are three main buried valleys within the study area that are filled predominantly by fine-grained sediments deposited in the Champlain Sea, a short-lived inland sea that inundated the St. Lawrence valley during deglaciation of the region.

The regional aquifer of the SW Quebec system is different from the Paloluoma BBV system in that the former consists of elongated glaciofluvial deposits directly overlying fractured sedimentary rocks. It is thus a mixed porous/fractured aquifer system (rock/sediment interface). In contrast, the Paloluoma BBV hydrostratigraphy contains more interlayered aquifers-aquitards and the sequence is overlying igneous rocks for which little is still known about its fracture network and density. However, the two studies are similar to one another in the sense that both study areas were inundated by a postglacial inland sea which deposited several meters of fine-grained material layering the buried valleys of comparable size, which provide semi-confined to confined conditions. Moreover, the Quaternary aquifers from both studies consist, at least in part, of glaciofluvial deposits mostly composed of coarse sand and gravel. Future studies of the Paloluoma BBV should provide important new information about the underlying fractured bedrock and what role it plays in the regional groundwater system.

Regarding assessing hydraulic parameters and building models to determine sustainable pumping rates, the two studies follow a similar workflow. Both studies begin with characterizing the aquifer system and hydrogeology, which is followed by assessing hydraulic parameters like recharge and hydraulic conductivity. While the workflow is similar, there are differences in methods between the two studies. For example, when assessing hydraulic parameters, the Savard et al. study used lysimeters, monitored water levels from observation wells, and applied a water balance method to estimate local recharge. Of these approaches, the Paloluoma BBV study applied a water balance method to estimate recharge, but also applied the groundwater flux method. The rate of recharge is 45 mm/a and 50 mm/a for the Savard et al. study and the Paloluoma BBV study, respectively. These rates are similar as the climates of the two regions are also similar (SW Quebec is under the Dfb Köppen climate classification whereas West Finland is under the Dfc classification; the main difference being that the summers are warmer in SW Quebec compared to West Finland). Recharge areas are also similar as they occur via coarse material or by bedrock outcrops in both studies. Savard et al. took things a step further and estimated recharge at the regional scale using the Darcy method (Nimmo et al., 1994; Sammis et al., 1982). Since the study area for the Paloluoma BBV is much smaller than the aquifer system of SW Quebec, it was not necessary to estimate recharge at a greater scale. Another key difference between the two studies is that the region of SW Quebec is more populated and its aquifer system is pumped at a higher rate than the Paloluoma BBV region and system.

Another aquifer system to compare with the Paloluoma BBV study is the Waterloo Moraine in Ontario, Canada. The Waterloo Moraine has been highly studied because it provides the main source of freshwater for a fast-growing municipality (Bajc et al., 2014, 2018; Blackport et al., 2014; Meyer et al., 2014). It lies in a complex interlobate glaciofluvial zone, similar to the Paloluoma BBV zone but there are no moraine-type (positive-relief) features within the Paloluoma BBV region because it is a valley; sediments filled a depression instead of forming a broad positive-relief deposit on the landscape. This difference of course has implications for the hydrogeological system. Nonetheless, the similar interlobate setting influenced by oscillating ice margins and glacial lake impoundments have led to highly heterogeneous hydrostratigraphy in both cases. When it comes to hydrostratigraphic delineation, both studies implemented similar strategies. As previously mentioned, the Paloluoma BBV 14 hydrostratigraphic layered model was delineated using borehole to bedrock logs and glacial history. In comparison, Bajc and Shirota (2007) delineated 19 hydrostratigraphic layers for the Waterloo Moraine using borehole logs, glacial history, and geophysical profiles. To analyse the effect of varying pumping rates, both regions were modelled using the finite element method. Meyer et al. (2014) explored

varying pumping rates, groundwater recharge and climate variability, to produce multiple realizations of capture zone data to reduce subjectivity. While the Paloluoma BBV study explored most of these variables, one variable it did not explore is climate variability. This can be explored in future research. Also, the Paloluoma BBV aquifer system is not as heavily exploited as the Waterloo Moraine, which supports a much larger population. Studies surrounding the Waterloo Moraine have also explored possible negative environmental effects that could result from mismanagement of the aquifer. For example, if left unmanaged, sensitive surface water features could be subjected to more than a 10% reduction in baseflow (Meyer et al., 2014). Such studies should also be performed for the Paloluoma BBV region in the future.

In support of managing groundwater, there has been an extensive monitoring system deployed across the Waterloo Moraine area that helps support various efforts including drinking water source protection, low water response, climate change studies, planning application and academic research. This system continuously records water levels and temperature on an hourly basis (GRCA, 2020). The Paloluoma region could also benefit from implementing such a monitoring system.

4.4 Implications and Recommendations

The knowledge gathered from this study and the data/results presented by the flow model provides the first step towards the protection of the groundwater resource and is part of an ongoing process to ensure sustainable management of the Paloluoma BBV. From this study, an overall improved understanding of the Paloluoma BBV was achieved. The resultant groundwater flow model explored exploitation opportunities and analysed flux dynamics under a maximum realistic pumping scenario. The flow model results coupled with the three-month long pumping tests from 2014 and 2015, which in itself expresses sustainable extraction, have established a good understanding of the system and demonstrates some certainty regarding sustainable extraction.

This maximum pumping scenario, while achievable, may undergo some consideration as multiple wells were active and there may be some degree of interaction between these wells. Moreover, under this maximum pumping scenario, neighbouring watersheds, specifically to the west, are impacted, which may govern further investigation around the Paloluoma region. This impact is largely from Siivilä 1 as it exploits shallower aquifers and draws water from the west boundary. Therefore, pumping rates at Siivilä 1 could be reduced to mitigate these outcomes and instead, increasing the pumping rate at Siivilä 3 may be explored. Likewise, in the future, the flow model can be

used as a tool to make effective decisions surrounding the sustainability of the GW resource system. Future research in the region should be emphasized around the sustainability of each pumping scenario and work towards constructing a monitoring and management plan that considers the adverse effects of over-pumping. These adverse effects include but are not limited to 1- changes in surface water bodies, 2- changes to biota, 3- reduction in aquifer storage, and 4- changes in groundwater quality. While groundwater quality is not an issue for the Paloluoma BBV groundwater system currently, increased exploitation may reduce subsurface residence times, which may cause contaminated water to be drawn. A monitoring system should be implemented to characterize and detect changes in groundwater geochemistry over time. Also, it is important to monitor the water levels to ensure they do not fall below safe levels. The monitoring system will ensure that the productive aquifer system is not exploited beyond its means. Furthermore, as the nearby municipalities grow, anthropogenic use should also be measured. As previously mentioned, this study has indicated important uncertainties about the system, which itself will also drive future research. Applying the practises and knowledge from this study towards assessing an aquifer, especially one as complex as this one, will benefit researchers and industry members when considering similar areas.

Bibliography

Abbaspour, K. C. (2005). Calibration of hydrologic models: When is a model calibrated? *International Congress on Modelling and Simulation: Advances and Applications for Management and Decision Making, MODSIM05*, 2449–2455.

Anderson, M. P. & Woessner, W. W. (1992). *Applied Groundwater Modeling. Simulation of flow and advective transport* (2nd ed.). Elsevier Inc.

Bajc, A. F., Marich, A. S., Priebe, E. H. & Rainsford, D. R. B. (2018). Evaluating the groundwater resource potential of the dundas buried bedrock valley, southwestern Ontario: An integrated geological and hydrogeological case study. *Canadian Journal of Earth Sciences*, *55*(7), 659–676. https://doi.org/10.1139/cjes-2016-0224

Bajc, A. F., Russell, H. A. J. & Sharpe, D. R. (2014). A three-dimensional hydrostratigraphic model of the Waterloo Moraine area, southern Ontario, Canada. *Canadian Water Resources Journal*, *39*(2), 95–119. https://doi.org/10.1080/07011784.2014.914794

Bajc, A. F. & Shirota, J. (2007). *Three-dimensional mapping of surficial deposits in the Regional Municipality of Waterloo, southwestern Ontario. Groundwater Resources Study 3.*

Barthel, R., Stangefelt, M., Giese, M., Nygren, M., Seftigen, K. & Chen, D. (2021). Current understanding of groundwater recharge and groundwater drought in Sweden compared to countries with similar geology and climate. *Https://Doi.Org/10.1080/04353676.2021.1969130*. https://doi.org/10.1080/04353676.2021.1969130

Beaudry, C., Lefebvre, R., Rivard, C. & Cloutier, V. (2018). Conceptual model of regional groundwater flow based on hydrogeochemistry (Montérégie Est, Québec, Canada). *Canadian Water Resources Journal*, *43*(2), 152–172. https://doi.org/10.1080/07011784.2018.1461579

Betancur, T., Palacio T., C. A. & Escobar M., J. F. (2012). Conceptual Models in Hydrogeology, Methodology and Results. In *Hydrogeology - A Global Perspective*. InTech. https://doi.org/10.5772/28155

Bianchi, M., Turner, A. K., Lark, M. & Courrioux, G. (2021). Uncertainty in Geological Models. In *Applied Multidimensional Geological Modeling: Informing Sustainable Human Interactions with the Shallow Subsurface* (pp. 273–294). Wiley.

Bierkens, M. F. P. & Wada, Y. (2019). Non-renewable groundwater use and groundwater depletion: a review. *Environmental Research Letters*, *14*(6), 063002. https://doi.org/10.1088/1748-9326/ab1a5f

Blackport, R. J., Meyer, P. A. & Martin, P. J. (2014). Toward an understanding of the Waterloo Moraine hydrogeology. *Canadian Water Resources Journal*, *39*(2), 120–135. https://doi.org/10.1080/07011784.2014.914795

Boulton, G. S., Dongelmans, P., Punkari, M. & Broadgate, M. (2001). Palaeoglaciology of an ice sheet through a glacial cycle: the European ice sheet through the Weichselian. *Quaternary Science Reviews*, *20*, 591–625.

Bredehoeft, J. D. (2005). The conceptualization model problem - Surprise. *Hydrogeology Journal*, *13*(1), 37–46. https://doi.org/10.1007/s10040-004-0430-5

Cloutier, V., Lefebvre, R., Savard, M. M., Bourque, E. & Therrien, R. (2006). Hydrogeochemistry and groundwater origin of the Basses-Laurentides sedimentary rock aquifer system. *Hydrogeology Journal*, *14*, 573–590. https://doi.org/10.1007/s10040-005-0002-3

Cooper, H. H. & Jacob, C. E. (1946). A generalized graphical method for evaluating formation constants and summarizing well field history. *Am Geophys. Union Trans.*, *27*, 526–534.

Cummings, D. I., Russell, H. A. J. & Sharpe, D. R. (2012). Buried-valley aquifers in the Canadian prairies: Geology, hydrogeology, and origin. In *Canadian Journal of Earth Sciences* (Vol. 49, Issue 9, pp. 987–1004). https://doi.org/10.1139/E2012-041

De Graaf, I. E. M., Van Beek, L. P. H., Wada, Y. & Bierkens, M. F. P. (2014). *Dynamic attribution of global water demand to surface water and groundwater resources: Effects of abstractions and return flows on river discharges*. https://doi.org/10.1016/j.advwatres.2013.12.002

DHI-WASY. (2016). *FEFLOW 7.0 User Guide*. 124.

Diersch, H. J. G. (2014). *FEFLOW: Finite element modeling of flow, mass, and heat transport in porous and fractured media*. Springer-Verlag.

Domenico, P. A. & Schwartz, F. W. (1990). *Physical and Chemical Hydrogeology*. John Wiley and Sons.

Dreimanis, A., Goldthwait, R. P. & Matsch, C. L. (1989). Tills: their genetic terminology and classification. In *Genetic Classification of Glaciogenic Deposits* (pp. 17–84). A.A. Balkema.

Dyke, A. S. (2009). Laurentide ice sheet. In *Encyclopedia of Earth Sciences Series* (pp. 45–51). Springer Netherlands. https://doi.org/10.1007/978-1-4020-4411-3_128

Enemark, T., Peeters, L. J. M., Mallants, D. & Batelaan, O. (2019). Hydrogeological conceptual model building and testing: A review. *Journal of Hydrology*, *569*(July 2018), 310–329. https://doi.org/10.1016/j.jhydrol.2018.12.007

Evans, D. J. A., Phillips, E. R., Hiemstra, J. F. & Auton, C. A. (2006). Subglacial till: Formation, sedimentary characteristics and classification. *Earth-Science Reviews*, *78*(1–2), 115–176. https://doi.org/10.1016/j.earscirev.2006.04.001

Eyles, C. H., Eyles, N., Dalrymple, R. W. & James, N. P. (2010). Glacial Deposits. In *Facies Model 4, Geotext 6* (pp. 73–104). St. John's, Nfld.: Geological Association of Canada.

Fetter, C. W. (2001). *Applied Hydrogeology* (4th ed.). Prentice-Hall Inc.

Freeze, R. A. & Cherry, J. A. (1979). *Groundwater* (1st ed.). Prentice-Hall Inc.

Gleeson, T., Alley, W. M., Allen, D. M., Sophocleous, M. A., Zhou, Y., Taniguchi, M. & Vandersteen, J. (2011). *Towards Sustainable Groundwater Use: Setting Long-Term Goals, Backcasting, and Managing Adaptively*. https://doi.org/10.1111/j.1745-6584.2011.00825.x

GRCA Groundwater Resources Group. (2020). *Regional Groundwater Monitoring in the Grand River Watershed*.

Hantush, M. S. (1959). Nonsteady flow to flowing wells in leaky aquifers. *Journal of Geophysical Research*, *64*(8), 1043–1052.

Haworth, T. J., Glover, S. C. O., Koepferl, C. M., Bisbas, T. G. & Dale, J. E. (2018). Synthetic observations of star formation and the interstellar medium. *New Astronomy Reviews*, *82*, 1–58. https://doi.org/10.1016/j.newar.2018.06.001

Healy, R. W. (2010). *Estimating Groundwater Recharge*. Cambridge University Press. https://books.google.ca/books?hl=en&lr=&id=xAr3FoL2KngC&oi=fnd&pg=PR1&ots=htARJJNj7e&sig=RUw3sWlQXP8h66XBvYb9iWtaP8U&redir_esc=y#v=onepage&q&f=false

Hickin, A. S., Kerr, B., Turner, D. G. & Barchyn, T. E. (2008). Mapping Quaternary paleovalleys and drift thickness using petrophysical logs, northeast British Columbia, Fontas map sheet, NTS 94I. *Canadian Journal of Earth Sciences*, *45*(5), 577–591. https://doi.org/10.1139/E07-063

Janos, D., Molson, J. W. & Lefebvre, R. (2018). Regional groundwater flow dynamics and residence times in Chaudière-Appalaches, Québec, Canada: Insights from numerical simulations. *Canadian Water Resources Journal*, *43*(2), 214–239. https://doi.org/10.1080/07011784.2018.1437370

Jørgensen, F. & Sandersen, P. B. E. (2006). Buried and open tunnel valleys in Denmark-erosion beneath multiple ice sheets. *Quaternary Science Reviews*, *25*, 1339–1363. https://doi.org/10.1016/j.quascirev.2005.11.006

Katko, T. S. (2016). *Finnish Water Services: Experiences in Global Perspective*. IWA Publishing.

Kazemi, G. A., Lehr, J. H. & Perrochet, P. (2006). *Groundwater Age* (1st ed.). John Wiley & Sons, Inc.

Kietäväinen, R. (2015). *Kurikan Kuusistonloukon syväpohjaveden isotooppitutkimukset*.

Kløve, B., Kvitsand, H. M. L., Pitkänen, T., Gunnarsdottir, M. J., Gaut, S., Gardarsson, S. M., Rossi, P. M. & Miettinen, I. (2017). Overview of groundwater sources and water-supply systems, and associated microbial pollution, in Finland, Norway and Iceland. *Hydrogeology Journal*, *25*(4), 1033–1044. https://doi.org/10.1007/s10040-017-1552-x

Konikow, L. F. & Kendy, E. (2005). Groundwater depletion: A global problem. *Hydrogeology Journal*, *13*, 317–320. https://doi.org/10.1007/s10040-004-0411-8

Kresic, N. (1997). *Quantitative Solution in Hydrogeology and Groundwater Modelling*. Lewis Publishers.

Kresic, N. & Mikszewski, A. (2013). *Hydrogeological Conceptual Site Models: Data Analysis and Visualization*. Taylor & Francis Group.

Kruseman, G. P. (1994). *Analysis and Evaluation of Pumping Test Data Second Edition (Completely Revised)*.

Kurki, V., Lipponen, A. & Katko, T. S. (2013). Managed aquifer recharge in community water supply: The Finnish experience and some international comparisons. *Water International*, *38*(6), 774–789. https://doi.org/10.1080/02508060.2013.843374

Lavigne, M. A., Nastev, M. & Lefebvre, R. (2010). Numerical simulation of groundwater flow in the Chateauguay River aquifers. *Canadian Water Resources Journal*, *35*(4), 469–486. https://doi.org/10.4296/cwrj3504469

Lefebvre, R., Maltais, I., Paradis, D. & Michaud, Y. (2011). Recharge assessment from daily soil moisture

balance and well hydrographs for the Portneuf unconfined aquifers. *Proceedings of Geohydro 2011*, 1–8. https://www.researchgate.net/publication/235342181_Recharge_assessment_from_daily_soil_moisture_balance_and_well_hydrographs_Portneuf_unconfined_aquifer_Canada

Limaye, A. S., Crosson, W. L. & Laymon, C. A. (2006). Estimating accuracy in optimal deconvolution of synthetic AMSR-E observations. *Remote Sensing of Environment*, *100*, 133--142. https://doi.org/10.1016/j.rse.2005.10.008

Luoma, S. (2012). *South Finland Office Land Use and Environment 30.03*. http://tupa.gtk.fi/raportti/arkisto/57_2012.pdf

Maxey, G. B. (1964). Hydrostratigraphic units. *Journal of Hydrology*, *2*(2), 124–129. https://doi.org/10.1016/0022-1694(64)90023-X

Meyer, P. A., Brouwers, M. & Martin, P. J. (2014). A three-dimensional groundwater flow model of the Waterloo Moraine for water resource management. *Canadian Water Resources Journal*, *39*(2), 167–180. https://doi.org/10.1080/07011784.2014.914800

Misstear, B. D. R., Brown, L. & Johnston, P. M. (2009). Estimation of groundwater recharge in a major sand and gravel aquifer in Ireland using multiple approaches. *Hydrogeology Journal*, *17*, 693–706. https://doi.org/10.1007/s10040-008-0376-0

Mook, W. G. (2006). *Introduction to Isotope Hydrology: Stable and Radioactive Isotopes of Hydrogen, Carbon, and Oxygen* (1st ed.). Taylor & Francis Group.

Nair, A. S. & Indu, J. (2020). Reservoir Water Surface Area Detection using Satellite observations for synthetic SWOT data simulation. *Proceedings of the 2020 International Conference on Smart Innovations in Design, Environment, Management, Planning and Computing, ICSIDEMPC 2020*, 160–163. https://doi.org/10.1109/ICSIDEMPC49020.2020.9299637

Nash, J. E. & Sutcliffe, J. V. (1970). River flow forecasting through conceptual models part I — A discussion of principles. *Journal of Hydrology*, *10*(3), 282–290. https://doi.org/10.1016/0022-1694(70)90255-6

Nimmo, J. R., Stonestrom, D. A. & Akstin, K. C. (1994). The feasibility of recharge rate determinations using the steady-state centrifuge method. *Soil Science Society of America Jounral*, *58*(1), 49–56.

Nironen, M. (2005). Chapter 10 Proterozoic orogenic granitoid rocks. *Developments in Precambrian Geology*, *14*(C), 443–479. https://doi.org/10.1016/S0166-2635(05)80011-8

Nironen, M. (2017). GUIDE TO THE GEOLOGICAL MAP OF FINLAND – BEDROCK 1:1 000 000. *Geological Survey of Finland, Special Paper*, *60*, 41–76.

Pandian, R. S., Nair, I. S. & Lakshmanan, E. (2016). Finite element modelling of a heavily exploited coastal aquifer for assessing the response of groundwater level to the changes in pumping and rainfall variation due to climate change. *Hydrology Research*, *47*(1), 42–60. https://doi.org/10.2166/nh.2015.211

Pasanen, A. H. & Okkonen, J. S. (2017). 3D geological models to groundwater flow models: Data integration between GSI3D and groundwater flow modelling software GMS and FeFlow. *Geological Society Special Publication*, *408*(1), 71–87. https://doi.org/10.1144/SP408.15

Person, M., McIntosh, J., Bense, V. & Remenda, V. H. (2007). Pleistocene hydrology of North America: The role of ice sheets in reorganizing groundwater flow systems. *Reviews of Geophysics*, *45*(3). https://doi.org/10.1029/2006RG000206

Pétré, M. A., Rivera, A. & Lefebvre, R. (2019). Numerical modeling of a regional groundwater flow system to assess groundwater storage loss, capture and sustainable exploitation of the transboundary Milk River Aquifer (Canada – USA). *Journal of Hydrology*, *575*, 656–670. https://doi.org/10.1016/j.jhydrol.2019.05.057

Punkari, M. (1997). Glacial and glaciofluvial deposits in the interlobate areas of the Scandinavian Ice Sheet. *Quaternary Science Reviews*, *16*(7), 741–753. https://doi.org/10.1016/S0277-3791(97)00020-6

Putkinen, N., Eyles, N., Putkinen, S., Ojala, A. E. K., Palmu, J.-P., Sarala, P., Väänänen, T., Räisänen, J., Saarelainen, J., Ahtonen, N., Rönty, H., Kiiskinen, A., Rauhaniemi, T. & Tervo, T. (2017). High-resolution LiDAR mapping of glacial landforms and ice stream lobes in Finland. *Bulletin of the Geological Society of Finland*, *89*, 64–81. https://doi.org/10.17741/bgsf/89.2.001

Putkinen, N., Lindsberg, E., Paalijärvi, M., Valjus, T., Forss, H., Hakala, P. & Wennman, K. (2018). *Kurikan Paloluoman ja Häjyluoman alueiden syväpohjavesitutkimukset 2015 – 2016 : Vaihe 3*.

Putkinen, N., Paalijarvi, M., Okkonen, J. & Putkinen, S. (2015). *KURIKAN KUUSISTONLOUKON ALUEEN*

SYVÄPOHJAVESITUTKIMUKSET 2014 - 2015 : VAIHE 2 : POHJAVEDEN KOEPUMPPAUS.

Putkinen, N., Putkinen, S., Valjus, T. & Levaniemi, H. (2012). *Kurikan Kuusistonloukon pohjavesialueen geologinen rakenneselvitys*.

Refsgaard, J. C., Christensen, S., Sonnenborg, T. O., Seifert, D., Højberg, A. L. & Troldborg, L. (2012). Review of strategies for handling geological uncertainty in groundwater flow and transport modeling. *Advances in Water Resources*, *36*, 36–50. https://doi.org/10.1016/j.advwatres.2011.04.006

Rey, N., Rosa, E., Cloutier, V. & Lefebvre, R. (2018). Using water stable isotopes for tracing surface and groundwater flow systems in the Barlow-Ojibway Clay Belt, Quebec, Canada. *Canadian Water Resources Journal*, *43*(2), 173–194. https://doi.org/10.1080/07011784.2017.1403960

Ritter, A. & Muñoz-Carpena, R. (2013). Performance evaluation of hydrological models: Statistical significance for reducing subjectivity in goodness-of-fit assessments. *Journal of Hydrology*, *480*, 33–45. https://doi.org/10.1016/j.jhydrol.2012.12.004

Rivard, C., Lefebvre, R. & Paradis, D. (2014). Regional recharge estimation using multiple methods: An application in the Annapolis Valley, Nova Scotia (Canada). *Environmental Earth Sciences*, *71*(3), 1389–1408. https://doi.org/10.1007/s12665-013-2545-2

Rivera, A. (2007). *GROUNDWATER MODELLING: FROM GEOLOGY TO HYDROGEOLOGY*. https://www.researchgate.net/publication/229005360_GROUNDWATER_MODELLING_FROM_GEOLOGY_TO_HYDROGEOLOGY

Ross, M., Parent, M. & Lefebvre, R. (2005). 3D geologic framework models for regional hydrogeology and land-use management: A case study from a Quaternary basin of southwestern Quebec, Canada. *Hydrogeology Journal*, *13*(5–6), 690–707. https://doi.org/10.1007/s10040-004-0365-x

Rushton, K. R. (2003). *Groundwater Hydrology*. John Wiley & Sons Ltd.

Sammis, T. W., Evans, D. D. & Warrick, A. W. (1982). WATER RESOURCES BULLETIN COMPARISON OF METHODS TO ESTIMATE DEEP PERCOLATION RATES1. *Water Resources*, *18*(3), 465–470.

Sandersen, P. B. E. & Jørgensen, F. (2003). Buried Quaternary valleys in western Denmark-occurrence and inferred implications for groundwater resources and vulnerability. *Journal of Applied Geophysics*, *53*(4), 229–248. https://doi.org/10.1016/j.jappgeo.2003.08.006

Savard, M. M., Nastev, M., Paradis, D., Lefebvre, R., Martel, R., Cloutier, V., Murat, V., Bourque, E., Ross, M., Lauziere, K., Parent, M., Hamel, A., Lemieux, J. M., Therrien, R., Bolduc, A., Rocher, M., Salad Hersi, O., Kirkwood, D., Castonguay, S. & Gelinas, P. (2013). Canadian Inventory of Groundwater Resources: Integrated regional hydro- geological characterization of the fractured aquifer system of southwestern Quebec. In *Geological Survey of Canada, Bulletin 587*. https://doi.org/10.4095/291347

Scanlon, B. R., Healy, R. W. & Cook, P. G. (2002). Choosing appropriate techniques for quantifying groundwater recharge. *Hydrogeology Journal*, *10*, 18–39. https://doi.org/10.1007/s10040-0010176-2

Sophocleous, M. (2000). From safe yield to sustainable development of water resources-the Kansas experience. *Journal of Hydrology*, *235*(1–2), 27–43. http://www-ne.cr.usgs.gov/highplains/hpactivities.html

Sophocleous, Marios. (2010). Review: groundwater management practices, challenges, and innovations in the High Plains aquifer, USA-lessons and recommended actions. *Hydrogeology Journal*, *18*, 559–575. https://doi.org/10.1007/s10040-009-0540-1

Stroeven, A. P., Hättestrand, C., Kleman, J., Heyman, J., Fabel, D., Fredin, O., Goodfellow, B. W., Harbor, J. M., Jansen, J. D., Olsen, L., Caffee, M. W., Fink, D., Lundqvist, J., Rosqvist, G. C., Strömberg, B. & Jansson, K. N. (2016). Deglaciation of Fennoscandia. *Quaternary Science Reviews*, *147*, 91–121. https://doi.org/10.1016/j.quascirev.2015.09.016

Stumpf, A. J. & Ismail, A. (2013). High-resolution seismic reflection profiling: an aid for resolving the Pleistocene stratigraphy of a buried valley in central Illinois, USA. *Annals of Glaciology*, *54*(64), 10–20. https://doi.org/10.3189/2013AoG64A602

Sutcliffe, O. E., Dowdeswell, J. A., Whittington, R. J., Theron, J. N. & Craig, J. (2000). Calibrating the Late Ordovician glaciation and mass extinction by the eccentricity cycles of Earth's orbit. *Geology*, *28*(11), 967–970. https://doi.org/10.1130/0091-7613(2000)28<967:CTLOGA>2.0.CO;2

Theis, C. V. (1941). The effect of a well on the flow in a nearby stream. *American Geophysical Transactions*, *22*(3), 734–738.

Usman, M., Liedl, R., Arshad, M. & Conrad, C. (2018). 3-D Numerical Modelling of Groundwater Flow for Scenario-Based Analysis and Management. *Water SA*, *44*(2), 146–154.

https://doi.org/10.4314/wsa.v44i2.01

Van Der Kamp, G. (2001). Methods for determining the in situ hydraulic conductivity of shallow aquitards-an overview. *Hydrogeology Journal*, *9*(5), 5–16. https://doi.org/10.1007/s100400000118

Van Der Kamp, Garth & Maathuis, H. (2012). The Unusual and Large Drawdown Response of Buried-Valley Aquifers to Pumping. *Ground Water*, *50*(2), 207–215. https://doi.org/10.1111/j.1745-6584.2011.00833.x

Vélez-Nicolás, M., García-López, S., Ruiz-Ortiz, V. & Sánchez-Bellón, Á. (2020). Towards a sustainable and adaptive groundwater management: Lessons from the Benalup Aquifer (Southern Spain). *Sustainability*, *12*(5215). https://doi.org/10.3390/su12125215

Vižintin, G., Ravbar, N., Janež, J., Koren, E., Janež, N., Zini, L., Treu, F. & Petrič, M. (2018). Integration of models of various types of aquifers for water quality management in the transboundary area of the Soča/Isonzo river basin (Slovenia/Italy). *Science of the Total Environment*, *619–620*, 1214–1225. https://doi.org/10.1016/j.scitotenv.2017.11.017

Wen, J.-C., Wu, C.-M., Tian-Chyi, &, Yeh, J. & Tseng, C.-M. (2010). Estimation of effective aquifer hydraulic properties from an aquifer test with multi-well observations (Taiwan). *Hydrogeology Journal*, *18*, 1143–1155. https://doi.org/10.1007/s10040-010-0577-1

Zhou, Y. & Li, W. (2011). A review of regional groundwater flow modeling. *Geoscience Frontiers*, *2*(2), 205–214. https://doi.org/10.1016/j.gsf.2011.03.003

Zhu, L., Gong, H., Chen, Y., Li, X., Chang, X. & Cui, Y. (2016). Improved estimation of hydraulic conductivity by combining stochastically simulated hydrofacies with geophysical data. *Scientific Reports*, *6*. https://doi.org/10.1038/srep22224

Appendix I: Cross-section comparisons between preliminary GTK model (top) and final 3D hydrostratigraphic model (bottom) for select locations.

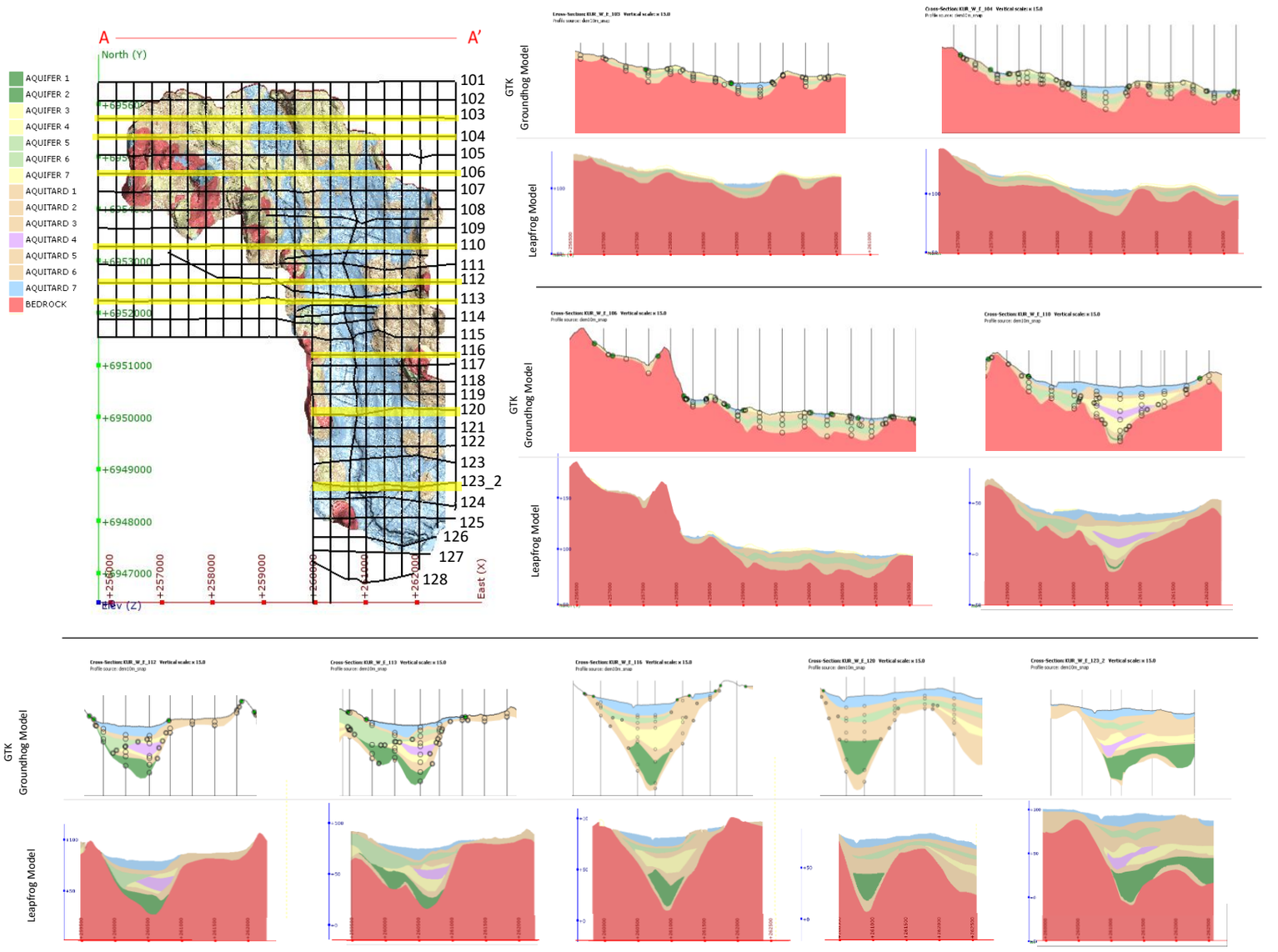

Appendix II: Pumping test analysis for observation wells: KUU19, 21, 22, and 23B during pumping at Siivilä 1.

Theis | **Hantush**

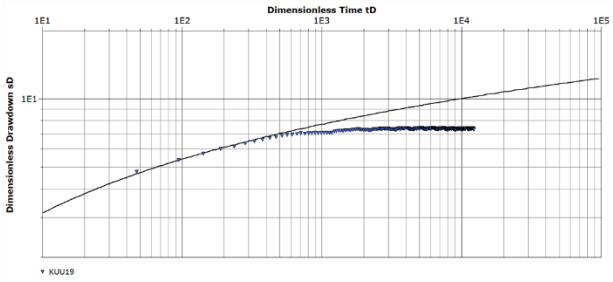

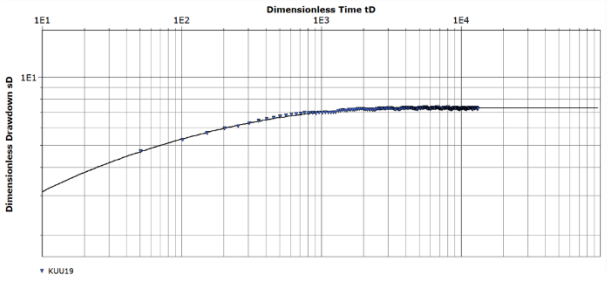

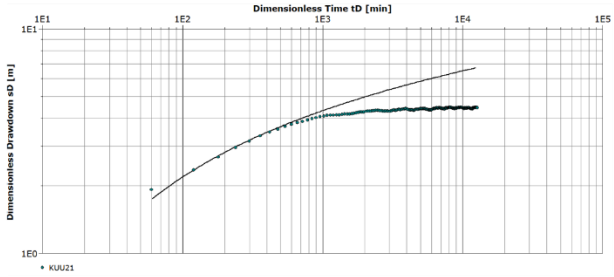

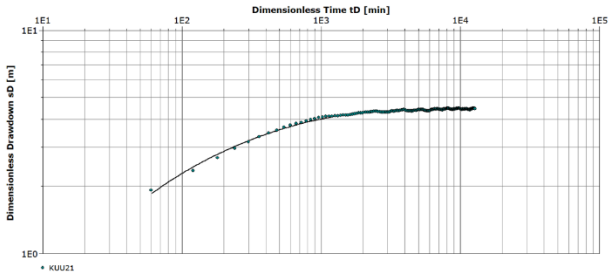

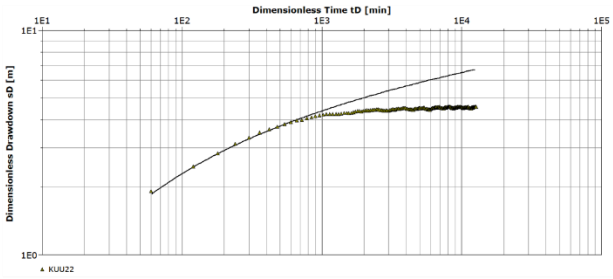

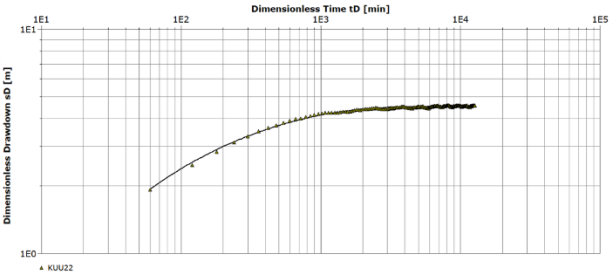

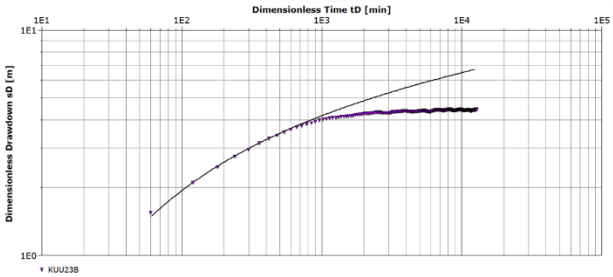

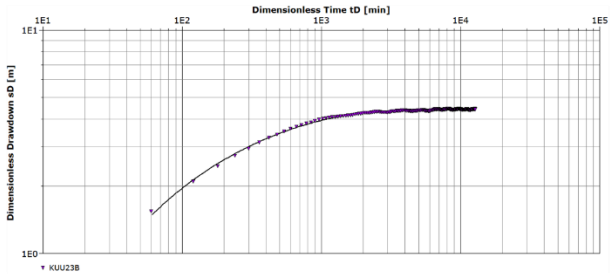

Appendix III: Pumping test analysis for observation wells: MIHP 3, 9, 10, and 12 during pumping at Siivilä 3.

Theis

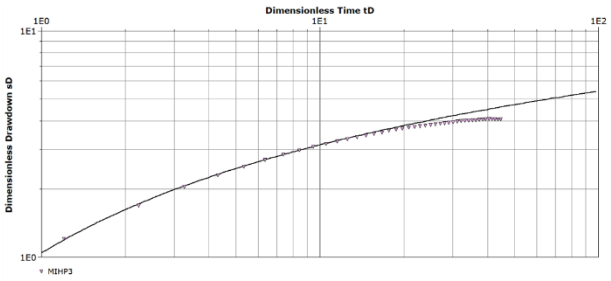

Hantush

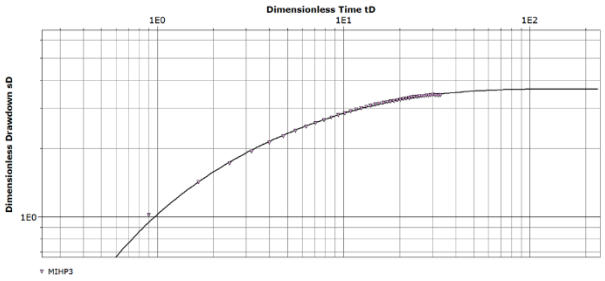

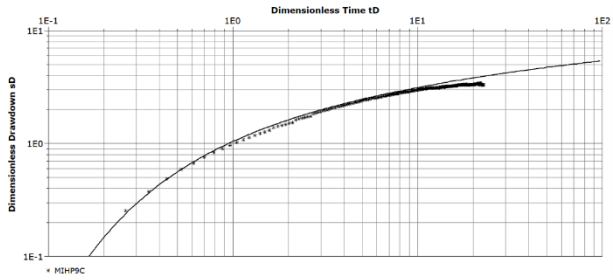

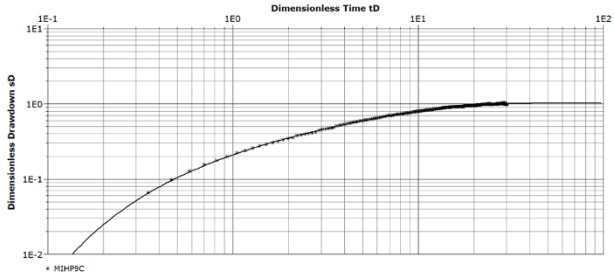

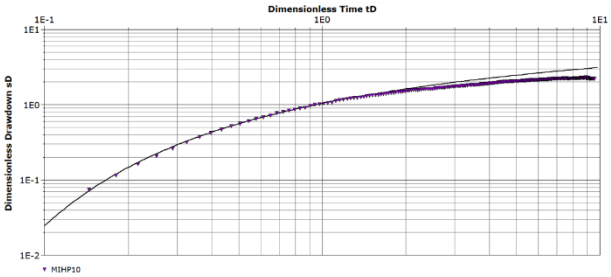

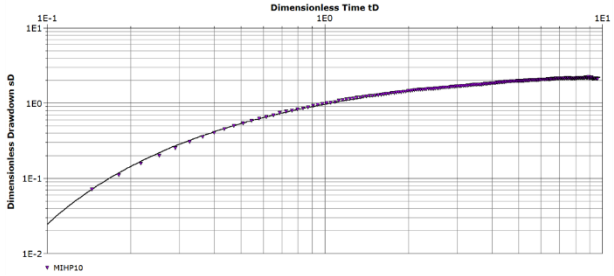

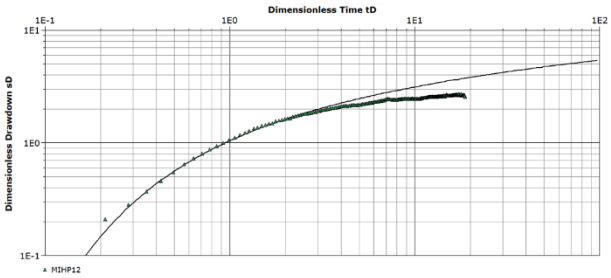

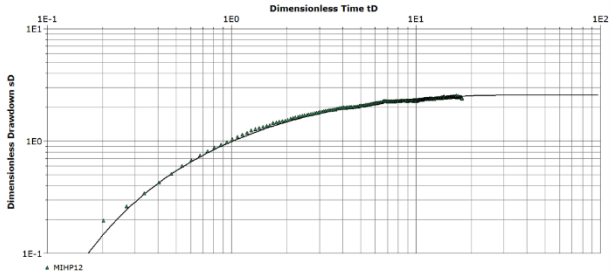

Appendix IV: Drawdown plots at observed wells during pumping at Siivilä 1 and Siivilä 3.